MODIFICATION OF POLYMERIC MEMBRANES FOR ENERGY SUSTAINABILITY AND CO_2CAPTURE

CHUA MEI LING

NATIONAL UNIVERSITY OF SINGAPORE

2014

MODIFICATION OF POLYMERIC MEMBRANES FOR ENERGY SUSTAINABILITY AND CO_2CAPTURE

CHUA MEI LING

(B.Eng. (CBE), NTU)

A THESIS SUBMITTED

FOR THE DEGREE OF DOCTOR OF PHILOSOPHY

DEPARTMENT OF CHEMICAL AND BIOMOLECULAR ENGINEERING

NATIONAL UNIVERSITY OF SINGAPORE

2014

DECLARATION

I hereby declare that this thesis is my original work and it has been written by me in its entirety. I have duly acknowledged all the sources of information which have been used in the thesis.

This thesis has also not been submitted for any degree in any university previously.

_____

Chua Mei Ling

29 July 2014

ACKNOWLEDGEMENTS

I would like to thankall the funding support and the support from my supervisor, my mentors, my seniors, fellow research students and my family and friends that I have received during my PhD study. Without them, I would not be able to accomplish much.

My supervisor, Professor Chung Tai-Shung Neal, has given me the opportunity to start this challenging yet rewarding PhD study. He has helped me to grow as a researcher. I would like to thank him for his guidance and encouragement. He has also referred mentors to help me. I would like to thank Dr. Xiao Youchang, Professor Shao Lu and Dr. Low Bee Ting for their valuable insight and suggestions for my research. The seniors and fellow research students have also contributed to improve my research.

This research is supported by the A*Star under its Carbon Capture & Utilisation (CCU) TSRP Program (SERC grant number 092 138 0020 (NUS grant numberR-398-000-058-305)), the National Research Foundation, Prime Minister's Office, Singapore under its Competitive Research Program (CRP Award No. NRF-CRP 5-2009-5 (NUS grant number R-279-000-311-281)) and the National University of Singapore (NUS) under the project entitled "Membrane research for CO_2 capture" (grant number R-279-000-404-133).

Special thanks to my husband, Mr. Cheang Kwai Sim, my beloved parents, siblings and friends who have been very supportive to my PhD study and research.

TABLE OF CONTENTS

Summary

Polymers, having a wide range of properties, are commonly used in the industries to fabricate gas separation membranes due to their low costs and ease of processing into different configurations.For efficient and effective gas separation, membranes with a high permeability and selectivity are desirable. However, there exist well-known tradeoff curves between permeability and selectivity for polymers. Other factors like CO_2-induced plasticization and mechanical strength need to be considered. The aim of this work is to employ modification methods to improve the physiochemical properties and the gas separation performance of the polyimide and poly(ethylene oxide) membranes for the separation of gas mixtures.

Attempts to cross-link a polyimide (PI) without sacrificing the permeability of the membrane are made by employing(1) chemical grafting usingthermally saccharide labile units such as glucose, sucrose and raffinose, (2) chemical modification of thermally labile unit and (3) ionic crosslinking by iron (III) acetylacetonate. These chemical modifications were followed by thermal annealing of the membranes. The polyimide was synthesized in the laboratory, modifications were performed, and membranes were fabricated and post-treated. Various characterization techniques such as TGA, DSC, FTIR, gel content and density measurement were employed to elucidate the structural changes.

For the first study using glucose, sucrose and raffinose as the thermally labile units, it is observed that when the grafted and annealed membranes are annealed from 200 to 400 °C, a substantial increase in gas permeability is achieved with moderate gas-pair selectivity. The annealed membranes show good flexibility with enhanced gas permeability and CO_2 plasticization resistance.

In this second study of chemical modification of thermally labile unit, annealing in air and incorporating β-CD and β-CD-Ferrocene are employed to change the molecular structure and improve the CO_2/CH_4 gas-pair separation and stability of polyimide membranes. A 55% increment in CO_2/CH_4

selectivity at the expense of permeability are observed for the PI membrane annealed under air at 400 °C compared to the as-cast membrane. A further twofold improvement in the permeability of the β-CD containing membrane annealed under air at 400 °C is achieved. With the inclusion of ferrocene, the membrane exhibits a decline in permeability with an improvement of CO_2/CH_4 selectivity to 47.3 when annealed in air at 400 °C.

By employing an ionic thermally labile unit, iron (III) acetylacetonate (FeAc) in the third study, coupled with low temperature annealing, it is observed that not only a cross-linked network is established, aparticular increment of more than 88 % in permeability is attained for the PI-6 wt% FeAc membrane as compared to pristine PI membrane.

In the fourth study, polyetheramine (PEA) was cross-linked with polyhedral oligomeric silsequioxane (POSS) for carbon dioxide/hydrogen (CO_2/H_2) and carbon/nitrogen (CO_2/N_2) separation. A high CO_2 permeability of 380 Barrer with a moderate CO_2/N_2 selectivity of 39.1 and a CO_2/H_2 selectivity of 7.0 are achieved at 35 °C and 1 bar for PEA:POSS 50:50 membrane. At higher upstream gas pressure during permeation tests, improvements are observed in both CO_2 permeability and ideal CO_2/H_2 and CO_2/N_2 selectivity due to the plasticization effect of CO_2.

LIST OF TABLES

LIST OF FIGURES

Chapter 1: Introduction

1.1 Gas separation processes and technologies

The separation of gas mixtures such as air, natural gas and olefin/paraffin are important in the oil and chemical industries to produce purified streams for further usage. An emerging gas separation process arise due to concerns of global warming is the carbon dioxide capture from flue gas streams. The following section entailsthe above-mentioned separation processes and its prevalent technology.

Air separation produces oxygen-enriched or nitrogen-enriched streams for a wide range of applications. Oxygen-enriched gas can be used for medical application, combustion enhancement in furnaces and fuel cells. Nitrogen-enriched gas is utilized in inert blanketing of hydrocarbon fuel and the preservation of agricultural products. The most common technology to separate air is cryogenic separation, which involves cooling air until it liquefies and selectively distilling the components at their respective boiling temperatures to separate them. This process can produce high purity gases but is energy-intensive and complex. Other technologies include pressure swing adsorption and membrane separation. Pressure swing adsorption (PSA) is based on the use of adsorbents such as zeolites and carbon molecular sieves. Both materials can result in oxygen and nitrogen production, depending on the operating steps. PSA is highly capital-intensive and energy-intensive.Membrane separation of air is primarily based on the use of polymeric hollow fiber technology in which oxygen permeates faster than nitrogen. Air is compressed and fed into the membrane assembly. Oxygen-rich gas is obtained as the low-pressure permeate and nitrogen-rich gas is obtained at the retentate at pressure close to the compressor discharge pressure. In practice, with the existing membrane properties, it is much easier to produce high purity nitrogen. Therefore, membranes have been used largely for nitrogen production [1]. The present O_2/N_2 separation factor for the best commercial polymer membranes ranges from 6-8.

(a) A cryogenic air separation flow diagram [2]

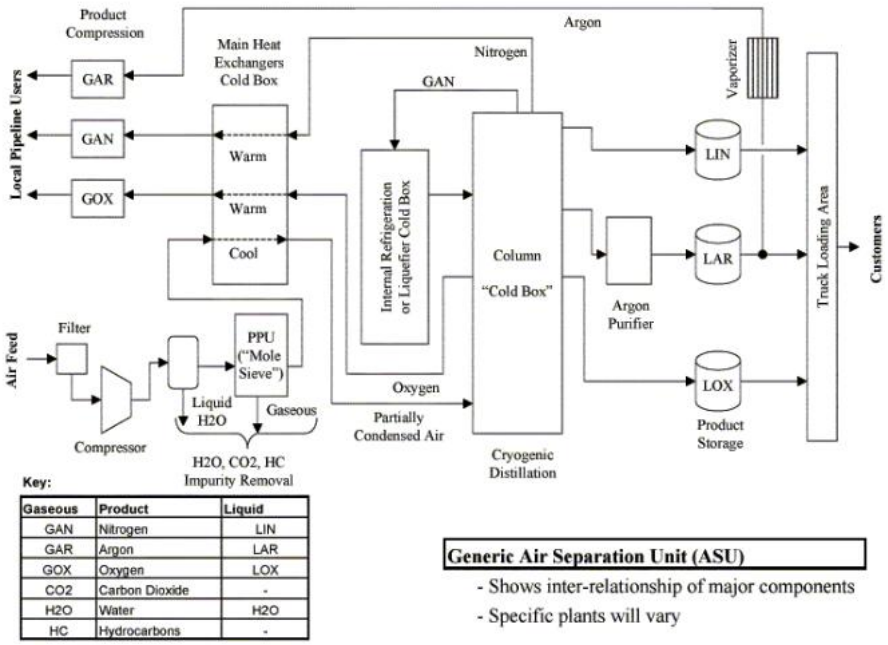

Gaseous	Product	Liquid
GAN	Nitrogen	LIN
GAR	Argon	LAR
GOX	Oxygen	LOX
CO2	Carbon Dioxide	-
H2O	Water	H2O
HC	Hydrocarbons	-

(b) PSA system for producing nitrogen-enriched streams [3]

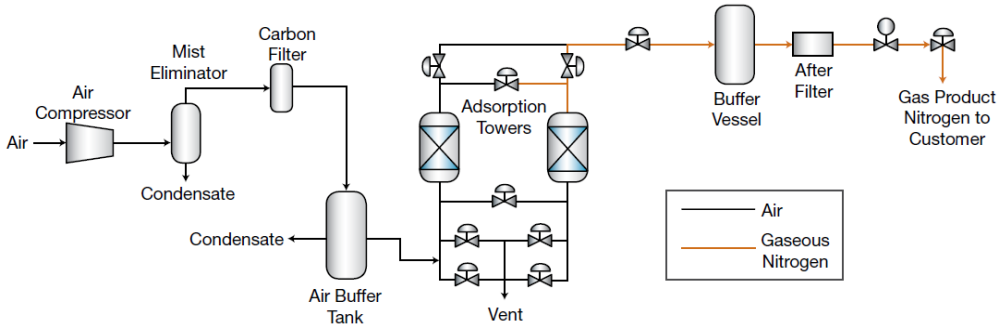

(c) Membrane system for generating nitrogen-enriched streams [3]

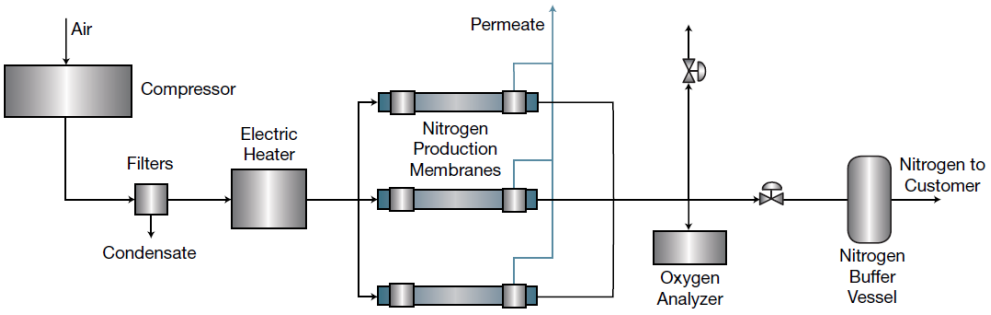

Figure 1.1 Schematics of air separation technologies

One of the separation processes in***natural gas purification*** is the removal of carbon dioxide from natural gas. Natural gas, a cleaner and more efficient fuel compared to coal and crude oil, is in rising demand in energy sector and also in chemical sector as petrochemical feedstock. Besides constituting methane as the key component, natural gas contains some undesirable impurities like other hydrocarbons, carbon dioxide, water, nitrogen and hydrogen sulfide. Thus, natural gas has to be purified to increase its fuel heating value, reduce transportation costs, pipeline corrosion and atmospheric pollution [4-5]. The conventional separation technology for carbon dioxide separation from light gases is amine absorption. A typical absorption process consists of two towers. In the first tower, which is operated at high pressure,an absorbent liquid, flowing countercurrent to the feed gas, absorbs the carbon dioxide in the feed gas. The liquid is then heated and fed to a low-pressure stripper tower where the sorbed component leaves as a low-pressure overhead gas.The regenerated liquid is recycled to the first tower. Heat exchangers are employed to reduce the cost of heating the absorbent liquid.

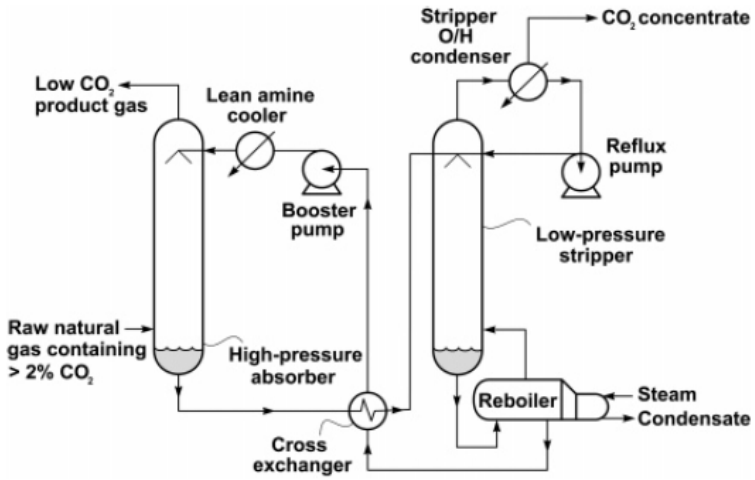

Figure 1.2 A typical natural gas amine absorber-stripper treatment process [4]

Amines are most commonly used sorbents for carbon dioxide. Amine absorption is a fully matured process. Despite its maturity, it suffers from drawbacks such as the need to regenerate solvent, large footprint for offshore applicationand lack of robustness for feed composition variations [6]. More and more offshore platforms require compact and environmentally friendly separation processes. Membrane technology is widely known to be a

promising alternative to amine absorption. It possesses competitive advantages like higher energy efficiency, smaller footprint, ease of scale-up and environmental friendliness [7]. The membrane market has grown over the last few decades and is likely to keep growing [8]. The nature of membrane technology makes it attractive for offshore applications. In addition, it can form hybrid system with amine absorption. Cellulose acetate is a glassy polymer commonly used for natural gas purification. The selectivity is about 12-15 under typical operating conditions. Other promising polymers include polyimide and polyaramide, which have selectivities of 20-25.

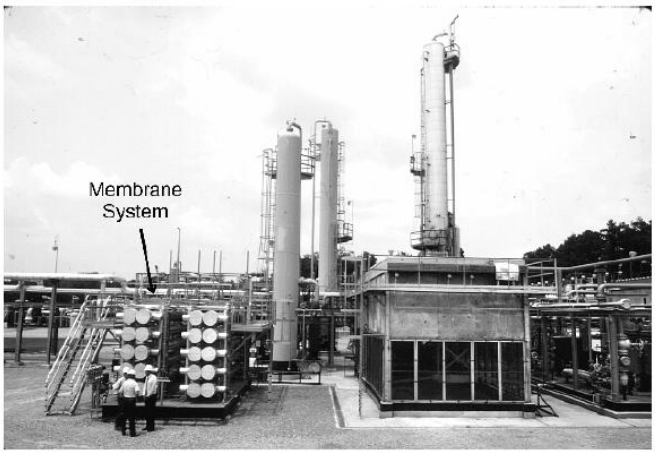

Figure 1.3 Size comparisons of membrane and amine system [9]

Similar to the removal of carbon dioxide from natural gas,amine absorption is the most mature and prevalent technology for***carbon dioxide capturefrom flue gas*** streams. Flue gas often refers to the gas emitted to the atmosphere from the power plants. It is produced from the combustion of fossil fuels. It contains mostly nitrogen from the combustion air, carbon dioxide, water vapor and oxygen. Particulate matter, carbon monoxide, nitrogen oxides and sulfur oxides are other pollutants that exist at a small percentage in the flue gas. It typically produced at atmospheric pressure and at large quantity. The increasing carbon dioxide emission to the atmosphere is one of the main contributing factors to global warming. The rising level of atmosphere carbon dioxide acts as trap for heat, causing the global temperature to increase. Hence, reduction in carbon dioxide emission becomes an important area of research. Separation of carbon dioxide from flue gas is one short term goal to achieve it.

Better fuel efficiency and utilizing alternate greener power sources are one of the mid-term goals and one of the long-term goals respectively. Membrane technology is a promising alternative to the expensive amine absorption for carbon dioxide capture from flue gas.

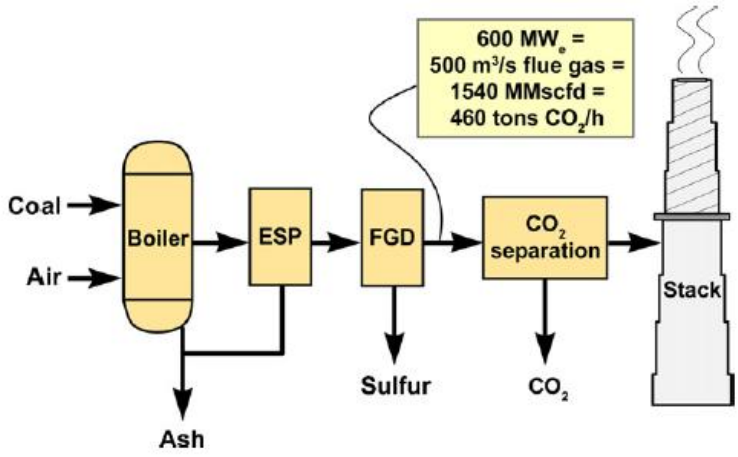

Figure 1.4 Simplified process flow diagram for a flue gas cleanup for a coal-fired power plant [10]

The ***separation of olefins from paraffins*** is an important process to the petrochemical industry. The streams containing olefins and paraffins are originated from steam cracking units, catalytic cracking units or dehydrogenation of paraffins. The separation is currently performed by cryogenic distillation, which is energy intensive and costly due to the close boiling point of the components [11]. Extensive research has been carried out to reduce the cost of the separation. Membrane technology has been considered as an attractive alternative.

1.2 Membranes for gas separation

Membrane is a thin film that acts as a selective barrier, preferentially allowing some particles to pass through while blocking others. It can be symmetric, asymmetric or composite structure. Membranes with symmetric structure are uniform throughout. It includes dense films and porous media that have cylindrical pores or sponge-type structure. Dense films are used intensively in laboratory scale for fundamental study of intrinsic membrane properties. Mircoporous membranes of defined pore structure are used to separate various chemical species by sieving.

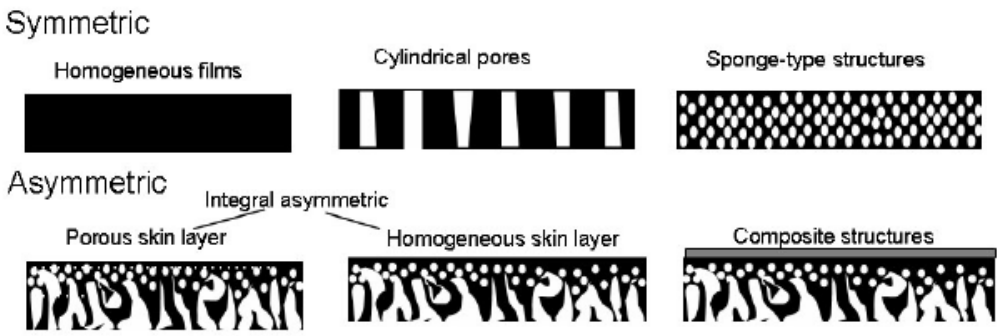

Figure 1.5 Structure of symmetric and asymmetric membranes

The flux of a symmetric membrane with the smallest thickness is still too low for practical interest. In the late 1950s, the breakthrough came when Loeb and Sourirajan discovered the formation of asymmetric membranes made of cellulose acetate for reverse osmosis [12]. Asymmetric membranes consist of a very thin, dense skin overlaying a porous, sponge mechanical support layer with little resistance to support. The structure is different on the top side and on the bottom structure. Since the selective layer is very thin, asymmetric membranes show much higher permeate flux than symmetric membranes. Hence, it is widely utilized in industries.

Asymmetric membranes can be used in plate-and frame type module, packaged in spiral-wound elements or developed into hollow fiber form. Hollow fiber membranes have higher surface area per volume compared to other configurations. The defects on the selective layer were found to be able to be treated by coating with highly permeable silicone rubber to form

composite membranes. Though membranes were known to have the potential to separate gases, the first synthetic membrane was only commercialized in 1980 due to the lack of technology to economically produce high performance membranes and modules [13].

Polymers, having a wide range of properties, are commonly used in the industries to fabricate gas separation membranes due to their low costs and ease of processing into different configurations. For efficient and effective gas separation, membranes with a high permeability and selectivity are desirable. However, there exist well-known tradeoff curves between permeability and selectivity for polymers [14-15]. Besides that, other factors like CO_2-induced plasticization and mechanical strength need to be considered [16].

Polymers can be generally classified as glassy and rubbery. Glassy polymers behave below the glass transition temperature. They have fixed and rigid polymer chains, which primarily have the capability to discriminate gas pairs according to their sizes.One glassy polymer of interest is polyimide containing 4,4′-(hexafluoroisopropylidene) diphthalic anhydride (6FDA), which will be discussed in details in the next section. However, similar to other glassy polymers, they are also prone to be plasticized by high sorbing gases like carbon dioxide (CO_2). Occurrence of plasticization is often marked by the upward increase in CO_2 permeability at high upstream pressures [6]. CO_2 swells up the polymer chains, resulting an increase in inter-chain spacing and chain mobility. In mixed gas tests, there will be an increase in permeability of all components, leading to a loss in membraneselectivity.

Rubbery polymers are at a state above the glass transition temperature. They have flexible polymer chains and they separate gases according to condensability of the gases. Poly(ethylene oxide), a rubbery material, has gained interests as a feasible material to fabricate carbon dioxide-selective membranes [17-19]. Its strong affinity to carbon dioxide due to the polar ether groups present allows preferential removal of carbon dioxide. However, its shortcomings such as tendency to crystallize due to its semi-crystalline nature and weak mechanical strength have restricted its applications.

1.3 Modification of polymeric membranes for gas separation

Extensive research has been performed to improve the physiochemical properties and the gas separation performance of polymeric membranes. Some of the approaches for modifying polyimide membranesinclude molecularly tailoring the structure to obtainnew materials and modifying existing polyimide materials by heat treatment, grafting side groups on polymer backbone and cross-linking[6].Incorporating PEO with other monomers as copolymers or as polymer blends or crosslinking it are some of the strategies done to overcome the drawbacks of PEO and improve the gas separation performance [18].

In this study, dense films will be used in laboratory scale for fundamental study of intrinsic membrane properties. Attempts to cross-link a polyimide (PI) without sacrificing the permeability of the membrane are made by employing (1) chemical grafting usingthermally saccharide labile units, (2) chemical modification of thermally labile unit and (3) ionic crosslinking. These chemical modifications were followed by thermal annealing of the membranes. The detailed methodology, results and discussion are in Chapter 3-6. In Chapter 7, polyetheramine (PEA) was cross-linked with polyhedral oligomeric silsequioxane (POSS) for enhanced gas separation. The modifications show improvements in the physiochemical properties and the gas separation performance of the membranes.

References:

[1] D. R. Paul, Y. P. Yampol'skii, Polymeric gas separation membranes, CRC Press, Inc (1994).

[2] Universal Industrial Gases, Inc. Overview of cryogenic air separation and liquefier systems. Retrieved from www.uigi.com/cryodist.html

[3] S. Ivanova, R. Lewis, Producing nitrogen via pressure swing adsorption, Aiche CEP June (2012) 38-42.

[4] R. W. Baker, K. Lokhandwala, Natural gas processing with membranes: an overview, Ind. Eng. Chem. Res. 47 (2008) 2109-2121.

[5]B. D. Bhide, A. Voskericyan, S. A. Stern, Hybrid processes for the removal of acid gases from natural gas, J. Membr. Sci. 140 (1998) 27–49.

[6] Y. Xiao, B. T. Low, S. S. Hosseini, T. S. Chung, D. R. Paul, The strategies of molecular architecture and modification of polyimide-based membranes for CO_2 removal from natural gas – A review, Prog. Polym. Sci. 34 (2009) 561-580.

[7] W. J. Koros, G. K. Fleming, Membrane-based gas separation, J. Membr. Sci.83 (1993) 1–80.

[8] D. F. Sanders, Z. P. Smith, R. Guo, L. M. Robeson, J. E. McGrath, D. R. Paul, B. D. Freeman, Energy-efficient polymeric gas separation membranes for a sustainable future: A review, Polymer 54 (2013) 4729-4761.

[9] T. Cnop, D. Dortmundt, M. Schott, Continued development of gas separation membranes for highly sour service, retrieved from www.uop.com.

[10] T. C. Merkel, H. Lin, X. Wei, R. Baker, Power plant post-combustion carbon dioxide capture: An opportunity for membranes, J. Membr. Sci. 359 (2010) 126-139.

[11] R. L. Burns, W. J. Koros, Defining the challenges for C_3H_6/C_3H_8 separation using polymeric membranes, J. Membr. Sci. 211 (2003) 299-309.

[12] S. Loeb, S. Sourirajan, Seawater demineralization by means of an osmoticmembrane,Adv. Chem38 (1963) 117-132.

[13] R. W. Baker, Future directions of membrane gas separation technology, Ind. Eng. Chem. Res. 41 (2002) 1393-1411.

[14] L. M. Robeson, The upper bound revisited, J. Membr. Sci. 320 (2008) 390-400.

[15] B. D. Freeman, Basis of permeability/selectivity tradeoff relations in polymeric gas separation membranes, Macromolecules 32 (1999) 375-380.

[16] A. Bos, I. G. M. Pünt, M. Wessling, H. Strathmann, Plasticization-resistant glassy polyimide membranes for CO_2/CH_4 separations, Sep. Purif. Technol. 14 (1998) 27-39.

[17] H. Lin, B. D. Freeman, Materials selection guidelines for membranes that remove CO_2 from gas mixtures, J. Mol. Struct. 739 (2005) 57-74.

[18] S. L. Liu, L. Shao, M. L. Chua, C. H. Lau, H. Wang, S. Quan, Recent progress in the design of advanced PEO-containing membranes for CO_2 removal, Prog. Polym. Sci. 38 (2013) 1089-1120.

[19] C. H. Lau, P. Li, F. Li, T. S. Chung, D. R. Paul, Reverse-selective polymeric membranes for gas separation, Prog. Polym. Sci. 36 (2013) 740-766.

Chapter 2: Background and literature review

Fundamental understanding on the gas transport properties of the membranes is essential in order to design high-performance polymeric membranes. In the next few sections, the gas transport mechanism, the factors affecting the gas transport and the modification methods will be discussed.

2.1 Gas transport mechanisms

The transport mechanism depends on the structure of the membrane. For the porous membranes, the mean free path of the gases and the diameter of the pores determine the transport properties through the membrane. The mean free path of gases refers to the average distance travelled by the gas molecule between collisions.

Table 2.1 Mean free path of gases at 0 °C and 1 atm [1]

Gas	Mean free path x 10^{10} (m)
Carbon dioxide	397
Hydrogen	1123
Nitrogen	600
Oxygen	647

Based on the ratio of the mean free path of the gases and the diameter of the pore, there are four fundamental gas transport mechanisms in porous membranes:

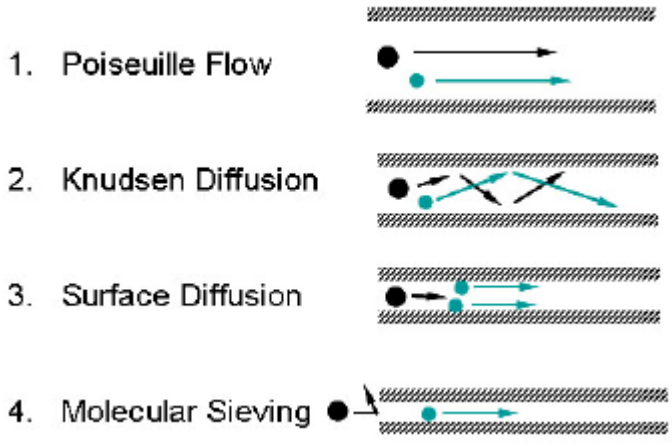

Figure 2.1 Transport mechanisms in porous membranes

(1) Poiseuille flow, where the mean pore diameter is much larger than the mean free path of the gases. The gases collide exclusively with each other. This type of transport mechanism is observed for porous membrane supports. There is no separation obtained for this transport mechanism.

(2) Knudsen diffusion

When the pore size becomes smaller than the mean free path, Knudsen diffusion dominates. A way to define Knudsen diffusion is to calculate the Knudsen diffusion number. If the Knudsen diffusion number is more than 10, the separation is termed as Knudsen diffusion. Gas molecules interact with the pore walls much more frequently than with each other, allowing the lighter molecules to be preferentially diffuse through pores to achieve separation. The lower limit for pore diameter is set to be 20Å. The highest attainable separation factor between two different gas molecules A and B is the square root of the ratio of the two gas molecular weight.

(3) Surface diffusion

The driving force for separation according to surface diffusion is based on the concentration of the adsorbed phase of the gas. The more condensable gas will be selectively adsorbed and the less condensable gas will be retained due to the reduced pore size. The pore size region for surface diffusion to take place is about 5Å $<d_p<$ 10Å or up to three times the diameter of the molecules.

(4) Molecular sieving

Molecular sieving occurs when there is precise size discrimination between the gas molecules through ultramicropores ($d_p<$ 5Å). High selectivity is achieved through size and shape separation of the gases. The pore diameter is small enough to allow the permeation of smaller molecules while blocking the larger molecules to diffuse through. Carbon molecular sieve membranes and zeolites are typical membranes dominated by this transport mechanism.

For non-porous membranes, the transport mechanism is described by the*solution-diffusion model* [2]. It occurs in the absence of direct continuous

pathways for gas transport across the membrane.The feed gas is sorbed at the high activity interface, diffused down the concentration gradient and desorbed at the low activity interface[3]. The diffusion process occurs through the transient opening of polymer chains in the membrane, as shown in Fig. 2.2. Membrane performance is characterized primarily by the flux of the gas component across the membrane and the selectivity in separating the gases.

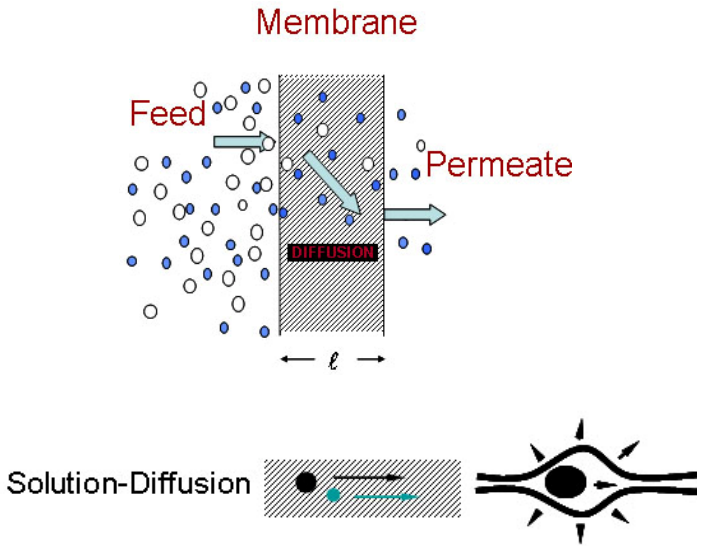

Figure 2.2 Schematic for the solution-diffusion mechanism across the membrane

2.2 Solution-diffusion mechanism

Gas permeability and selectivity are two important parameters for the gas separation performance of the membranes. Gas permeability is a measure of the transport flux of a penetrant through a membrane. It is normalized by the driving force and the thickness of the membrane. The pure gas permeability can be measured using a constant volume method and be computed using Equation2.1, where Q (cm^3 (STP)/s) is the pure gas flux, l (cm) is the thickness of the membrane, A (cm^2) is the membrane area and ΔP (cm Hg) is the pressure drop across the membrane. The pure gas flux can be further expressed by the rate of increase in the downstream pressure (dp/dt (torr/s)), the downstream volume of the permeation cell (V (cm^3)), and the operating temperature of the permeation cell (T (K)). p_2 (psia) is the upstream feed gas pressure [4]. The permeate side was kept under vacuum before the testing. The unit of permeability is Barrer where 1 Barrer = 10^{-10} cm^3 (STP)-cm/cm^2 sec cmHg.

$$P = \frac{Ql}{A\Delta P} = \frac{273\times10^{10}}{760}\frac{Vl}{AT\left[\frac{p_2\times76}{14.7}\right]}\left(\frac{dp}{dt}\right) \tag{2.1}$$

To account for non-ideality at high pressures, the pressure drop across the membrane could be replaced by the fugacity difference [5]. The fugacity difference was determined using the Peng-Robinson equation of state for both pure gas and binary gas mixture.

The *ideal selectivity* of gas A to gas B was obtained by taking the ratio of the pure gas permeability of A to B, as shown in Equation2.2.

$$\alpha_{A/B} = \frac{P_A}{P_B} \tag{2.2}$$

Based on the solution-diffusion model, the permeability is the product of gas diffusivity coefficient, D (cm^2/s) and gas solubility coefficient, S (cm^3 (STP)/cm^3 polymer cmHg) and the ideal selectivity is the product of

diffusivity selectivity of gas A to B and solubility selectivity of gas A to B. The diffusivity coefficient (kinetic parameter) measures the mobility of the gas in a membrane while the solubility coefficient (thermodynamic parameter) is an indicator how much gas can be taken up by the membrane. Variations in the diffusion and sorption properties of polymers arise much from the nature of the polymer (glassy or rubbery).

$$P = D \times S \tag{2.3}$$

$$\alpha_{A/B} = \frac{D_A}{D_B} \times \frac{S_A}{S_B} \tag{2.4}$$

The permeability of abinary gas mixturecan be determined by the equations as follows [4],

$$P_A = \frac{y_A}{x_A} \frac{273 \times 10^{10}}{760} \frac{Vl}{AT\left[\frac{p_2 \times 76}{14.7}\right]} \left(\frac{dp}{dt}\right) \tag{2.5}$$

$$P_B = \frac{(1-y_B)}{1-x_B} \frac{273 \times 10^{10}}{760} \frac{Vl}{AT\left[\frac{p_2 \times 76}{14.7}\right]} \left(\frac{dp}{dt}\right) \tag{2.6}$$

where y_A is the mole fraction of penetrant A in the permeate and x_A is the mole fraction of penetrant A in the feed gas.

2.3 Gas transport in glassy polymers

2.3.1 Free volume concept and the non-equilibrium nature of glassy polymers

The free volume concept of polymer is extended from Cohen and Turnbull's explanation for the self-diffusion process in a liquid of hard spheres. The sum of the free volume V_f, which are spaces not occupied by polymer molecules, and the occupied volume $V_o$theoretically made up thespecific volume V_g of a polymer. The occupied volume, which consists of Van der Waals volume of the polymer and the excluded volume, is given by 1.3 times of Van deer Waals volume [6].

$$V_g = \frac{1}{\rho} = V_o + V_f \qquad (2.7)$$

Figure 2.3 shows the plot of specific volume of polymer as a function of temperature. As the temperature is cooled to below the glass transition temperature (T_g), a rapid decrease in thermal expansion coefficient is observed at T_g. Hence, glassy polymers, as illustrated in Figure2.3, exhibit a specific volume that is larger than the specific volume of an equivalent hypothetical rubber. This non-equilibrium nature of glassy polymers results in significant differences in the sorption and diffusion properties of glassy and rubbery polymers. Unlike liquid-like rubbers, glassy polymer chains do not have rapid and large scale segmental motions. Due to this restricted chain mobility, glassy polymers have entangled molecular chains with immobile molecular backbones in frozen conformations that are more size and shape selective to gas permeants.

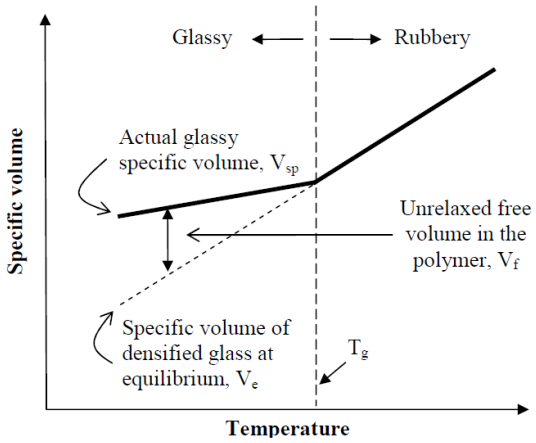

Figure 2.3Plot of the specific volume of polymer as a function of temperature

2.3.2 Effect of pressure on transport parameters of glassy polymers

2.3.2.1 Sorption

Sorption isotherms for glassy polymer are typically nonlinear (concave to the pressure axis) due to the presence of excess free volume in polymer.The dual-mode sorption model, given by Equation2.8, has been widely used to describe sorption in this case [7].

$$C = C_D + C_H = k_D p + \frac{C'_H bp}{1+bp} \tag{2.8}$$

whereC_D is the gas concentration at Henry sites and C_H is the gas concentration at Langmuir sites. k_D refers to the Henry law constant, C'_H is the Langmuir sorption capacity constant and b is a measure of the affinity of gas molecules to the Langmuir sites.

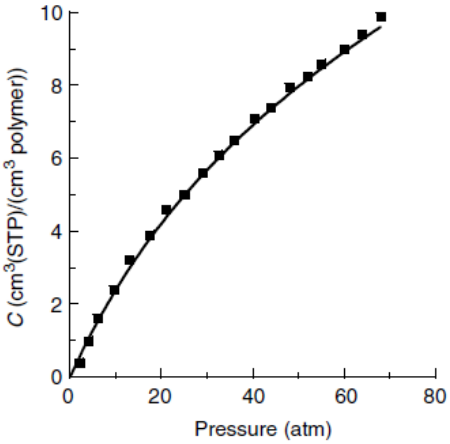

Figure 2.4 A typical sorption isotherm for glassy polymers (Argon in polysulfone at 25 °C [8])

As depicted in the equation, the sorption of gases is postulated to take place in both the Henry and Langmuir sites of the polymer. The Henry's law parameter (k_D) represents gas sorption into the densified equilibrium matrix and Langmuir sorption capacity (C'_H) takes into account sorption into the non-equilibrium excess free volume. Both are in local chemical equilibrium with each other. At low to moderate pressure, gas sorption occurring at the Langmuir sites is dominant over that at the Henry sites. At high pressures, the Langmuir sites become saturated and the gas is added into the higher mobility Henry's law sites. Excessive sorption can lead to swelling of the polymer

matrix, causing the diffusion coefficients to increase tremendously. This is the onset for plasticization. A sigmoidal-shaped sorption isotherm such as the one in Figure 2.5 is seen.

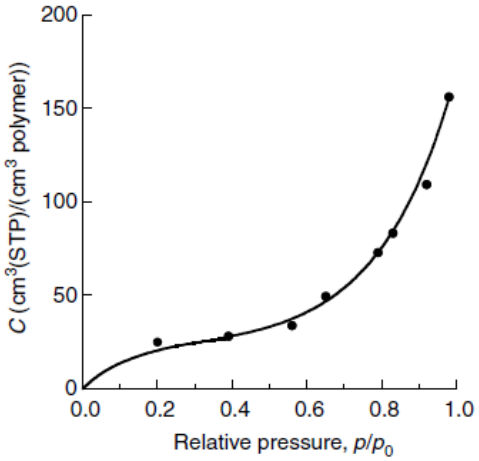

Figure 2.5 Sigmoidal-shaped sorption isotherm in glassy polymers (vinyl chloride monomer in poly(vinyl) chloride [9])

2.3.2.2 Diffusion

Figure 2.6 is characteristic of diffusion coefficients for many penetrants at relatively low concentrations in glassy polymers. The line fits the transport model based on dual-mode concepts.

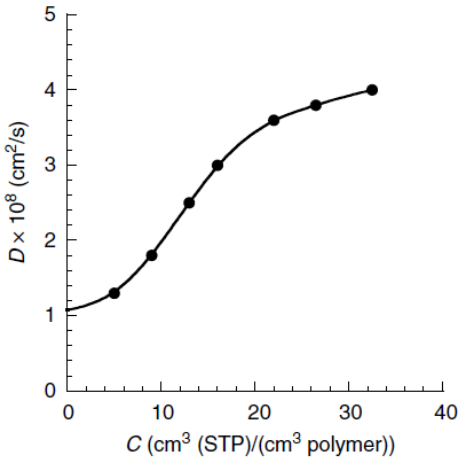

Figure 2.6A typical diffusion coefficient plot in glassy polymers (CO_2 in polycarbonate at 35 °C [10])

2.3.2.3 Permeability

Based on the solution-diffusion model, the sorption and diffusion behavior determine the permeability in polymers. As mentioned previously, the characteristic excess free volume in glassy polymers results the polymer having Henry and Langmuir sites. The sorption and diffusion behavior can be described by the dual-mode concepts. Figure 2.7 shows the permeability plot for glassy polymers. A decrease in gas permeability with increasing pressure is often seen.

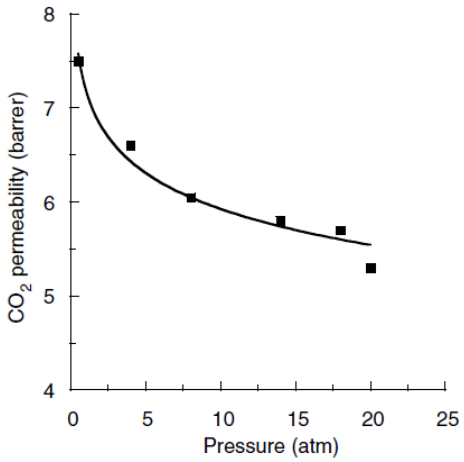

Figure 2.7 Influence of upstream pressure on permeability of glassy polymers (CO_2 in Lexan polycarbonate [11])

However, at higher penetrant concentration, plasticization may occur and it often leads to an increase in permeability as seen in Figure 2.8.

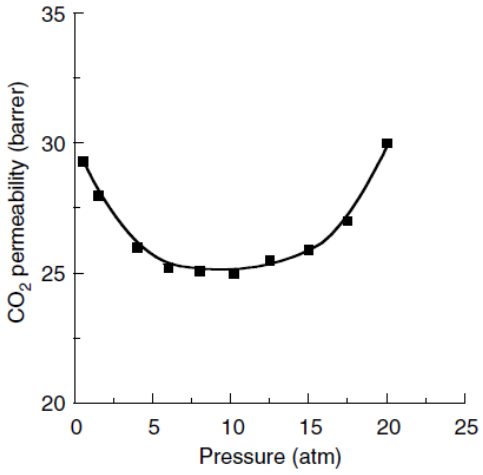

Figure 2.8Plasticization phenomenain glassy polymers (CO_2 in polytetrabromophenolphthalein at 35 °C [12])

2.3.2.4 Selectivity

Gas selectivity is derived from the permeability data. For the separation of light gas mixtures, the mixed-gas selectivity can be expected to be the same as the pure-gas mixture due to similar transport properties. However, in the presence of more condensable component, the mixed-gas and pure-gas selectivity values are often different.

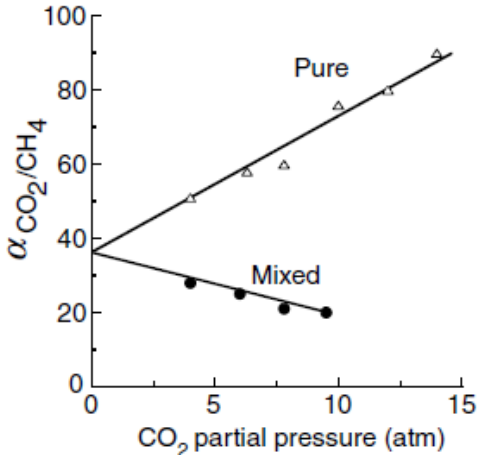

Figure 2.9 Comparison of pure-gas with mixed-gas selectivity of glassy polymers (CO_2/CH_4 in cellulose acetate [13])

The sorption of a more condensable component such as CO_2increases the free volume of the polymers, which in turn causes the increase in the pure-gas selectivity with increasing pressure. As compared, the light gases have lesser effect on free volume. As a result, the selectivity based on pure gas permeation increases with pressure. However, in mixed gas permeation, the selectivity decreases with increasing CO_2 partial pressure. This could be explained by the increased free volume caused by the CO_2 sorption. Diffusivity increases with the increased free volume, causing the diffusivity selectivity of the membrane to decrease and the overall mixed-gas selectivity to decrease. The size-sieving ability of glassy polymers decreases.

2.3.3 Effect of temperature on transport parameters of glassy polymers

The temperature dependence of gas transport can be described by the Arrhenius-van't Hoff equations [14], where E_D and E_P are the activation energies of diffusion and permeation respectively and ΔH_S is the enthalpy of sorption. E_D is always positive. E_D and E_P are typically independent of temperature for transport in glassy polymers. Therefore, permeability increases with temperature.

$$D = D_0 e^{-E_D/RT} \tag{2.9}$$

$$S = S_0 e^{-\Delta H_S/RT} \tag{2.10}$$

$$P = P_0 e^{-E_P/RT} \tag{2.11}$$

2.3.4 Effect of gas and polymer properties on gas transport

The kinetic diameter, as shown in Table 2.2, is one of the widely used scales of penetrant size for gas diffusion [7]. The diffusion coefficient of gas molecules generally decreases with the increase in gas molecule size. The critical temperature, another gas property, is an indicator of its solubility in polymers. The higher the critical temperature, the more condensable it is. As glassy polymers discriminate gas pairs according to their sizes, the larger the difference between the kinetic diameters of the gas pair, the higher the diffusivity selectivity.For penetrants with similar kinetic size, the selectivity of glassy polymer is generally lower.

Table 2.2: Kinetic diameter and critical temperature of gases

Gas	Kinetic diameter (Å)	Critical temperature (K)
H_2	2.89	33.2
O_2	3.46	154.6
N_2	3.64	126.2
CO_2	3.3	304.2
CH_4	3.8	190.6

C_2H_6	-	305.3
C_3H_6	4.5	365.2
C_3H_8	4.3	369.9

Besides the kinetic diameter of the gas molecule, gas diffusion in glassy membranes is also dependent on the free volume and its distribution in polymer, which is related to itschemical structure.The connector groups, bulky side chains, polarity and hydrogen bonding in side chains, para versus meta linkages, cis/trans configuration are some of the structural variations attempted to produce polymers with enhanced gas separation performance. In general, polymer inter-chain spacing and chain mobility influence the permeability while polymer rigidity affects the selectivity. To achieve both high permeability and selectivity, a rigid polymer with high inter-chain spacing and mobility is desirable.

2.3.5 Challengesforpolyimide membranes

Aromatic polyimide, a rigid glassy polymer with exceptional high chemical, thermal and mechanical properties and excellent gas separation properties,is a class of potential materials for fabricating gas separation membranes. Despite the many merits, there are some challenges for this material, which are listed in this section.

2.3.5.1Upper bound relationship

As discussed earlier, the key parameters for gas separation are permeability and selectivity. It is observed that a tradeoff exist between these two. As permeability of the more permeable gas component increases, the selectivity generally decreases and vice versa. Polymers with best combination of permeability and selectivity are generally glassy and have rigid structures with poor chain packing [15].

This trade-off was shown to be related to an empirical upper bound relationship, as shown in Fig. 2.10[17-18]. It can be expressed by Equation 2.12, where P_A is the permeability of the more permeable gas component, α is the selectivity and n is the slope of the log-log upper bound [17].

$$P_A = k\alpha_{A/B}^{n} \qquad (2.12)$$

Compared to the upper bound curve, only a minority of aromatic polyimides falls close or above the trade-off line.

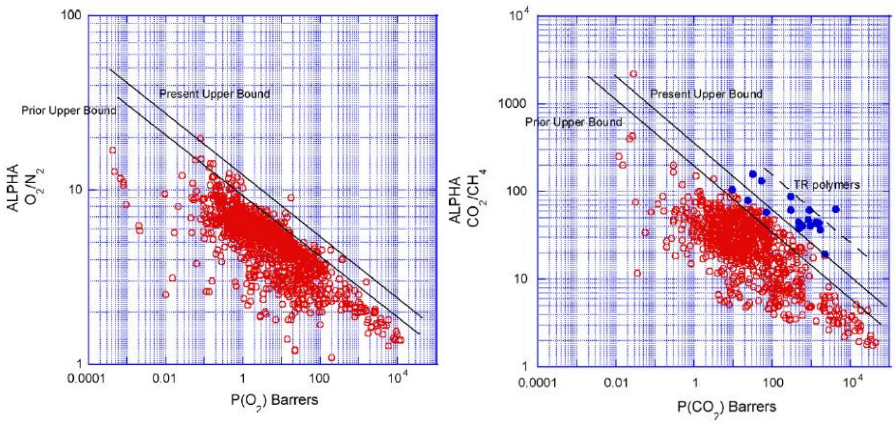

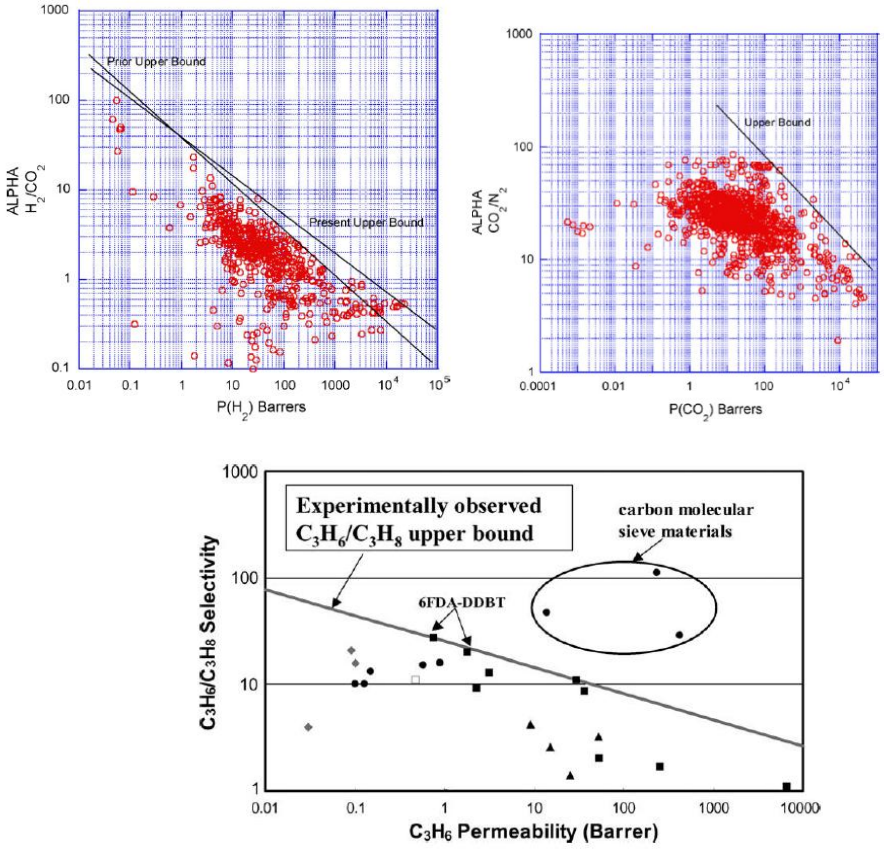

Figure 2.10 Upper bound relationships for different gas pairs

2.3.5.2Plasticization

Plasticization, as mentioned in the previous sections, is the phenomenon where the polymer is swelled by high concentration of highly sorbing component and results in the increase of free volume and polymer chain mobility, which in turn leads to increase in diffusion coefficient and decrease in diffusion selectivity. CO_2 is one of the highly sorbing gases. For polyimides, the permeability of CO_2 increases with pressure until plasticization occurs and the permeability then increases with the increasing pressure. The typical plasticization pressure for polyimides for gas separation lies in the range of 10 – 35 bar. Plasticization can cause decrease in selectivity of membranes under mixed gas conditions in separations such as natural gas purification.

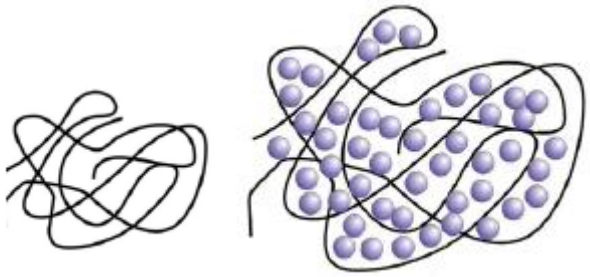

Figure 2.11 Plasticization effect on the polymer chains

Considering the adverse impacts of CO_2-induced plasticization on the performance of polyimide membranes, any effort toward its suppression or even elimination would improve the viability of the membranes.

2.3.5.3 Physical aging

The non-equilibrium nature of glassy polymers results in the tendency for polymer chains to undergo physical aging to attain the equilibrium state. In the process of physical aging, the polymer chains undergo gradual molecular rearrangement, leading to the densification of the polymer matrix and the corresponding reduction in the free volume. Overcoming this problem is a challenge for membrane researchers.

2.3.6 Modification methods

Some approaches undertaken to improve polyimide membranes include molecularly tailoring the structure to obtainbetter materials and modifying existing polyimide materials by heat treatment, grafting side groups on polymer backbone and cross-linking. The implications of the search for better materials and cross-linking treatments are discussed in details in the following section.

2.3.6.1 Search for better materials

Polyimide can be synthesized via atwo-step polycondensation of monomers with dianhydride functional group and monomers with diamine functional group, using poly (amic acid) as the intermediate. High molecular weight is dependent upon the use of high purity monomers, the exclusion of moisture, the choice of solvent and the maintenance of low to moderate reaction temperature [21].

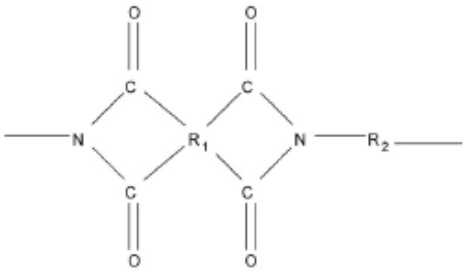

Figure 2.12General structure of polyimide

Numerous dianhydrides and diamines have been derived to molecularly design polyimide to improve the properties of the membranes [22-27]. The spatial linkage configurations, the type of bridging unit and the bulkiness and polarity of pendant groups are found to have an impact on the gas transport properties. Among various polyimides, aromatic polyimides containing 4,4′-(hexafluoroisopropylidene) diphthalic anhydride (6FDA) are of great interest. The bulky CF_3 group in 6FDA reduces chain packing and also increases chain stiffness due to steric hindrance. Hence, 6FDA-based polyimide membranes display good gas permeability and selectivity.

2.3.6.2 Cross-linking treatments

Cross-linking can be obtained by radiation (ultraviolet, ion beam etc), thermal treatment and chemical treatment [27]. UV irradiation of the polyimide containing benzophenone moiety brought cross-linking between the polymer chains, resulting a significant enhancement in gas selectivity at the expense of permeability [28]. Through exposure to ion beam irradiation, there were simultaneous increments of permeability and selectivity in Matrimid membranes. However, the ion beam led to degradation of the polymer backbone [29-30].

Extensive research efforts have also been focused on modifying the polymer properties via thermal treatment. Thermal treatment of polyimides such as Matrimid and 6FDA-based polymers at elevated temperatures for short periods of time has shown increased resistance to plasticization compared to untreated membranes [31-37]. In a study by Barsema et al., they observed structure densification of Matrimid when annealing it below the glass transition temperature (T_g), forming a charge transfer complex at above T_g and transiting it to a carbon membrane at a higher annealing temperature [32]. Decarboxylation occurred at 15 °C above $T_g$for the 6FDA-based polymer containing cross-linkable carboxylic acid, generating phenyl radicals to form linkages and a more open matrix [33-34]. Thermal treatment of 6FDA-based polymers grafted with thermally labile units such as cyclodextrin and saccharrides not only induced thermal cross-linking, but also led to the decomposition of thermally labile units to form microvoids, resulting simultaneous enhancements in permeability, selectivity and the integrity of the polymer backbone [35-37]. There are varying results obtained for cross-linking polyimides via thermal treatment. However, thermal treatment at elevated temperatures incurs a higher cost for membrane fabrication. It may also compromise the mechanical strength of the resultant membranes.

Chemical cross-linking is another commonly employed method. Hayes found that diamino cross-linked polyimide membranes at ambient temperature with an increased O_2/N_2 selectivity [38-39]. Chung and his co-workers further explored the use of different diamines and multi-arm amines with various

immersion times as cross-linkers to post-treat polyimide flat sheet and hollow fiber membranes [40-49]. The modified membranes showed an enhanced CO_2/CH_4 selectivity and plasticization resistance but the permeability decreased [40]. Drawbacks of this method include methanol swelling, reversibility of amidation reaction at high temperatures and considerable time to dry the membranes [48-50]. Vapor-phase cross-linking was devised as an alternative to solution-phase cross-linking of polyimides. Another chemical cross-linking method is to synthesize the polyimide containing carboxylic acid that can be cross-linked by diols [51-52]. Coupled with thermal treatment, the transesterification reaction occurred and brought forth cross-linking reaction with the removal of pendant diol groups. As a result, it improves plasticization resistance and increases permeability.

From the above research findings, the preferred cross-linking method would be one that (1) causes a minimum loss in membrane permeability, (2) occurs at low temperatures, (3) integrity of polymer backbone is kept and (4) resistance to plasticization

2.4 Gas transport in rubbery polymers

Rubbery polymers are solution-selective. The separation of gases through rubbery membranes is dependent on the affinity between the gas penetrants and the polymer matrix.

2.4.1 Effect of pressure on transport parameters of rubbery polymers

2.4.1.1 Sorption

The sorption and diffusion properties differ in rubbery polymers. The sorption of gases in rubbery polymers is similar to that in low molecular liquid. Gas concentration (C) often obeys the Henry's law,

$$C = k_D p \tag{2.13}$$

wherek_D is the Henry constant and p is the pressure of the gas. The concentration of light gases absorbed increases with increasing pressure. Theoretically, the sorption coefficient in this case is a constant ($S = \frac{C}{p} = k_D$).

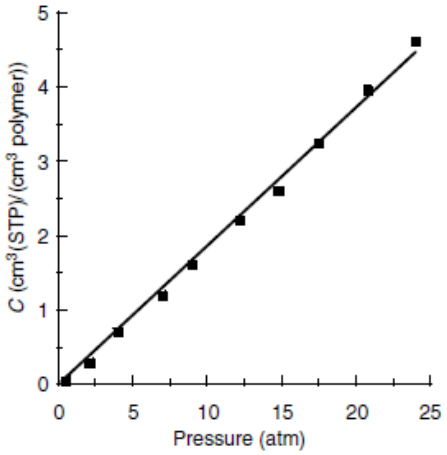

Figure 2.13Atypical sorption isotherm based on Henry's law (O_2 in PDMS at 35 °C [53])

For high sorbing gases such as carbon dioxide, the penetrant concentration may deviate from Henry's law at high pressure. The Flory-Huggins model is often applied for describing the sorption under these circumstances [7].

$$\ln a = \ln\left(p/p_{sat}\right) = \ln\phi_v + \left(1-\phi_v\right) + \chi\left(1-\phi_v\right)^2 \tag{2.14}$$

where$a$ is the activity of the gas, p is the pressure of the gas and $p_{sat}$is the saturated vapor pressure at the experiment condition.

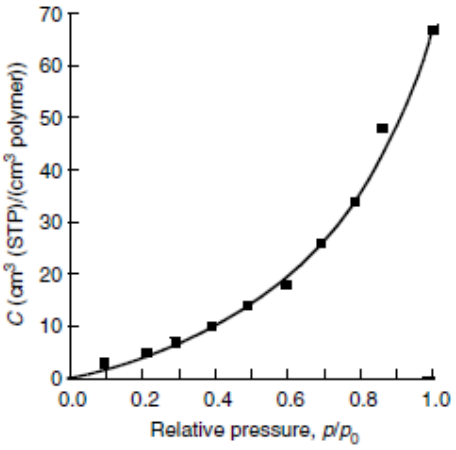

Figure 2.14 Sorption isotherm based on Flory-Huggins model (acetone in PDMS at 28 °C [54])

The isotherm, as shown as above, is convex to the pressure axis. χ is the Flory-Huggins interaction parameter and is correlated to solubility parameter as follows,

$$\chi = \beta + \frac{V_2(\delta_1 - \delta_2)^2}{RT} \tag{2.15}$$

whereβ is a constant, $V_2$is the partial molar volume of the gas in the polymer, δ_1 and δ_2 are the solubility parameter of the polymer and the gas respectively, R is the ideal gas constant and T is the absolute temperature.

The obtained volume fraction of the amount of gas dissolved in the polymer (ϕ_v) is related to the partial molar volume of the gas in the polymer (V_2) and the concentration of the gas dissolved (C). Hence, the solubility of the gas in the membrane can be determined.

$$\phi_v = \frac{(C/22414)V_2}{1+(C/22414)V_2} \tag{2.16}$$

2.4.1.2 Diffusion

As shown in Figure 2.15, the diffusion coefficients for low-sorbing gases are usually independent of gas concentration in the polymer.

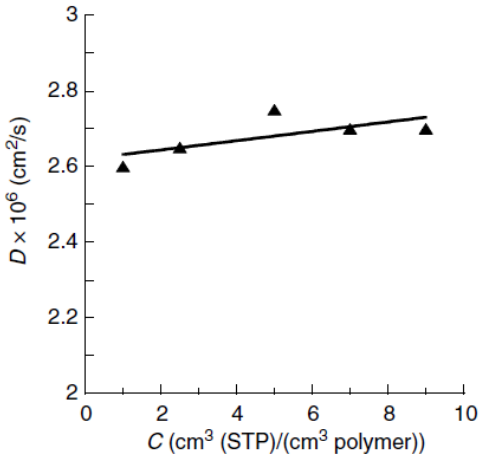

Figure 2.15 Independence of diffusion coefficient on concentration for low-sorbing gases in rubbery polymers (O_2 in Telfon AF1600[55])

Plasticization due to sorption of condensable gases results in a linear or even exponential increase in diffusion coefficients. The increased sorption of condensable gases in the polymer causes increase in the free volume and diffusion coefficient.

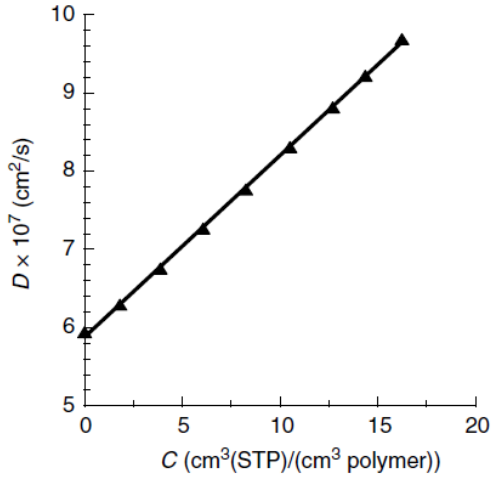

Figure 2.16 Dependence of diffusion coefficient on concentration for condensable gases in rubbery polymers (CO_2 in crosslinked poly(ethylene glycol diacrylate) at 35 °C [56])

2.4.1.3 Permeability

The permeability of low-sorbing gases in rubbery polymers exhibits little or no change with increasing pressure. Plasticization by condensable gases causes the permeability to increase with pressure as the sorption follows the Flory-Huggins model.

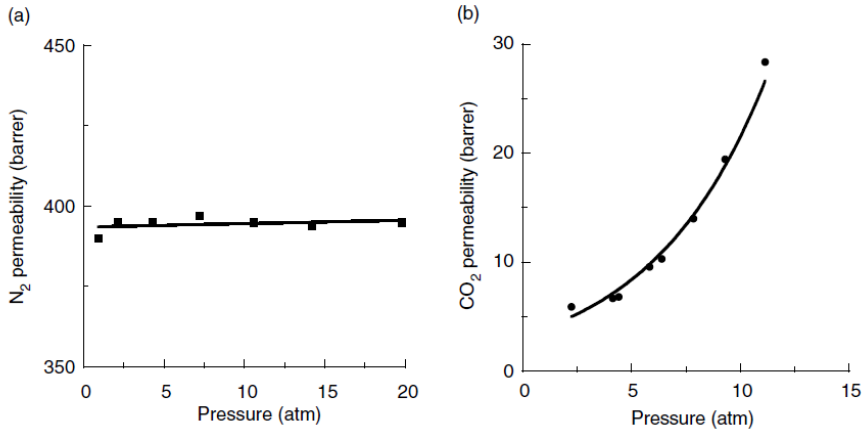

Figure 2.17 Influence of upstream pressure on permeability coefficients of rubbery polymers (a) low-sorbing gases (N_2 in PDMS at 35 °C [54]); (b) plasticization (crosslinked poly (ethylene glycol diacrylate) at -20 °C[57])

2.4.1.4 Selectivity

For the separation of light gases, the pure-gas and mixed-gas selectivities for rubbery polymers can be equivalent or nearly so, which is similar to that for glassy polymers. The light gases penetrate the polymer matrix as if they were the only penetrant in the polymer. They do not have influence on each other. When the mixture contain a more condensable component, the mixed-gas selectivity may differ from the pure-gas selectivity.

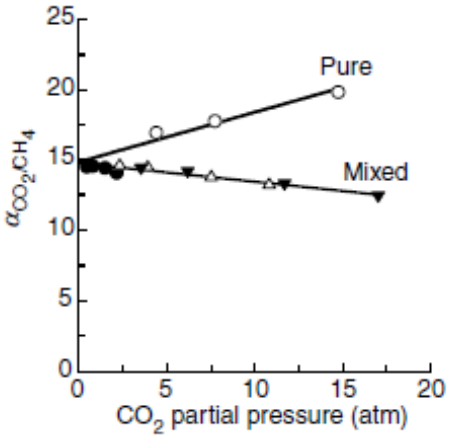

Figure 2.18 Comparison of pure-gas and mixed-gas selectivity for rubbery polymers [58]

2.4.2 Limitations and modification methods for poly(ethylene oxide)

Poly(ethylene oxide) (PEO), a semi-crystalline polymer, has gained interests as a feasible rubbery material to fabricate carbon dioxide-selective membranes for carbon dioxide/hydrogen (CO_2/H_2) and carbon dioxide/nitrogen (CO_2/N_2) separations. Its strong affinity to carbon dioxide due to the polar ether groups present allows preferential removal of carbon dioxide. However, its shortcomings such as tendency to crystallize due to its semi-crystalline nature and weak mechanical strength have restricted its applications [59].

Incorporating PEO with other monomers as copolymers or as polymer blends or crosslinking it are some of the strategies done to overcome the drawbacks of PEO and improve the gas separation performance. Okamoto and co-workers fabricated PEO-segmented copolymers with various hard segments [60]. Peinemann's group blended different low molecular weights of poly(ethylene glycol) (PEG) with synthesized PEO-PBT (Poly(butylene terephthalate) and commercial Pebax® respectively [61-62]. Enhancement in the gas separation performance of the membranes was observed. CO_2 permeability increased by eight-fold to more than 850 Barrer for the Pebax membrane blended with 50 wt% of PEG-dimethyl ether. The CO_2/N_2 selectivity was 31. Reijerkerk et al. also attempted to blend an additive, PDMS (poly(dimethyl siloxane))-PEG, into Pebax with the aim to enhance the membraneperformance with the aid of highly permeable and flexible PDMS and highly selective PEO [63]. CO_2 permeability was improved by five times to 530 Barrer at 50 wt% of PDMS-PEG. The increase in permeability was mainly ascribed to the increase in diffusivity due to the incorporation of PDMS. Freeman's group applied ultraviolet light to crosslink different ratios of PEG diacrylate (PEGDA) and PEG methyl ethyl acrylate (PEGMEA) [64]. The resultant structure had a hyperbranched network in which crystallisation of PEO was restricted. Siloxane-based monomers were incorporated with PEO acrylates with the intention to increase permeability [65-66]. The CO_2 permeability was enhanced while the selectivity decreased. Shao and Chung also explored the addition of silane as acrosslinking agent to form PEO-based membranes. This strategy hindered the formation of crystals which in turn

increased the permeability of PEO [67]. Further studies by grafting PEG methacrylate (PEGMA) and blending PEG into the polymer matrix had improved the performance of the membranes significantly by 5 folds and 2.5 folds, respectively [68-69]. Thus, combining with highly permeable groups and fabricating it as an organic-inorganic hybrid network seems to be a promising strategy to enhance the inherent properties of CO_2-selective PEO.

References:

[1] W. J. Moore, Physical Chemistry, Longmans Green, New York (1958).

[2] J. G. Wijmans, R. W. Baker, The solution-diffusion model: a review, J. Membr. Sci. 107 (1995) 1-21.

[3] W. J. Koros, G. K. Fleming, S. M. Jordan, T. H. Kim, H. H. Hoehn, Polymeric membrane materials for solution-diffusion based permeation separations, Prog. Polym. Sci. 13 (1988) 339-401.

[4] L. Shao, T. S. Chung, In situ fabrication of cross-linked PEO/silica reverse-selective membranes for hydrogen purification, Int. J. Hydr. Energy 34 (2009) 6492-6504.

[5] B. Kraftschik, W. J. Koros, Cross-linkable polyimide membranes for improved plasticization resistance and permselectivity in sour gas separations, Macromolecules 46 (2013) 6908–6921.

[6] A. Bondi, van der Waals volumes and radii, J. Phys. Chem. 68 (1964) 441-451.

[7] Y. Yampolskii, I. Pinnau, B. D. Freeman, Materials science of membranes for gas and vapor separation, John Wiley & Sons Ltd (2006).

[8] V. Bondar, Y. Kamiya, Y. P. Yampolskii, On pressure dependence of the parameters of the dual-mode sorption model, J. Polym. Sci. Part B: Polym. Phys. 34 (1996) 369–378.

[9] A. R. Berens, The solubility of vinyl chloride in poly(vinyl chloride), Die Angewandte Makromolekulare Chemie 47 (1975) 97–110.

[10] W. J. Koros, D. R. Paul, A. A. Rocha, Carbon dioxide sorption and transport in polycarbonate, J. Polym. Sci. Part B: Polym. Phys. 14 (1976) 687–702.

[11] V. T. Stannett, The transport of gases in synthetic polymer membranes – a historic perspective, J. Membr. Sci. 3 (1978) 97–115.

[12] R. T. Chern, C. N. Provan, Gas-induced plasticization and the permselectivity of poly(tetrabromophenolphthalein) to a mixture of carbon dioxide and methane, Macromolecules 24 (1991) 2203–2207.

[13] S. Y. Lee, B. S. Minhas, M. D. Donohue, Effect of gas composition and pressure on permeation through cellulose acetate membranes, AIChE Symposium Series 84 (1988) 93–101.

[14] K. Ghosal, B. D. Freeman, Gas separation using polymer membranes: An overview, Polym. Adv. Technol. 5 (1994) 673–697.

[16] D. F. Sanders, Z. P. Smith, R. Guo, L. M. Robeson, J. E. McGrath, D. R. Paul, B. D. Freeman, Energy-efficient polymeric gas separation membranes for a sustainable future: A review, Polymer 54 (2013) 4729-4761.

[17] L. M. Robeson, The upper bound revisited, J. Membr. Sci. 320 (2008) 390-400.

[18] B. D. Freeman, Basis of permeability/selectivity tradeoff relations in polymeric gas separation membranes', Macromolecules 32 (1999) 375–380.

[19] R. L. Burns, W. J. Koros, Defining the challenges for C_3H_6/C_3H_8 separation using polymeric membranes, J. Membr. Sci. 211 (2003) 299-309.

[20] H. Ohya, V. V. Kudryavtsev, S. I. Semenova, Polyimide membranes: applications, fabrications and properties, Kodansha Japan and Gordon and Breach Science Publishers, 1996.

[21] C. E. Sroog, Polyimides, J. Polym. Sci.: Macromol. Rev. 11 (1976) 161-208.

[22] Y. Álvarez-Gallego, S. P. Nunes, A. E. Lozano, J. G. de la Campa, J. de Abajo, Synthesis and properties of novel polyimides bearing sulfonated benzimidazole pendant groups, Macromol. Rapid Commun. 28 (2007) 611–622.

[23] D. Ayala, A. E. Lozano, J. de Abajo, C. García-Perez, J. G. de la Campa, K. V. Peinemann, B. D. Freeman, R. Prabhakar, Gas separation properties of aromatic polyimides, J. Membr. Sci. 215 (2003) 61–73.

[24] S. X. Cheng, T. S. Chung, R. Wang, R. H. Vora, Gas-sorption properties of 6FDA-durene/1,4-phenylenediamine (pPDA) and 6FDA-durene/1,3-phenylene- diamine (mPDA) copolyimdes, J. Appl. Polym. Sci. 90 (2003) 2187–2193.

[25] M. R. Coleman, W. J. Koros, Isomeric polyimides based on fluorinated dianhydrides and diamines for gas separation applications, J. Membr. Sci. 50 (1990) 285–297.

[26] S. A. Stern, Y. Mi, H. Yamamoto, Structure/permeability relationships of polyimide membranes applications to the separation of gas mixtures, J.Polym. Sci. Part B: Polym. Phys. 27 (1989) 1887–1909.

[27] Y. Xiao, B. T. Low, S. S. Hosseini, T. S. Chung, D. R. Paul, The strategies of molecular architecture and modification of polyimide-based membranes for CO_2 removal from natural gas – A review, Prog. Polym. Sci. 34 (2009) 561-580.

[28] H. Kita, T. Inada, K. Tanaka, K. I. Okamoto, Effect of photocrosslinking on permeability and permselectivity of gases through benzophenone-containing polyimide, J. Membr. Sci. 87 (1994) 139-147.

[29] J. Won, M. H. Kim, Y. S. Kang, H. C. Park, U. Y. Kim, S. C. Choi, S. K. Koh, Surface modification of polyimide and polysulfone membranes by ion beam for gas separation, J. Appl. Polym. Sci. 75 (2000) 1554–60.

[30] L. Hu, X. Xu, M. R. Coleman, Effect of H+ and N+ irradiation on structure and permeability of the polyimide Matrimid, Sep. Sci. Tech. 43 (2008) 4030-4055.

[31] A. Bos, I. G. M. Pünt, M. Wessling, H. Strathmann, Plasticization-resistant glassy polyimide membranes for CO2/CH4 separations, Sep. Purif. Tech. 14 (1998) 27-39.

[32] J. N. Barsema, S. D. Klijnstra, J. H. Balster, N.F.A. van der Vegt, G. H. Koops, M. Wessling, Intermediate polymer to carbon membranes based on Matrimid PI, J. Membr. Sci. 238 (2004) 93-102.

[33] A. M. Kratochvil, W. J. Koros, Decarboxylation-induced cross-linking of a polyimide for enhanced CO2 plasticization resistance, Macromolecules 41 (2008) 7920-7927.

[34] W. Qiu, C.-C. Chen, L. Xu, L. Cui, D. R. Paul, W. J. Koros, Sub-Tg cross-linking of a polyimide membrane for enhanced CO2 plasticization resistance for natural gas separation, Macromolecules 44 (2011) 6046-6056.

[35] Y. C. Xiao, T. S. Chung, Grafting thermally labile molecules on cross-linkable polyimide to design membrane materials for natural gas purification and CO2 capture, Energy & Environ. Sci. 4 (2011) 201-208.

[36] M. Askari, Y. C. Xiao, T. S. Chung, Natural gas purification and olefin/paraffin separation using cross-linkable 6FDA-Durene/DABA co-polyimides grafted with α, β and γ-cyclodextrin, J. Membr. Sci. 390-391 (2012) 141-151.

[37] M. L. Chua, Y. C. Xiao, T. S. Chung, Effects of thermally labile saccharide units on the gas separation performance of highly permeable polyimide membranes, J. Membr. Sci. 415-416 (2012) 375-382.
[38] R. A. Hayes, Polyimide gas separation membranes, E. I. Du Pont de Nemours and Company, US patent 4,717,393 (5 January 1988).
[39] R. A. Hayes, Amine-modified polyimide membranes, E. I. Du Pont de Nemours and Company, US patent 4,981,497 (1 January 1991).
[40] Y. Liu, R. Wang, T. S. Chung, Chemical cross-linking modification of polyimide membranes for gas separation, J. Membr. Sci. 189 (2001) 231–239.
[41] C. Cao, T. S. Chung, Y. Liu, R. Wang, K. P. Pramoda, Chemical cross-linking modification of 6FDA-2,6-DAT hollow fiber membranes for natural gas separation, J. Membr. Sci. 216 (2003) 257–68.
[42] P. S. Tin, T. S. Chung, R. Wang, Y. Liu, S. L. Liu, K. P. Pramoda, Effects of crosslinking modification on gas separation performance of Matrimid membranes, J. Membr. Sci. 225 (2003) 77–90.
[43] L. Shao, T. S. Chung, S. H. Goh, K. P. Pramoda, Polyimide modification by a linear aliphatic diamine to enhance transport performance and plasticization resistance, J. Membr. Sci. 256 (2005) 46–56.
[44] Y. C. Xiao, T. S. Chung, M. L. Chng, Surface characterization, modification chemistry and separation performance of polyimide and PAMAM dendrimer composites, Langmuir 20 (2004) 8230–8238.
[45] L. Shao, T. S. Chung, S. H. Goh, K. P. Pramoda, Transport properties of cross-linked polyimide membranes induced by different generations of diaminobutane (DAB) dendrimers, J. Membr. Sci. 238 (2004) 153-163.
[46] B. T. Low, Y. C. Xiao, T. S. Chung, Y. Liu, Simultaneous occurrence of chemical grafting, cross-linking, and their etching on the surface of polyimide membranes and their impact on H_2/CO_2 separation, Macromolecules 41 (2008) 1297-1309.
[47] L. Shao, C. H. Lau, T. S. Chung, A novel strategy for surface modification of polyimide membranes by vapor-phase ethylenediamine (EDA) for hydrogen purification, Int. J. Hydrogen Energy 34 (2009) 8716-8722.
[48] C. H. Lau, B. T. Low, L. Shao, T. S. Chung, A vapor-phase surface modification method to enhance different types of hollow fiber membranes for

industrial scale hydrogen separation, Int. J. Hydrogen Energy 35 (2010) 8970-8982.

[49] H. Wang, D. R. Paul, T. S. Chung, Surface modification of polyimide membranes by diethylenetriamine (DETA) vapor for H_2 purification and moisture effect on gas permeation, J. Membr. Sci. 430 (2013) 223-233.

[50] C. E. Powell, X. J. Duthie, S. E. Kentish, G. G. Qiao, G. W. Stevens, Reversible diamine cross-linking of polyimide membranes, J. Membr. Sci. 291 (2007) 199-209.

[51] C. Staudt-Bickel, W. J. Koros, Improvement of CO_2/CH_4 separation characteristic of polyimides by chemical crosslinking, J. Membr. Sci. 155 (1999) 145–154.

[52] J. D. Wind, C. Staudt-Bickel, D. R. Paul, W. J. Koros, Solid-sate covalent cross-linking of polyimide membranes for carbon dioxide plasticization reduction, Macromolecules 36 (2003) 1882–1888.

[53] T. C. Merkel, V. Bondar, K. Nagai, B. D. Freeman, I. Pinnau, Gas sorption, diffusion, and permeationin poly(dimethylsiloxane), J. Polym. Sci. Part B: Polym. Phys. 38 (2000) 415–434.

[54] A. Singh, B. D. Freeman, I. Pinnau, Pure andmixed gas acetone/nitrogen permeation propertiesof polydimethylsiloxane, J. Polym. Sci. Part B: Polym. Phys. 32 (1998) 289–301.

[55] A. Y. Alentiev, V. P. Shantarovich, T. C. Merkel, V. Bondar, B. D. Freeman and Y. P. Yampolskii,Gas and vapor sorption, permeation, and diffusion in glassy amorphous Teflon AF1600, Macromolecules35 (2002) 9513–9522.

[56] H. Lin, B. D. Freeman, Gas and vapour solubility in crosslinked poly(ethylene glycoldiacrylate), Macromolecules38 (2005) 8394–8407.

[57] H. Lin, E. van Wagner, B. D. Freeman, L. G. Toy, P. Ragubuir, New membrane materials for CO_2/H_2 separation and a model for pure and mixed gas permeability, Science, 311 (2006) 639–642.

[58] H. Lin, E. van Wagner, B. D. Freeman, I. Roman, High performance polymer membranes for natural gas sweetening, Advanced Materials 18 (2006) 39–44.

[59] H. Lin, B. D. Freeman, Materials selection guidelines for membranes that remove CO_2 from gas mixtures, J. Mol. Struct. 739 (2005) 57-74.

[60] M. Yoshino, K. Ito, H. Kita, K. I. Okamoto, Effects of hard segment polymers on CO_2/N_2 gas-separation properties of poly(ethylene oxide)-segmented copolymers, J. Polym. Sci. B: Polym. Phys. 38 (2000) 1707-1715.

[61] W. Yave, A. Car, S. S. Funari, S. P. Nunes, K. V. Peinemann, CO_2-Philic polymer membrane with extremely high separation performance, Macromolecules 43 (2010) 326-333.

[62] W. Yave, A. Car, K. V. Peinemann, Nanostructured membrane material designed for carbon dioxide separation, J. Membr. Sci. 350 (2010) 124-129.

[63] S. R. Reijerkerk, M. H. Knoef, K. Nijimeijer, M. Wessling, Poly(ethylene glycol) and poly(dimethyl siloxane): Combining their advantages into efficient CO_2 gas separation membranes, J. Membr. Sci. 352 (2010) 126-135.

[64] H. Lin, B. D. Freeman, Plasticization-enhanced hydrogen purification using polymeric membranes, Science 311 (2006) 639-642.

[65] V. A. Kusuma, G. Gunawan, Z. P. Smith, B. D. Freeman, Gas permeability of cross-linked poly(ethylene-oxide) based on poly(ethylene glycol) dimethacrylate and a miscible siloxane co-monomer, Polymer 51 (2010) 5734-5743.

[66] V. A. Kusuma, B. D. Freeman, S. L. Smith, A. L. Heilman, D. S. Kalika, Influence of TRIS- based co-monomer on structure and gas transport properties of cross-linked poly(ethylene oxide), J. Membr. Sci. 359 (2010) 25-36.

[67] L. Shao, T. S. Chung, In situ fabrication of cross-linked PEO/silica reverse-selective membranes for hydrogen purification, Int. J. Hydrogen Energy 34 (2009) 6492-6504.

[68] C. H. Lau, S. L. Liu, D. R. Paul, J. Z. Xia, Y. C. Jean, H. Chen, L. Shao, T. S. Chung, Silica nanohybrid membranes with high CO_2 affinity for green hydrogen purification, Adv. Energy Mat. 1 (2011) 634-642.

[69] J. Z. Xia, S. L. Liu, C. H. Lau, T. S. Chung, Liquid-likepoly(ethylene glycol) supported in the organic-inorganic matrix for CO_2 removal, Macromolecules 44 (2011) 5268-5280.

Chapter 3: Research methodology

3.1 Materials

The polyimide used in this study was constituted of three monomers; namely, 4,4′-(hexafluoroisopropylidene) diphthalic anhydride (6FDA), 2,3,5,6-tetramethyl-1,4-phenylenediamine (durene diamine) and 3,5-diaminobenzoic acid (DABA). 6FDA was purchased from Clariant (99% purity), durene diamine from Sigma-Aldrich (99% purity) and DABA from Merck (99% purity). To achieve high molecular weights for polymer syntheses, 6FDA and DABA were further purified via sublimation and durene diamine was further purified by recrystallization from methanol. The solvents used were analytical grade N-methylpyrrolidone (NMP) (Merck) and technical grade methanol (Aik Moh Paints& Chemicals). NMP was used for polymer syntheses and membrane fabrication. It was purified via vacuum distillation at 70 °C. Methanol was used as received for polymer washing. Acetic anhydride (dehydrating agent) and triethylamine (aprotic organic base) of reagent grade for polymer syntheses were attained from Sigma Aldrich.

Figure 3.1 Structure of the monomers and the polyimide

Glucose, sucrose and raffinose, which were used in the first study, were also of reagent grade and were dried and kept in a dry box to minimize contact with moisture.

Glucose (S1) Sucrose (S2) Raffinose (S3)

Figure 3.2 Structure of glucose, sucrose and raffinose

For the second study, β-CD of reagent grade was purchased from Cyclolab. It was dried in vacuum before use. Ferrocene of 98% purity was acquired from Sigma Aldrich and used as received.The chemical structures of β-CD, ferrocene and the resultant inclusion complex are illustrated in Figure 3.3. The hollow, toroidal and truncated cone is β-CD.

β-CD β-CD-Ferrocene

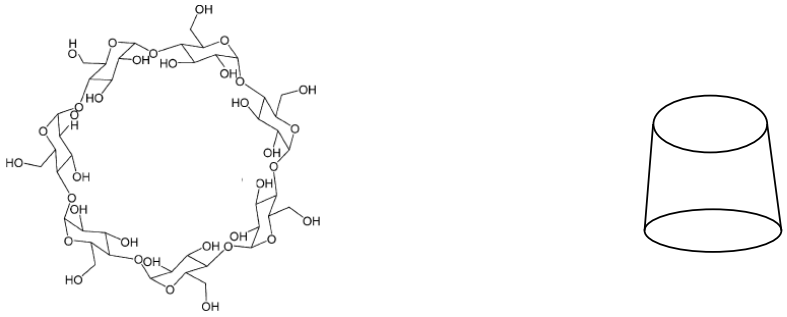

Figure 3.3Structure of β-CD andβ-CD-Ferrocene

In the third study, the reagents namely iron (III) acetylacetonate (97% purity), silver acetylacetonate (98% purity), zinc acetylacetonate, iron (III) chloride (99% purity) and acetylacetonate (99% purity) were purchased from Sigma Aldrich and were used as received.

Figure 3.4Structure of iron (III) acetylacetonate

The starting materials for the fabrication of membranes based on polyetheramine (PEA) and polyhedral oligomeric silsequioxane (POSS) are

poly(propylene glycol)-block-poly(ethylene glycol)-block-poly(propylene glycol) bis(2-aminopropyl ether) (PEA) with M_n 2000 g/mole (approximately 85 wt% of PEO) and glycidyl polyhedral oligomeric silsesquioxane (POSS®).Poly(propylene glycol)-block-poly(ethylene glycol)-block-poly(propylene glycol) bis(2-aminopropyl ether)was purchased from Sigma-Aldrich and was chosen as the source for PEO due to its low cost and widespread availability. It has also high PEO content. The PPG content helps to decrease the crystallinity of the polymer. Glycidyl polyhedral oligomeric silsesquioxane (POSS®) cage mixture, acquired from Hybrid Plastics, Inc, was selected to react with PEA to form epoxy-amine crosslinked organic-inorganic hybrid membranes. Tetrahydrofuran (THF), obtained from Merck, was used as the solvent to dissolve PEA and POSS. All the chemicals were used as received. The respective chemical structure of the starting materials is illustrated in Figure 3.5.

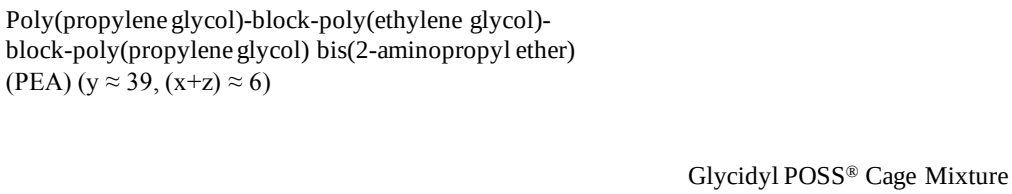

Figure 3.5 Starting materials for PEA-POSS

The gases used for permeation tests are hydrogen (H_2), oxygen (O_2), nitrogen (N_2), methane (CH_4), carbon dioxide (CO_2), ethane (C_2H_6), propylene (C_3H_6) and propane (C_3H_8). They were of at least 99.99% purity.

3.2 Membrane fabrication

For the synthesis of the chosen polyimide, the monomers, durene diamine and DABA, were dissolved in NMP in a predetermined amount and ratio (5:5 or 9:1). The solution was purged with purified N_2 for approximately thirty minutes. 6FDA was then added slowly to make up a total solid weight percent of 20. The solution was stirred at room temperature for 24 h to form a high molecular weight polyamic acid. A mixture of acetic anhydride and triethylamine of ratio 4:1 was added to the solution to induce chemical imidization for 24 h at room temperature. The polyimide solution was then precipitated and washed with methanol and dried in a vacuum oven [1].

For the grafting of glucose, sucrose or raffinose onto the side chains of the polymer, the dried polyimide was first dissolved in NMP to make a solution of 10 wt% solid concentration. Excess thermal labile unit was added to the solution and a small amount of p-toluenesulfonic acid was added to catalyze the esterification reaction. The solution was heated to 120 °C and purged with purified nitrogen gas. The reaction was carried out for 12 h.

The pristine polyimide and grafted polyimide powders were mixed equally in NMP (2 wt%) and filtered with Whatman's filter of pore size 1 μm before casting onto a leveled silicon wafer. The solvent was allowed to evaporate slowly at 70 °C in a vacuum oven. The dried films were peeled off from the wafer and the temperature was then gradually increased to 200 °C and held for 24 h to remove the residual solvent. The membranes were allowed to cool to room temperature naturallyand were stored in a dry box. The thermal annealing process was performed using a Centurion Neytech Qex vacuum furnace. The temperature was increased at a rate of 10 °C/min till the desired temperature and was held constant for 2 h. The membranes were stored in a dry box for further studies. The membrane sample was termed as PI-A-B where A can be S1 (glucose), S2 (sucrose) or S3 (raffinose) and B is the annealing temperature. For example, PI-SI-400 represents the membrane that consists of polyimide and polyimide grafted with glucose, annealed at 400 °C.

Figure 3.6 Structure of the grafted polyimide, where R represents glucose, sucrose or raffinose

For the second study, β-CD, another thermally labile unit,was modified with ferrocene to form inclusion complex. A typical process to obtain inclusion complexes from water soluble compounds is by co-crystallization of the compounds from an aqueous solution. As ferrocene is insoluble in water, this method could not be employed. In this study, the β-CD-ferrocene inclusion compound (fBCD) was prepared by directly adding ferrocene into a saturated aqueous solution of β-CD with a molar ratio of 4:1 and stirred at 60 °C for 1 day [2]. The product was washed thoroughly with water and tetrahydrofuran, and then dried in a vacuum oven.

Similar to the previous study, grafting β-CD and β-CD-Ferrocene onto the polyimide chains was performed by adding excess β-CD and β-CD-Ferrocene into a 10 wt% polyimide/NMP solution. The esterification reaction was carried out at 120 °C for 12 hours with a small amount of p-toluenesulfonic acid and with nitrogen purging. The solution was precipitated to obtain the grafted polymer. The product was washed with methanol and dried in a vacuum oven. The polyimide (PI) grafted with β-CD was termed as PIBCD while the one grafted with β-CD-Ferrocene was named as PIfBCD.

The polyimide and the grafted polymer were dissolved in the same ratio in NMP to constitute a 2 wt % solution. The solution was filtered with a Whatman's filter of pore size 1 μm and then casted onto a silicon wafer. The solvent was allowed to evaporate slowly in a vacuum oven, set at 70 °C. After the films were dried, they were peeled off from the wafer and the temperature of the vacuum oven was increased gradually to 200 °C to remove the residual solvent in the films. The membranes were annealed at 200 °C for 24 hours.

After that, they were cooled down naturally to room temperature and stored in a dry box.

Further annealing of the membranes was carried out in a Centurion Neytech Qex vacuum furnace. The temperature was raised at a rate of 10 °C/min and held at 400 °C for 2 hours. The annealed membranes were cooled down naturally and kept in the dry box. The PI membranes dried at 200 °C in vacuum and annealed at 400 °C in vacuum and air were termed as PI-200, PI-400 and PI-A400, respectively. Likewise, the PIBCD and PIfBCD membranes annealed at 400 °C in air were termed as PIBCD-A400 and PIfBCD-A400, respectively. The choice of annealing at 400 °C will be discussed later.

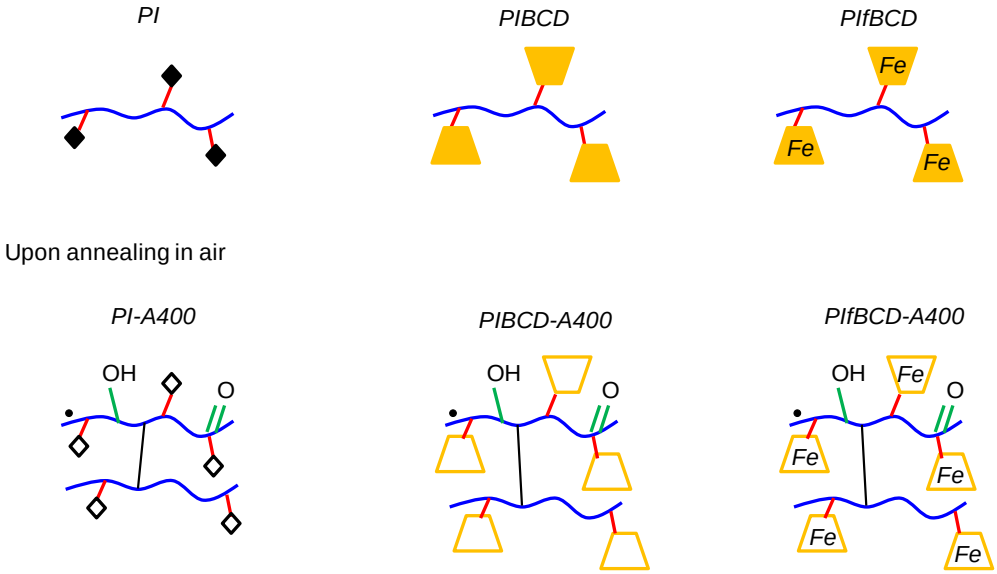

Figure 3.7 Proposed annealing mechanism for PI grafted with β-CD and β-CD-ferrocene

For the third study, a pre-determined amount of the metal additive was dissolved in a 2 wt% polyimide solution in NMP for solution casting. Each solution was filtered by a Whatman's filter with a pore size of 1 μm and then poured onto a silicon wafer in a vacuum oven. The solvent was evaporated slowly at 70 °C. After the films were dried, they were peeled off from the wafer and annealed in a Centurion Neytech Qex vacuum furnace at 10 °C/min and held at 200 °C for 30 minutes. They were then cooled down naturally and stored in a dry box. The pristine polyimide membrane was termed as PI. The blend membranes were named as PI-MN, where M represents the weight

percentage of additive and N is the additive. For example, PI-2 wt% FeAc refers to the membrane that consists of 2 wt% iron (III) acetylacetonate in the polyimide.

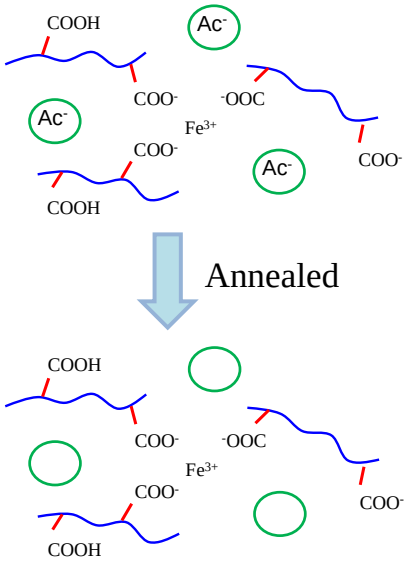

Figure 3.8 Proposed mechanisms for cross-linking of polyimide by iron (III) acetylacetonate

PEA and POSS were dissolved in THF at various compositions to prepare a homogeneous solution for the fabrication of PEA-POSS membranes.The solution containing 2 wt% solid concentration was then heated under reflux at 60°C for 3 hours to initiate the reaction between the epoxy groups in POSS and the amino groups in PEA. After sonicating for 10 minutes to remove the trapped gases, the solution was slowly casted onto a Telfon dish and placed in the oven at 40°C. A glass plate was used to cover the Telfon dish to allow slow evaporation of the solvent. The dried membrane was peeled off and further annealed under vacuum at 120°C for 12 hours. The membrane preparation procedure is depicted in Figure 3.9. All the membrane samples were kept in the dry box after fabrication. The ratio of PEA to POSS is represented by PEA:POSS X:Y in the subsequent figures, where X and Y are the weight ratio of PEA and POSS, respectively.

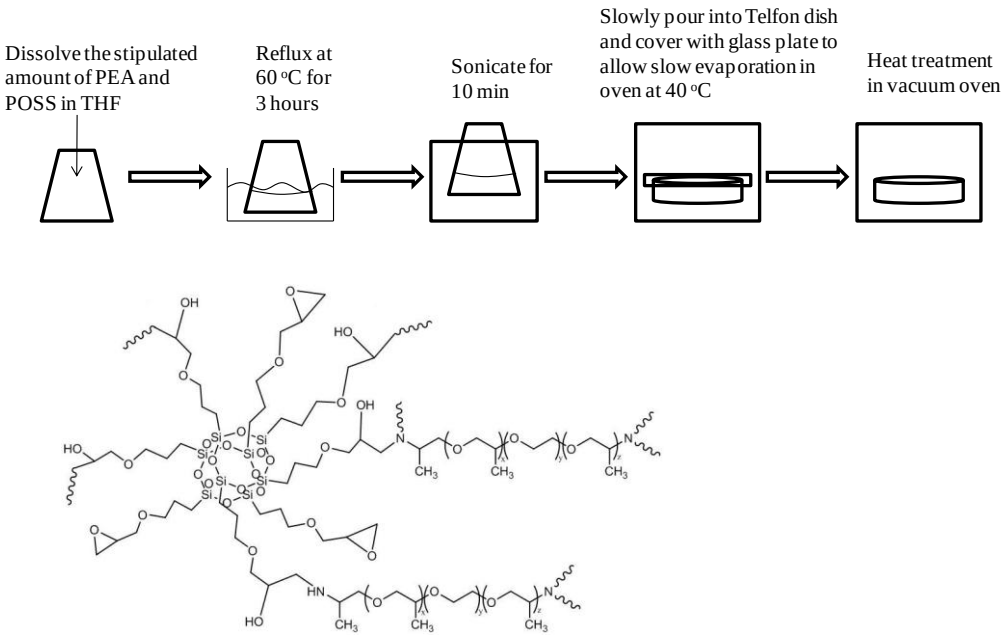

Figure 3.9Fabrication procedure and the resultant polymer network (y ≈ 39, (x+z) ≈ 6)

3.3 Material and membrane characterizations

3.3.1 Inherent viscosity

The inherent viscosity of the pristine polyimide was measured at 25 °C with an Ubbelohde viscometer. The viscometer was filled with the blank NMP till a certain level and placed in the water bath. The flow time was then measured. The polymer solution was prepared with aconcentration of 0.5 g/dL in NMP.The flow time of the polymer was determined in the similar manner.

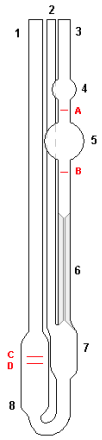

Figure 3.10 A Ubbelohde viscometer

With the flow times, the inherent viscosity (η) was derived, as shown in Equation 3.1.

$$\eta = \frac{\ln \eta_r}{c} = \frac{\ln(t/t_0)}{c} \qquad (3.1)$$

where$\eta_r$is the relative viscosity which the ratio between the polymer flow time (t) and the blank NMP flow time (t_0). $c$is the concentration of the polymer solution.

It is a simple and inexpensive viscometric method for measuring polymer molecular size. The higher the IV is, the higher the polymer molecular weight.

3.3.2 Scanning electron microscope

Scanning electron microscope and electron dispersive X-ray analysis (JEOL JSM-6360LA) were employed to examine the uniformity of the cross-section of the membranes.They were fractured by immersing in liquid nitrogen and breaking between two grips at low temperature. The fractured membrane was mounted onto a stub and coated for SEM observation. Elemental analysis was performed to map the elemental composition in the sample.

Figure 3.11 Scanning electron microscope (JEOL JSM-6360LA)

3.3.3 Fourier transform infrared spectrometry

A Perkin-Elmer Fourier Transform Infrared spectrometer-Attenuated Total Reflection (FTIR-ATR Spectrum 2000) was used to detect the bond vibration of the various groups of atoms in the polymer matrix to confirm the structure of the synthesized polymer. The wavenumber domain obtained ranged from 4000 cm^{-1} to 600 cm^{-1}.FTIR-ATR is a sampling technique that enables samples to be examined directly without further preparation. Themembrane sample to be analyzed was placed on the ATR crystal. A beam of infrared light entered the ATR crystal and went through multiple internal reflections when in contact with the sample surface. The detector collected the beam that exitedfrom the crystal. The spectrum was used to characterize the sample.

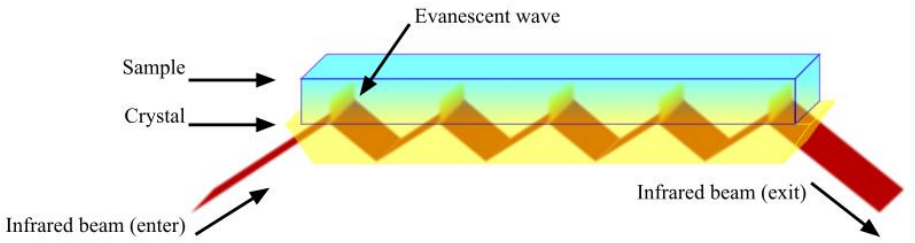

Figure 3.12 Attenuated total reflectance

3.3.4 X-ray photoelectron spectroscopy

X-ray photoelectron spectroscopy (XPS) measurements using Kraton AXIS Ultra^{DLD} were performed to analyze the elemental composition of the membranes. The X-ray source used was monochromatic Al Kα (hν = 1486.71 eV), operated at 5 mA and 15 kV. As shown in Figure 3.13, the X-ray beam hit the membrane sample and the kinetic energy and number of electrons escaped from the surface of the sample was measured.The raw elemental binding energy spectra were deconvoluted by using the XPS peak fitting software.

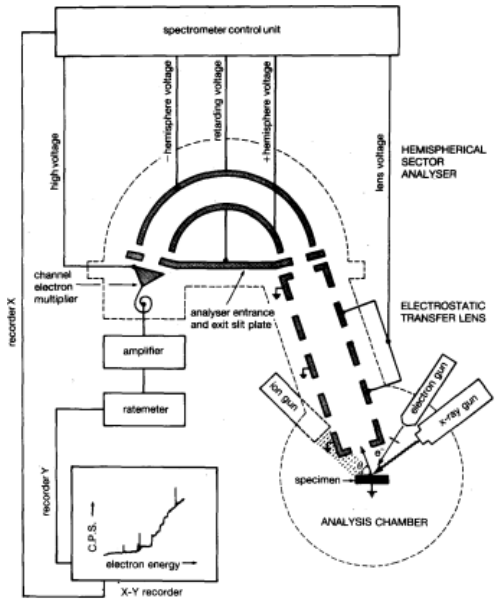

Figure 3.13 X-ray photoelectron spectroscopy

3.3.5 Density

The density of the polyimide membranes in this study, ρ (g/cm^3), was determined by using a Mettler Toledo balance and a density kit. The membrane weight was measured in air (W_{air} (g)) and in hexane (W_{liq} (g)), which is a non-solvent of polyimide. The measurements were then used to compute the density using the following equation, which is based on the Archimedean principle.

$$\rho = \frac{W_{air}}{W_{air} - W_{liq}} \rho_o \qquad (3.2)$$

where ρ_o (g/cm$_3$) is the density of hexane.

Figure 3.14Density kit

The density of the crosslinked PEO network was measured using a gas pycnometer (Quantachrome Ultrapyc 1200e) where helium was used to determine the volume of the samples. More membrane samples were required in this method.

Figure 3.15 Gas pycnometer

3.3.6 X-ray diffraction

The inter-chain spacing (d-spacing) of the membranes were analyzed at room temperature by anX-ray diffractometer (Bruker D8 advanced diffractometer). Ni-filtered Cu K_α rays at the wavelength of λ = 1.54 Å was used as the X-ray source. The X-ray beam hit on the membrane sample and the atomic planes in the membrane caused the X-rays to interfere with one another. The diffraction pattern was recorded.

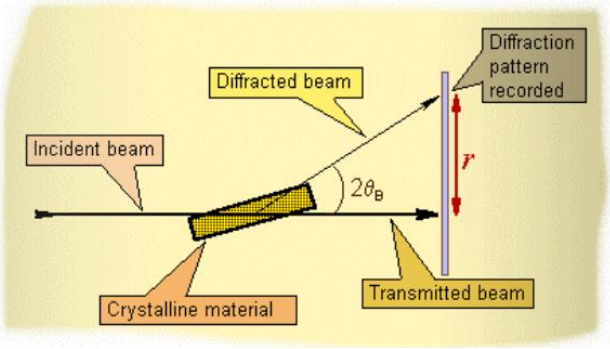

Figure 3.16 X-ray diffraction

The d-spacing of the membranes can be computed using the Bragg's law.

$$n\lambda = 2d\sin\theta \tag{3.3}$$

where*n* is an integer, λ is the wavelength of the X-ray source and θ is the diffraction angle.

3.3.7 Gel content

To examine the cross-linking extent of the membranes fabricated and annealed, the gel content was measured. The membranes were immersed in a selected solvent for 5 days and the insoluble portions were dried in a vacuum oven for 24 hours to remove the residual solvent. The gel content can be calculated using Equation 3.4, where M_1 is the mass of the insoluble portion and M_0 is the original mass of the membrane.

$$Gel\ content\ (\%) = \frac{M_1}{M_0} \times 100\% \tag{3.4}$$

3.3.8 Thermogravimetric analysis

Thermogravimetric analysis (TGA) was employed to analyze the decomposition profiles of the thermal labile units, the pristine polymer, the grafted polymers and the membranes. TGA was performed using either Perkin-Elmer TGA 7 or Shimadzu DTG-60. The sample was placed into the pan. The temperature was ramped at 10 °C/min from 25 °C to 800 °C or ramped at 10 °C/min and held at the desired temperature and duration to mimic the heating conditions in the furnace. Either N_2or air was used as the purging gas and the flow rate was maintained at 100 ml/min. The weight loss with temperature was measured.

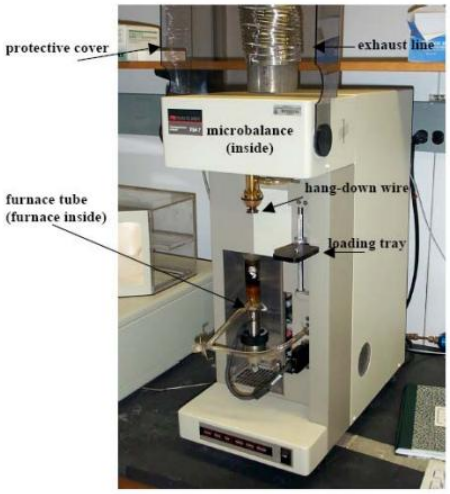

Figure 3.17 Thermogravimetric analyzer

3.3.9 Differential scanning calorimeter

A Differential Scanning Calorimeter (Mettler Toledo DSC822e) was employed to analyze the thermal property of the membranes. It is a thermoanalytical technique in which the difference in the amount of heat required to increase the temperature of a sample and reference is measured as a function of temperature.

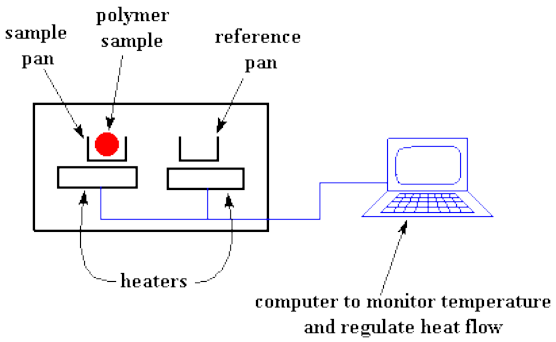

Figure 3.18 Differential scanning calorimetry

The calorimeter was employed to determine the glass transition temperature of polyimide membranes, T_g (°C) under N_2 environment (100 ml/min) at a ramping rate of 10 °C/min from 50 °C to 450 °C. Two cycles of heating and cooling were employed for every sample. The first cycle was to eliminate any thermal history. The second heating curve was used to determine the glass transition temperature.

The PEO-based membranes were tested under N_2 environment (100 ml/min) using the same DSC at temperatures ranging from -100 °C to 100 °C. The ramping rate was set at 10 °C/min. The first cycle of ramping and cooling of the sample was to eliminate any thermal history. The second heating curve was used for further analysis.

3.3.10 Mechanical strength

The mechanical strength of the PEO membranes was tested using a nano-indentor (Agilent Nanoindentor XP), as shown in Figure 3.19. A 5mN load was placed on the indentor tip and held on the surface of the membranes for 30 s. The displacement of the tip was measured and the Young's Modulus and the hardness of the membranes were derived. The entire procedure was repeated for 10 points on the membrane surface to obtain an average value.

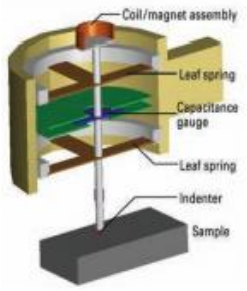

Figure 3.19 Schematic diagram of the mechanism in nanoindentor

3.3.11 Measurements of pure gas permeation

As mentioned previously, the pure gas permeability was measured using a constant volume method. The experimental setup is as shown in Figure 3.20[3].The volumes of the downstream compartments were calculated using standard polycarbonate and its published permeability data. Calibration for the volumes of the permeation cell and the checking of leakage rate were performed regularly. This was to ensure the accuracy of the data obtained.

The thickness and the area of membrane to be tested were measured and the membrane was mounted in the permeation cell. The temperature of the cell was controlled at 35 °C. The cell was kept under vacuum prior testing so as to remove any residue air or gas trapped in the membrane. During gas test, the pure gas was fed to the upstream till the desired pressure and the increase in the permeate pressure was measured. The permeability was determined and the ideal selectivity was the ratio of the pure gas permeabilities.

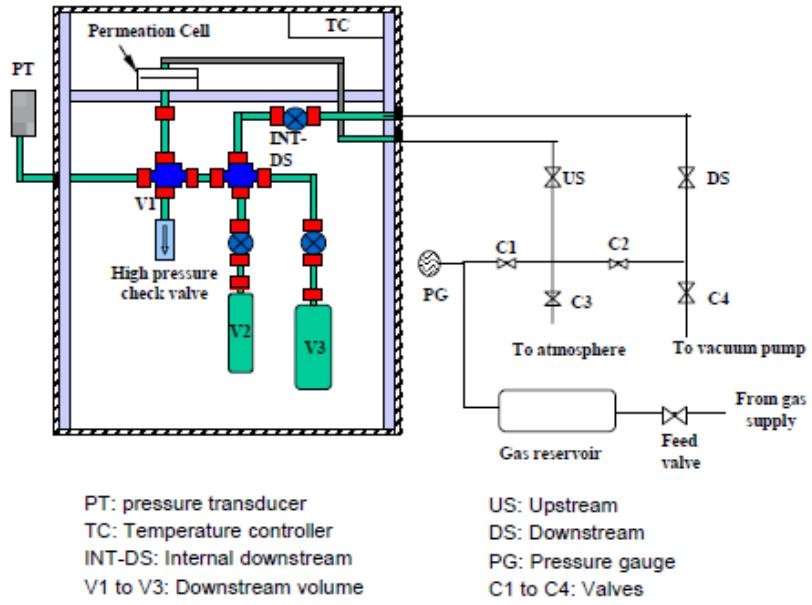

Figure 3.20Experimental setup of a pure gas permeation cell

3.3.12 Binary gas permeation tests

Binary gas tests were performed on the polyimide membranes using a gas mixture of CO_2/CH_4 50:50 (mole %) as the feed at 35 °C and at a CO_2 partial pressure of 2 bar. Binary gas tests using CO_2/H_2 and CO_2/N_2 50:50 mixtures were also performed on the PEA:POSS 50:50 membrane at 35 °C and a CO_2 partial pressure of 1 bar.

To test the mixed gas separation performance of the membranes, slight modifications were made to the pure gas permeation setup. As seen in Figure 3.21, the membrane was tested in a cross-flow configuration [4]. An additional valve was installed at the upstream to adjust the stage cut of the feed gas. The retentate flow rate could be controlled using the valve. At the downstream portion, a valve was added to introduce the accumulated permeate gas to a gas chromatographer (GC) for the analysis of the permeate composition. The GC used in our laboratory is Agilent 7890. During the gas test, the membrane was fed with the feed and the downstream pressure was accumulated and sent to the gas chromatograph to obtain the binary gas selectivity.

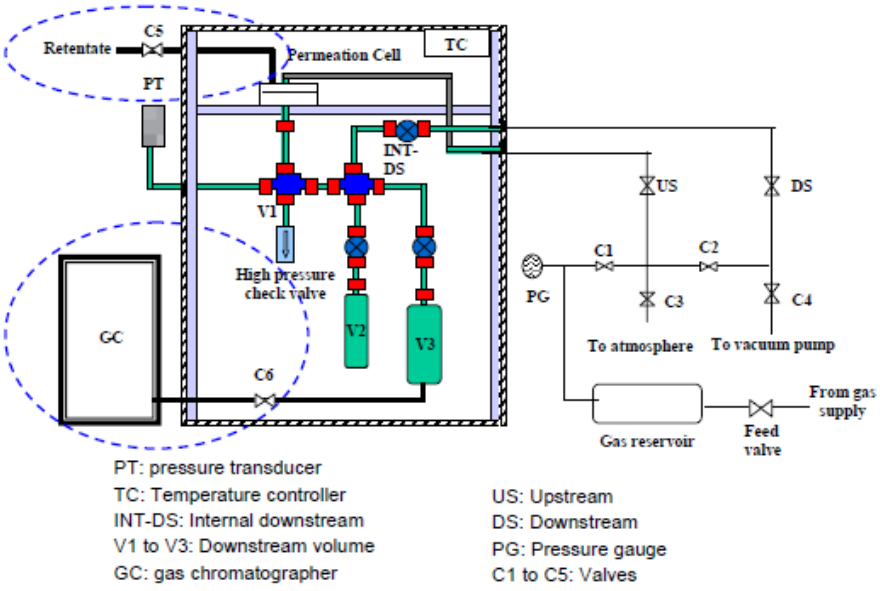

Figure 3.21Experimental setup of a mixed gas permeation cell

The gas chromatographer comprises of a valve switching system, which is connected to a 2-column assembly, an injection port and a vacuum pump. A thermal conductivity detector (TCD) is employed. Helium was used as the carrier gas.The 2-column assembly consists of a HP-PLOTQ column and a molecular sieve 5A column. As the gas permeation testing was performed at sub-atmospheric pressures, the leakage of air into the system was unavoidable. For the analysis of the permeate composition for the permeation of binary CO_2/CH_4 gas pair through the membrane, the PLOTQ column is sufficient to separate CO_2, CH_4 and air. For the analysis for the permeation of binary CO_2/N_2 and CO_2/H_2 gas pairs, the second molecular sieve column is needed in addition to the HP-PLOTQ column. For the CO_2/H_2 gas pair, the PLOTQ column could not separate air from H_2. For the CO_2/N_2 gas pair, the amount of air leakage would need to be determined in order to obtain the accurate nitrogen composition. The molecular sieve column could achieve this.

3.3.13 Gas sorption measurements

The gas solubility of the membranes can be determined experimentally by measuring its gas sorption using a Cahn Microbalance, as shown in Figure 3.22 [5].The sorption cell consists of a sample pan and a reference pan. The

microbalance was first calibrated with each gas as a function of pressure. The sorption of the empty pan was measured.

For the measurement of gas sorption of membranes, a total mass of 70 mg of films was placed on the sample pan. The system was evacuated for 24 h prior to testing and kept at a temperature of 35 °C. The gas was fed at the desired pressure.The gain in the polyimide membrane mass at different gas pressures from 0 to 30 atm at 35 °C was recorded. The gain in the mass of the PEA-POSS membranes at different feed gas pressures from 1 bar to 10 bar at 35 °C was measured. The amount of gas sorbed in the membranes was calculated after correction of buoyancy and the sorption of the empty pan.

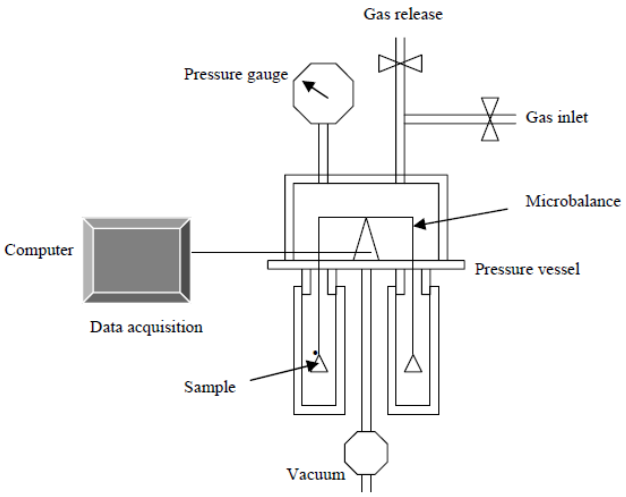

Figure 3.22Experimental setup of a microbalance sorption cell

References:

[1] Y. Liu, R. Wang, T. S. Chung, Chemicalcross-linkingmodification of polyimidemembranesfor gas separation, J. Membr. Sci. 189 (2001) 231–239.

[2] A. Harada, S. Takahashi, Preparation and properties of cyclodextrin inclusion compounds of organometallic complexes: Ferrocene inclusion compounds, J. Incl. Phenom. 2 (1984) 791-798.

[3] J. J. Shieh, T. S. Chung, Gaspermeability,diffusivity,andsolubilityofpoly(4-vinylpyridine) film, J. Polym. Sci. Part B: Polym. Phys. 37 (1999) 2851–2861.

[4] L. Shao, T. S. Chung, S. H. Goh, K. P. Pramoda, Polyimide modification by alinear aliphatic diamine to enhance transport performance and plasticizationresistance, J. Membr. Sci. 256 (2005) 46-56.

[5] S. X. Cheng, T. S. Chung, R. Wang, R. H. Vora, Gas-sorption properties of 6FDA–durene/1,4-phenylenediamine (pPDA) and 6FDA–durene/1,3-phenylene diamine (mPDA) copolyimides, J. Appl. Polym. Sci. 90 (2003) 2187-2193.

Chapter 4: Modification of polyimide with thermally labile saccharide units

4.1 Introduction

The separation of gas mixtures such as air, natural gas and olefin/paraffin are important in the oil and chemical industries to produce purified streams for further usage. An emerging gas separation process arise due to concerns of global warming is the carbon dioxide (CO_2) capture from flue gas streams [1-2]. Amine absorption, pressure swing adsorption and cryogenic distillation are some conventional technologies to separate such gas mixtures. Membrane technology is widely known to be a promising alternative [3]. It possesses competitive advantages like higher energy efficiency, smaller footprint, ease of scale-up and environmental friendliness [4].

Polymers, having a wide range of properties, are commonly used in the industries to fabricate gas separation membranes due to their low costs and ease of processing into different configurations [5]. Glassy polymeric membranes are often employed because they possess good capabilities to discriminate gas pairs according to their sizes. One of the common glassy polymers is the polyimide family. Not only it has exceptional thermal, chemical and mechanical properties due to its rigid structure, it also exhibits excellent gas separation properties. However, drawbacks of existing polyimide membranes restrict its broad applications. Though both high permeability and selectivity are desirable, a tradeoff exists between these two [6]. In addition, highly permeable polyimide membranes typically undergo CO_2-induced plasticization, in which CO_2 swells the polymer chains at high CO_2 partial pressures, resulting in an increase in inter-chain spacing and chain mobility [7]. The membrane in turn loses its intrinsic selectivity. In view of these challenges, increasing the permeability of the membranes with a minimum loss in selectivity and reducing CO_2-induced plasticization are required.

Extensive research has been done to molecularly design polyimide membranes to improve the properties of the membranes. One of the approaches is to search for better membrane materials. It can be done by varying chemical composition and configuration of the monomers used. It is found that

polyimide membranes containing 4,4′-(hexafluoroisopropylidene) diphthalic anhydride (6FDA) exhibit chain stiffness which effectively reduce chain packing. Several studies have shown that 6FDA-based polyimide membranes have shown good balance between high permeability and selectivity [8-11]. The other approach is to modify polyimide membranes by polymer blending, fabricating mixed matrix membranes, thermal annealing, grafting on polyimide backbone and cross-linking.

In the past few years, several studies have worked on improving the permeability of the membranes by incorporating thermally labile units such as sulfonated groups (–SO_3H), carboxylic acid groups (-COOH) and cyclodextrin in the polymer chains and decomposing them by annealing the membranes [12-16]. The resultant membranes exhibited higher gas permeability due to the microvoids left behind by the degraded thermally labile unit. However, the enhancement in permeability is often accompanied by the decline in selectivity. Cross-linking by applying ultra-violet radiation or adding chemical cross-linkers are some strategies employed to enhance selectivity and increase the CO_2-plasticization resistance of the membranes but oftensacrificingpermeability [17-19]. A novel scheme of combining the two strategies was proposedby Xiao et al. where they thermally treated a cross-linkable polyimide grafted with cyclodextrin up to 425 °C [14]. Not only did the new approach reduced CO_2-induced plasticization, it also enhanced gas permeability together with a minimum loss in selectivity. The resultant structure consisted of ultra-fine micropores derived from cross-linking reactions, connected integrally with microvoids from the decomposition of cyclodextrin.

In this work, we aim to investigate the effects of thermally labile units present in a cross-linkable 6FDA-based polyimide membrane on gas separation performance and CO_2 plasticization resistance. Three thermally labile units, glucose (S1), sucrose (S2) and raffinose (S3) are chosen to be studied in this work. Glucose (180 g/mol) is a monosaccharide, while sucrose (342 g/mol) is a disaccharide and raffinose (504 g/mol) is a trisaccharide. They are

commercially available low cost sugars. The methodology includes synthesizing a cross-linkable polyimide polymer, followed by grafting with the thermally labile units. Membranes fabricated will be annealed to decompose the thermally labile units. Analytical techniques will be performed to analyze the physiochemical properties of the membranes. In terms of gas separation performance, the membranes will be tested for the separation of the gas pairs O_2/N_2, CO_2/CH_4, CO_2/C_2H_6, CO_2/N_2 and C_3H_6/C_3H_8 at 2 atm and 35 °C. The resistance of the membranes to CO_2 plasticization will also be studied.

4.2 Results & discussion

4.2.1 Characterizations of the synthesized polymers

The pristine polyimide polymer was prepared via a standard two-step method, using poly(amic acid) as the intermediate [20]. During the synthesis of the polymer, a highly viscous polyamic acid solution was observed forming when the monomers, 6FDA, durene-diamine and DABA, were reacted together after several hours. After stirring for a day, the amic acid groups were converted to imide groups via chemical imidization. The yield is 96 wt% and the inherent viscosity of the polyimide measured is 0.79 g/dL. Figure 4.1 shows the residual weights and weight derivative curves of the pristine polymer and the grafted polymers when they were heated from 25 to 800 °C. As illustrated in the figure, the pristine polymer undergoes two decomposition stages. The first stage begins when the heating temperature reaches 400 °C. A decrease of approximately 5% of the weight of the polymer is observed. This could be attributed to the decarboxylation of the free carboxylic acid groups in the polymer side chains [16, 21]. The second decomposition stage, which is from 500 to 800 °C, resulted in a substantial 40 wt% decrease in the polymer weight. A broad tall peak in the weight derivative curve arises. The decline in weight in this temperature range may be due to the degradation of the polyimide backbone. The final residual weight at 800 °C is around 50 %.

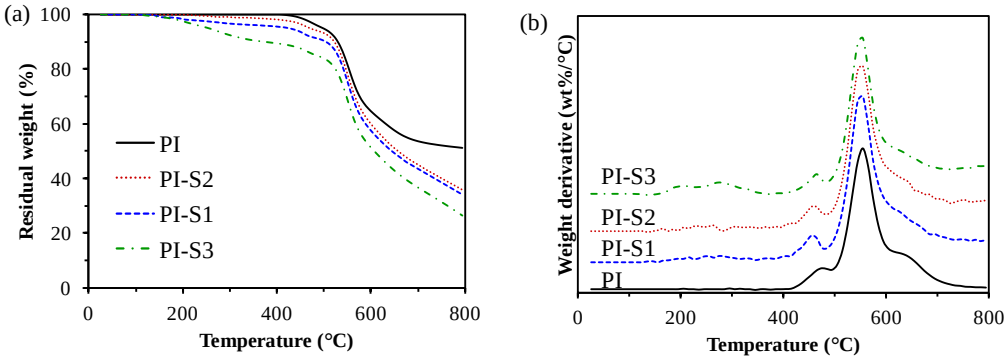

Figure 4.1 (a) TGA curves and (b) weight derivative curves of the synthesized polymers(S1: glucose,180 g/mol; S2: sucrose, 342 g/mol; S3: raffinose, 504 g/mol)

The grafted polymers have an additional decomposition stage from 200 to 400 °C. In this stage, PI-S1 showed a larger decline in the residual weight (around 5 %) compared to PI-S2 (around 2 %) and a huge drop can be seen in PI-S3 (around 10 %). To understand the reason behind the decreases in weight,

thermal analyses of the thermally labile units were performed. Figure4.2depicts the decomposition profiles. It can be observed that the thermally labile units decompose in two stages. The first stage occurs from 200 to 265 °C, as seen from the weight derivative plot. In this stage, it is postulated that the thermal labile units may undergo two processes. They are melted and may polymerize to form oligo- or polysaccharides, which is accompanied by the release of water. They may also decompose into smaller compounds, resulting in the formation of brown matter [22]. In the second stage from 265 to 800 °C, the brown matter and the oligo- or polysaccharides are both decomposed. It is also noticed that there are variations in the decomposition profiles of the three thermally labile units and amounts decomposed. S1 starts decomposing earlier and finishes later than S2 and S3. The relative weight losses in stage 1 and stage 2 are different. In addition, S1 also decomposes more than S2 and S3. The final residual weight follows the order, S1 (10 wt%) < S3 (18 wt%) < S2 (20 wt%). This may have an impact on gas separation performance, which will be discussed later. From the above thermal analyses of the polymers and the thermally labile units, it is proven that the decrease in weight of the polymers from 200 to 400 °C is due to the decomposition of the thermally labile units and it also shows that the thermally labile units are successfully grafted onto the polymer chains.

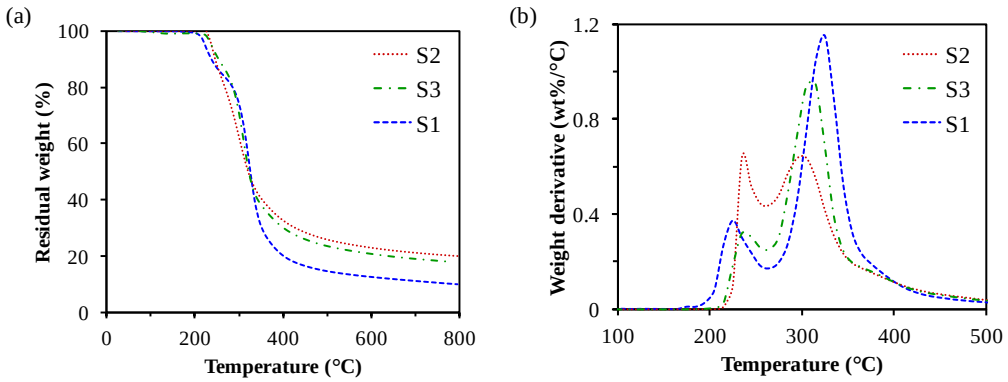

Figure 4.2 (a) TGA curves and (b) weight derivative curves of the thermally labile units (S1: glucose,180 g/mol; S2: sucrose, 342 g/mol; S3: raffinose, 504 g/mol)

As the thermally labile units decomposes in the temperature range of 200 to 400 °C, an annealing temperature of 400 °C for the pristine and grafted membranes is chosen for comparing the effect of the grafted thermally labile

units. In addition, the membrane grafted with S1 is annealed to a higher temperature of 425 °C to study the effect of annealing temperature on membrane properties.

4.2.2 Membrane structure verification and characterizations

As shown in Figure 4.3, the FTIR spectra confirm the structure of the membranes. The characteristic peaks of imide linkages at approximately 1780 cm^{-1} (symmetric stretching of the C=O bond), 1716 cm^{-1} (asymmetric stretching of the C=O bond), 1350 cm^{-1} (asymmetric stretching of the C-N bond) and 717 cm^{-1} (asymmetric bending of the C=O bond) are seen in the FTIR spectra of the pristine membrane. These peaks are consistent for the grafted membranes annealed at 400 °C, which indicate that the polyimide backbone is still intact. It is not degraded at the temperature. There seems to be a slight increase in the intensity of the broad band in the range of 3500 – 4000 cm^{-1}. This could be attributed to the stretching of the O-H bond of the grafted thermally labile unit.

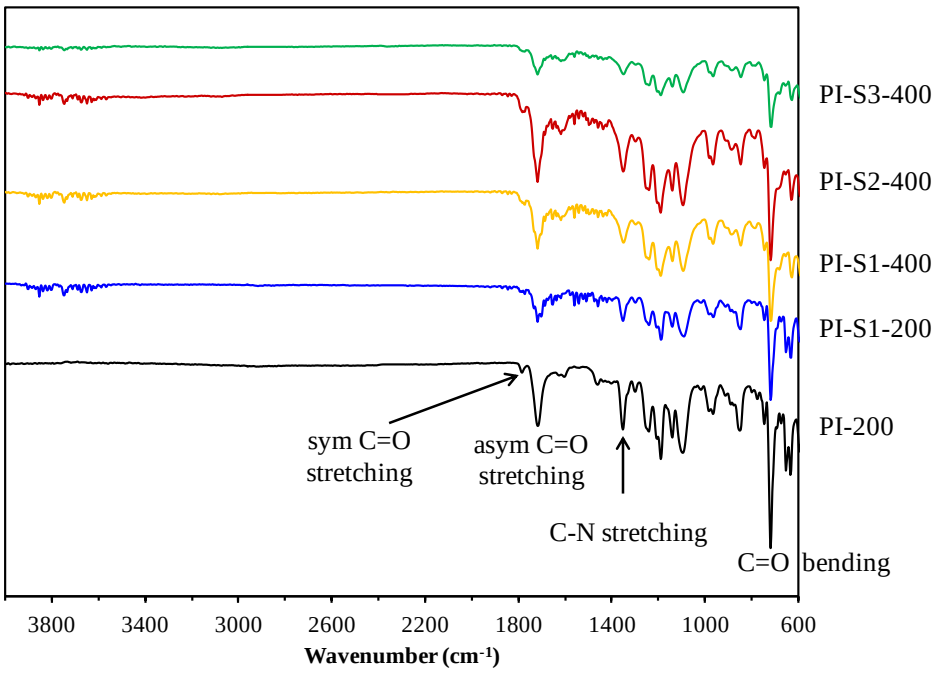

Figure 4.3 FTIR of the pristine and grafted membranes

The variation of the density of the membranes is listed in Table 4.1. The pristine membrane has the highest density of 1.390 g/cm^3. This could be due

to the tendency of carboxylic acid groups to form hydrogen bonds, hence causing the increase in the polymer packing density [23]. It is observed that the density of the grafted membranes follows the trend of PI-S1-200 < PI-S3-200 < PI-S2-200 and is smaller than the pristine membrane. When the thermally labile unit is grafted onto the side chains of the polymer, it is speculated that the following competing factors affect the packing density of the membranes: (1) the size of the thermally labile unit, (2) the thermally labile units disrupt the formation of strong hydrogen bonds between the carboxylic acid groups of the polymer chains, (3) hydrogen bonds form between the hydroxyl groups of the thermally labile unit and the carboxylic acid groups of the polymer, (4) cross-linking reactions between the thermally labile unit and the free carboxylic acid groups of the polymer. Taking PI-S3-200 as an example, it is grafted with the largest sugar (S3), thus it should show the lowest density. However, it has the most –OH groups, which may form a cross-linked structure or a structure with extensive hydrogen bonding. Therefore, the density of PI-S3-200 is in between that of PI-S1-200 and PI-S2-200.

Table 4.1 Density of the pristine and grafted membranes

	ρ (g/cm^3)
Samples treated at 200 °C	
PI-200	1.390
PI-S1-200	1.364
PI-S2-200	1.377
PI-S3-200	1.367
Samples treated at 400 °C	
PI-400	1.359
PI-S1-400	1.329
PI-S2-400	1.351
PI-S3-400	1.333
Sample treated at 425 °C	
PI-S1-425	1.298

The density of all the membranes annealed at 400 °C decreases. For the pristine membrane, the decrease in packing density could be attributed to the increase in the mobility of polymer chains [24]. The strong hydrogen bonds could also be broken at this high temperature. The grafted membranes have a

lower density than the pristine membrane. This could be ascribed to the decomposition of the thermally labile units, as mentioned earlier. The chemical bonds of the thermally labile units become unstable and smaller molecules are released, creating microvoids in the polymer matrix. Hence the packing density decreases [14].

The trend of the grafted membranes annealed at 400 °C is similar to that at 200 °C. The thermal analysis of the grafted membranes is as shown in Figure 4.4. It can be observed that PI-S3 in the membrane form (4 wt%) decomposes less than in the polymer form (10 wt%) from 200 to 400 °C. The thermally labile unit may experience polymerization and cross-linking reactions may occur when casted into a membrane form. As a result, PI-S3 decomposes lesser. The microvoids left behind by the higher amount of decomposition of the glucose unit in PI-S1 lead to a lower density of PI-S1-400 membrane compared with PI-S2-400 and PI-S3-400 membranes.

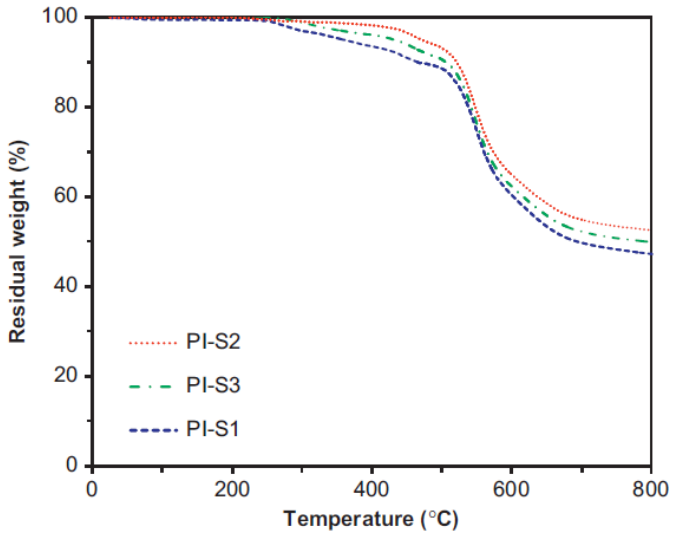

Figure4.4 TGA curves of the membranes fabricated

Figure 4.5 shows the XRD spectra of the membranes. The average inter-chain spacing (d-spacing) of PI-400 membrane is approximately 5.7 Å. It could be observed that the d-spacing of PI-400 membrane and PI-S2-400 membrane is close to each other and is smaller than that of PI-S1-400 and PI-S3-400 membrane (a higher diffraction angle results in a smaller d-spacing). This is in agreement with the variation in membrane density. The smaller the inter-chain

spacing, the higher is the packing density. A more obvious trend can be seen from the PI-S1 membranes annealed at different temperatures. It could be seen vividly that the d-spacing first increases and then decreases when the annealing temperature is varied from 200 to 400 to 425 °C. The increment of d-space when the annealing temperature is increased is in accordance with the variation in membrane density. The microvoids formed from the decomposition of glucose results in an increase in d-spacing. The decrease in d-spacing may be ascribed to the thermal-induced cross-linking reactions.

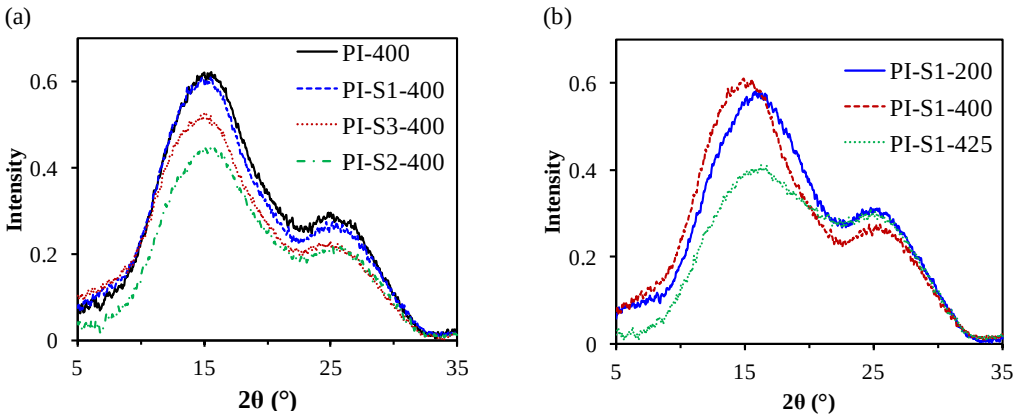

Figure 4.5 XRD spectra of the membranes
(a) Annealed at 400 °C (b) Annealed at 200 °C, 400 °C and 425 °C

4.2.3 Gas separation performance

As concluded from the previous results, the membrane properties are affected by the decomposition of the thermally labile unit, the polymerization of the thermally labile unit and the cross-linking reactions occurring in the membrane. This in turn has an impact on the gas separation performance. Table 4.2 lists the pure gas permeability and selectivity of the membranes for various gases, O_2, N_2, CO_2, CH_4, C_2H_6, C_3H_6 and C_3H_8. As predicted, the gas permeability of PI-200 membrane is the lowest. After the thermally labile units decompose, the permeability of the grafted membranes annealed at 400 °C increases substantially (four to six-fold increase in CO_2 permeability). This is contributed by the microvoids left in the polymer matrix after the release of the volatile decomposition products of the thermally labile unit. These microvoids increase the fractional free volume of the membranes. The gas permeability of the membranes increases with a slight decrease in selectivity.

Table 4.2 Pure gas permeability and selectivity of the membranes, tested at 2 atm and 35 ^{o}C

	Permeability (Barrer)							Selectivity				
	O_2	N_2	CO_2	CH_4	C_2H_6	C_3H_6	C_3H_8	O_2/N_2	CO_2/N_2	CO_2/CH_4	CO_2/C_2H_6	C_3H_6/C_3H_8
PI-200	18.4	4.3	83.6	2.8	2.4	-	-	4.3	19.5	29.6	34.8	-
PI-400	93.1	23.0	366	14.5	10.6	14.5	1.1	4.1	16.0	25.4	34.5	13.2
PI-S1-400	135	33.7	533	21.5	12.4	22.1	2.0	4.0	15.8	24.9	38.3	11.0
PI-S2-400	88.9	21.7	370	13.6	10.0	14.7	1.2	4.1	17.0	27.3	37.0	12.3
PI-S3-400	106	27.8	407	19.3	11.2	16.2	1.3	3.8	14.7	21.6	36.3	12.0
PI-S1-425	254	66.7	1389	51.5	33.8	59.0	4.2	3.8	20.8	26.9	41.0	14.1

The gas permeability of the membranes follows the same trend as the density and the d-spacing results. The PI-S1 membranes have the highest permeability since the density is the lowest and the d-spacing is the highest. The membrane annealed at 425 °C shows a high CO_2 permeability of 1389 Barrer with a moderate CO_2/CH_4 selectivity of 26.9. It is noted that the gas pair selectivity of PI-S1-425 membranes except for O_2/N_2 is higher than that of PI-S1-400 membranes because the thermal-induced cross-linking reactions at 425 °C decrease the d-spacing of the membrane. The CO_2/CH_4 selectivity increases from 24.9 for the PI-S1-400 membrane to 26.9 for the PI-S1-425 membrane. There may be a shift in the free volume distribution which favors the diffusion of CO_2 than that of CH_4 as the kinetic diameter of CO_2 is smaller than CH_4. On the other hand, less effect on O_2/N_2 gas pair due to their similar kinetic diameter [25].

When the gas separation performance of the membranes are compared with the Robeson's upper bound which is a representative of the performance of existing polymeric membranes, as shown in Figure 4.6, it falls slightly below the upper bound for O_2/N_2, CO_2/N_2 and CO_2/CH_4 gas pairs. The membranes have shown excellent C_3H_6/C_3H_8 separation performance. It is also observed that the membranes have good CO_2/C_2H_6 separation performance. Few studies have worked on the feasibility of using membranes for CO_2/C_2H_6 separation [26-27]. The cross-linked poly(ethylene oxide) membrane fabricated by Ribeiro Jr. et al. has a pure CO_2 permeability of approximately 330 Barrer with a CO_2/C_2H_6 selectivity of 6.6 at 35 °C and 2 atm [27]. It is challenging to separate CO_2 from C_2H_6 based on solubility selectivity as CO_2 and C_2H_6 have

similar condensability. Polyimide membranes in this study which are based on diffusivity selectivity have shown promising results for CO_2/C_2H_6 separation. The membranes have CO_2/C_2H_6 selectivity over 34.

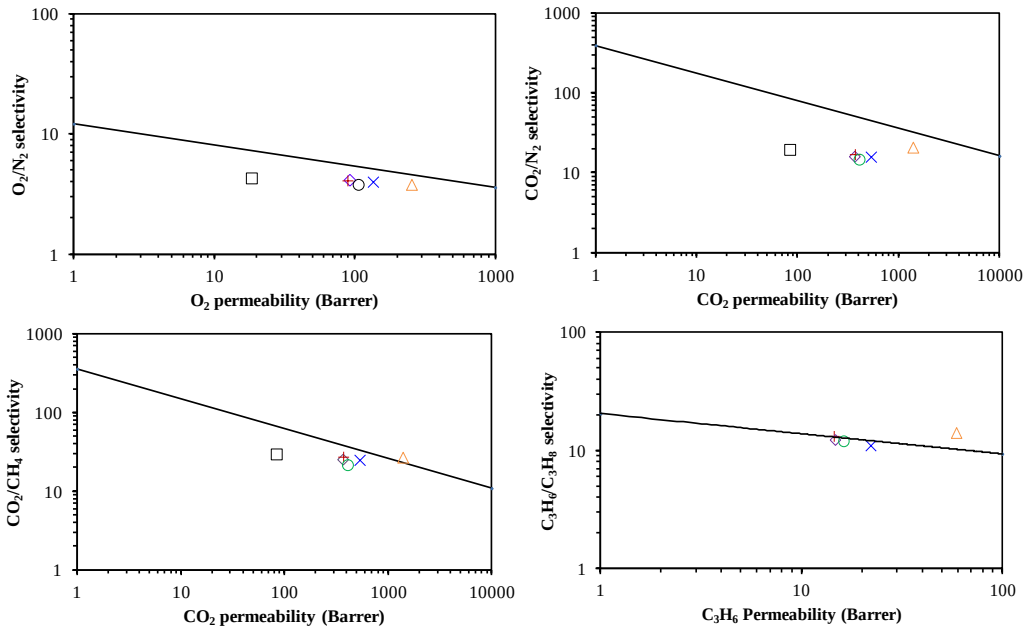

Figure 4.6 Comparison with upper bound plots
□ PI-200, ◊ PI-400, x PI-S1-400, + PI-S2-400, o PI-S3-400, Δ PI-S1-425

Figure 4.7 shows the variation of the relative CO_2 permeability of PI-S1 membranes when subjected to pure CO_2 feed pressure up to 30 atm. The increase in permeability of the pristine membrane at 15 atm is due to CO_2-induced plasticization. The pristine membrane is easily swollen by CO_2. After annealing at 400 °C, the membranes' resistance to CO_2 plasticization is enhanced. They do not exhibit plasticization up to 30 atm. The cross-linking reactions aid in the restrictions of polymer chain movement. It is also noted that although the membranes are annealed up to 425 °C, they are robust enough for gas permeability measurements. The picture in Figure 4.8 captures the flexibility of the PI-S1 membranes annealed at 200 °C and 425 °C. The mechanical strength of the membranes remains strong after annealing unlike carbon molecular sieve membranes.

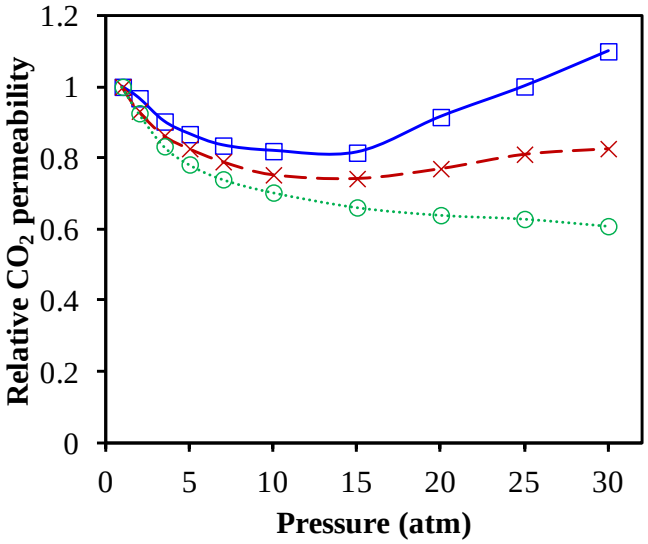

Figure 4.7 Resistance of the grafted membranes to CO_2 plasticization

PI-S1-200 PI-S1-425

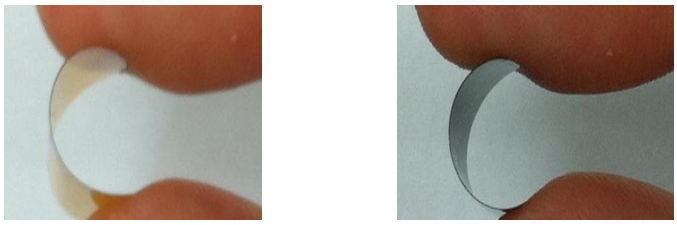

Figure 4.8 Mechanical strength of the PI-S1 membranes annealed at 200 ^{o}C and 425 ^{o}C

4.3 Conclusion

In this study, polyimide membranes grafted with glucose, sucrose and raffinose are prepared to study the effect of different molecular weight of the thermally labile unit on the properties of the membranes. The results show that the decomposition of the thermally labile unit from 200 to 400 °C leads to the formation of microvoids in the membrane, which in turn improves the gas permeability. The competing effects of the size and the decomposition behavior of the grafted unit, the formation/disruption of hydrogen bonds and the effect of cross-linking lead to PI-S1-400 membrane having a higher permeability than PI-S2-400 and PI-S3-400 membranes. The gas separation performance of the membranes falls slightly below the upper bound for O_2/N_2, CO_2/N_2 and CO_2/CH_4 gas pairs. The membranes have shown excellent C_3H_6/C_3H_8 separation performance. It is also observed that the membranes have promising results for CO_2/C_2H_6 separation withselectivity over 34. Increasing the annealing temperature of PI-S1 membrane to 425 °C shows a high CO_2 permeability of 1389 Barrer and an enhanced CO_2/CH_4 selectivity of 26.9 due to the thermally-induced cross-linking reactions. It is also noted that the annealed membranes do not exhibit plasticization up to a CO_2 feed pressure of 30 atm. The cross-linking reaction between the polyimide chains suppresses the swelling of the chains by carbon dioxide.

References:

[1] C. E. Powell, G. G. Qiao, Polymeric CO_2/N_2 gas separation membranes for the capture of carbon dioxide from power plant flue gases, J. Membr. Sci. 279 (2006) 1-49.

[2] A. Hussain, M. B. Hagg, A feasibility study of CO_2 capture from flue gas by a facilitated transport membrane, J. Membr. Sci. 359 (2010) 140-148.

[3] R. W. Baker, Future directions of membrane gas separation technology, Ind. Eng. Chem. Res. 41 (2002) 1393-1411.

[4] D. R. Paul, Y. P. Yampol'skii, Polymeric gas separation membranes, CRC Press, Boca Raton, FL, 1994.

[5] L. Shao, B. T. Low, T. S. Chung, A. Greenberg, Polymeric membranes for the hydrogen economy: Contemporary approaches and prospects for the future, J. Membr. Sci. 327 (2009) 18-31.

[6] L. M. Robeson, The upper bound revisited, J. Membr. Sci. 320 (2008) 390-400.

[7] Y. Xiao, B. T. Low, S. S. Hosseini, T. S. Chung, D. R. Paul, The strategies of molecular architecture and modification of polyimide-based membranes for CO_2 removal from natural gas – A review, Prog. Polym. Sci. 34 (2009) 561-580.

[8] S. A. Stern, Y. Mi, H. Yamamoto, A. Clair, Structure/permeability relationships of polyimide membranes. Applications to the separation of gas mixtures, J. Polym. Sci. Part B: Polym. Phys. 27 (1989) 1887-1909.

[9] S. X. Cheng, T. S. Chung, R. Wang, R. H. Vora, Gas-sorption properties of 6FDA-durene/1,4-phenylenediamine (pPDA) and 6FDA-durene/1,3-phenylenediamine (mPDA) copolyimdes, J. Appl. Polym. Sci. 90 (2003) 2187-2193.

[10] K. Tanaka, H. Kita, M. Okano, K. Okamoto, Permeability and permselectivity of gases in fluorinated and non-fluorinated polyimides, Polymer 33 (1992) 585-592.

[11] M. R. Coleman, W. J. Koros, Isomeric polyimides based on fluroinated dianhydrides and diamines for gas separation applications, J. Membr. Sci. 50 (1990) 285-297.

[12] M. N. Islam, W. Zhou, T. Honda, K. Tanaka, H. Kita, K. Okamoto, Preparation and gas separation performance of flexible pyrolytic membranes

by low-temperature pyrolysis of sulfonated polyimides, J. Membr. Sci. 261 (2005) 17-26.

[13] E. M. Maya, A. Tena, J. Abajo, J. G. Campa, A. E. Lozano, Partially pyrolyzed membranes (PPMs) derived from copolyimides having carboxylic acid groups. Preparation and gas transport properties, J. Membr, Sci. 349 (2010) 385-392.

[14] Y. Xiao, T. S. Chung, Grafting thermally labile molecules on cross-linkable polyimide to design membrane materials for natural gas purification and CO_2 capture, Energy & Environ. Sci. 4 (2011) 201-208.

[15] M. Askari, Y. Xiao, T. S. Chung, Natural gas purification and olefin/paraffin separation using cross-linkable 6FDA-Durene/DABA co-polyimides grafted with α, β and γ-cyclodextrin, J. Membr. Sci. 390-391 (2012) 141-151.

[16] A. M. Kratochvil, W. J. Koros, Decarboxylation-induced cross-linking of a polyimide for enhanced CO_2 Plasticization Resistance, Macromolecules 41 (2008) 7920-7927.

[17] H. Kita, T. Inada, K. Tanaka, K. Okamoto, Effect of photocrosslinking on permeability and permselectivity of gases through benzophenone-containing polyimide, J. Membr. Sci. 87 (1994) 139-147.

[18] Y. Liu, R. Wang, T. S. Chung, Chemical cross-linking modification of polyimide membranes for gas separation, J. Membr. Sci. 189 (2001) 231-239.

[19] L. Shao, T. S. Chung, S. H. Goh, K.P. Pramoda, Polyimide modification by a linear aliphatic diamine to enhance transport performance and plasticization resistance, J. Membr. Sci. 256 (2005) 46-56.

[20] M. K. Ghosh and K. L. Mittal, Polyimides: Fundamental and applications, Marcel Dekker, Inc., New York (1996).

[21] W. Qiu, C. C. Chen, L. Xu, L. Cui, D. R. Paul, W. J. Koros, Sub-T_g cross-linking of a polyimide membrane for enhanced CO_2 plasticization resistance for natural gas separation, Macromolecules 44 (2011) 6046-6056.

[22] F. Orsi, Kinetic studies on the thermal decomposition of glucose and fructose, J. of Thermal Analysis 5 (1973) 329-335.

[23] R. M. Huertas, E. M. Maya, J. Abajo, J.G. Campa, Effect of 3,5-Diaminobenzoic acid content, casting solvent, and physical aging on gas

permeation properties of copolyimides containing pendant acid groups, Macromol. Res. 19 (2011) 797-808.

[24] L. Shao, T. S. Chung, K. P. Pramoda, The evolution of physicochemical and transport properties of 6FDA-durene toward carbon membranes; from polymer, intermediate to carbon, Micropor. Mesopor. Mater. 84 (2005) 59-68.

[25] B. T. Low, N. Widjojo, T. S. Chung, Polyimide/polyethersulfone dual-layer hollow fiber membranes for hydrogen enrichment, Ind. Eng. Chem. Res. 49 (2010) 8778–8786.

[26] S. Kelman, H. Lin, E. S. Sanders, B. D. Freeman, CO_2/C_2H_6 separation using solubility selective membranes, J. Membr. Sci. 305 (2007) 57–68.

[27] C. P. Ribeiro Jr., B. D. Freeman, D. R. Paul, Pure- and mixed-gas carbon dioxide/ethane permeability and diffusivity in a cross-linked poly(ethylene oxide) copolymer, J. Membr. Sci. 377 (2011) 110– 123.

Chapter 5: Modification of polyimide via annealing in air and incorporation of β-CD and β-CD–ferrocene

5.1 Introduction

Natural gas, a cleaner and more efficient fuel compared to coal and crude oil, is in rising demand in energy sector and also in chemical sector as petrochemical feedstock. Besides constituting methane (CH_4) as the key component, natural gas contains some undesirable impurities like other hydrocarbons, carbon dioxide, water, nitrogen and hydrogen sulfide. Thus, natural gas has to be purified to increase its fuel heating value, reduce transportation costs, pipeline corrosion and atmospheric pollution [1-2]. One of the separation processes in natural gas purification is the removal of carbon dioxide (CO_2) from natural gas.

Membrane separation offers a promising alternative to conventional separation technologies such as amine absorption for CO_2 separation from light gases [3-5]. It possesses a higher energy efficiency and smaller footprint. It is easy to scale-up and is environmental friendly. Polymers are a suitable group of materials for fabricating membranes for gas separation due to their low costs and ease of processing into various configurations. A commonly used polymer is aromatic polyimide - a rigid glassy polymer with exceptional high chemical, thermal and mechanical properties and excellent gas separation properties [6]. For efficient and effective gas separation, membranes with a high permeability and selectivity are desirable. However, there exist well-known tradeoff curves between permeability and selectivity [7-9]. Besides that, other factors like CO_2-induced plasticization and mechanical strength need to be considered.

The gas transport in polyimide membranes is governed by (1) the penetrate size, (2) polymer chain mobility and (3) size and distribution of free volume[2]. The selective permeation of CO_2 over CH_4 for most polyimide membranes is attributed to the smaller kinetic diameter and highercondensability of CO_2. The chain mobility and the free volume of the membranes are affected by the molecular structure and the interactions between polymer chains and gas molecules. Some approaches undertaken to improve polyimide membranes include molecularly tailoring the structure to

obtainnew materials and modifying existing polyimide materials by heat treatment, grafting side groups on polymer backbone and cross-linking [2]. Numerous polyimide structures have been developed in literatures by varying the monomer structures [10-15]. Among various polyimides, aromatic polyimides containing 4,4′-(hexafluoroisopropylidene) diphthalic anhydride (6FDA) are of great interest. The bulky CF_3 group in 6FDA reduces chain packing and also increases chain stiffness due to steric hindrance. As a result, 6FDA-based polyimide membranes display good gas permeability and selectivity.

Thermal annealing is also employed to improve the performance of polyimides. Pyrolysis of polyimides at elevated temperatures (550 – 900 ˚C) has been studied to attain carbon molecular sieve membranes with superior permeability and selectivity[16-20].Despite the outstanding separation performance, the polyimide structure was not sustained. The resultant carbon membranes often show weak mechanical strength and high processing costs that limited their industrial applications. Another recent area of interest is the thermal rearrangement of polyimides to polybenzoxazoles. The single imide bond linkages are thermally rearranged to a stiff and rigid benzoxazole with formation of additional free volume. Higher permeability and selectivity of thermally rearranged polyimides are achieved [21-24].

A low temperature pyrolysis method involving polyimides containing thermally labile groups has also been developed in various studies [25-31]. In a similar manner, microvoids were formed during thermal annealing. The decomposition of thermally labile groups such as sulfonated groups, carboxylic acid groups, cyclodextrin and saccharide units on the side group of the polyimide backbone creates microvoids that result in a higher free volume for gas transport. Hence, enhancements in membrane permeability were achieved. In addition, increases in gas-pair selectivity and CO_2 plasticization resistance due to thermal induced cross-linking were observed in the studies by Chung and his coworkers. The polymer used was a 6FDA-based polyimide containing 3,5-diaminobenzoic acid (DABA), which was cross-linkable upon annealing. By decomposing the grafted thermally labile units, they produced

highly permeable membranes with improved selectivity and plasticization resistance. Furthermore, the toughness and flexibility of the membranes were retained after annealing at 425 °C. One of the thermally labile units used is β-cyclodextrin (β-CD). β-CD is an oligomer consisting seven α-D-glucose units bound together in a ring. The geometry of β-CD is of a hollow, toroidal and truncated cone with hydrophilic surface and hydrophobic cavity [32]. It decomposes to smaller molecules at temperatures from 300 °C to 400 °C. Its unique structure can be altered by forming inclusion with guest molecules, such as metallocene.

Several factors affect the thermal annealing process as well as membrane properties. In our previous studies, an increase in thermal treatment temperature on thermally labile membranes resulted in the enhancement of gas separation performance. Membranes thermally treated from different thermally labile groups such as α, β, γ-cyclodextrin and saccharides also exhibited different resistance against CO_2 induced plasticization. Heat treatment environments also play an important role on separation performance. Meier-Haack et al. showed that the asymmetric polyamide-6 membrane dried in air had a lower flux but a higher water/2-propanol selectivity compared to that dried in vacuum as the removal rate of the entrapped water in the polymer matrix was slower [33]. Wang et al. observed interference of oxygen in air to the thermal rearrangement of polyimides [24]. The O_2 induced degradation led to structural changes of polybenzoxazole that resulted in enhancements in both gas permeability and selectivity at the expense of mechanical properties. Chen et al. found that the presence of trace oxidizer in the purge gas and varying the soaking time had a negligible effect on the thermal cross-linking of 6FDA-based polyimide hollow fibers consisting of carboxylic acid [34]. On the other hand, cross-linking under open air conditions resulted in decrease in both permeance and selectivity. Densification of the skin and transition layer was observed.

From the above-mentioned studies, it would be interesting to study the change in molecular structure and gas separation performance of thermally labile polyimides annealed in air. β-CD and β-CD with a guest molecule will also be

incorporated. Ferrocene, one type of metallocene, is chosen as the guest molecule in this study. It consists of two cyclopentadienyl rings bound on opposite sides of a central iron atom and is available commercially at a reasonable cost. The 6FDA-polyimide containing 3,5-diaminobenzoic acid (DABA) will be synthesized and then grafted with β-CD and β-CD-Ferrocene (fBCD). Membranes will be fabricated and annealed under air environment. Material characterizations will be performed and gas separation performance of the membranes will be tested.

5.2 Results and discussion

5.2.1 Characterizations of the membranes fabricated and annealed

By employing the standard two-step method, naming the formation of poly(amic acid) from the purified monomers as the intermediate followed by chemical imidization, a highly viscous polyimide polymer solution was prepared. The measured inherent viscosity of the polymer obtained is 0.86 g/dL. The β-CD-Ferrocene product was also successfully synthesized with a high yield of 93 %. Figure 5.1d shows the existence of iron element across the PIfBCD membrane. β-CD-Ferrocene is uniformly distributed among the polymer chains. This is attributed to the chemical grafting of β-CD onto the polymer chains and the hydrophilic attraction of DABA with β-CD.

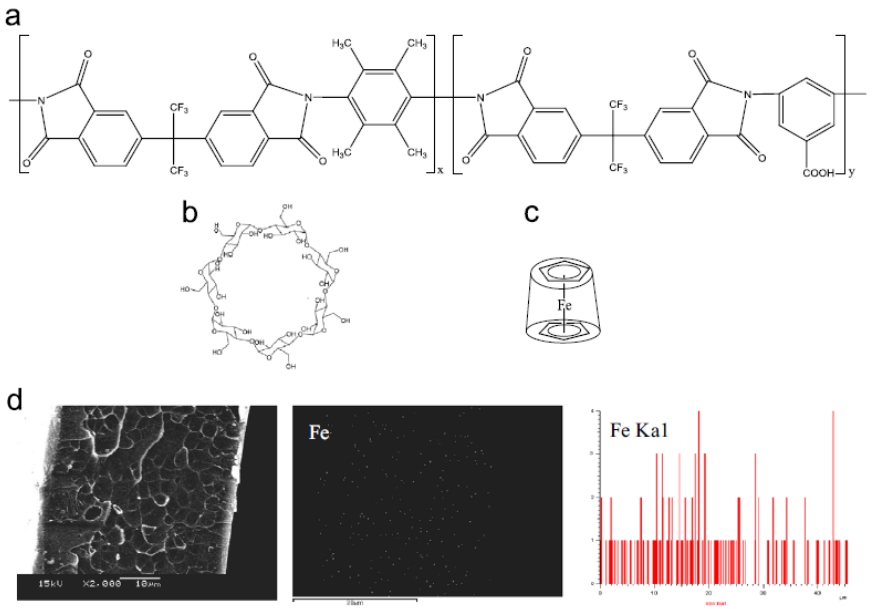

Figure 5.1 (a) Chemical structure of the polyimide containing carboxylic acid, (b) Chemical structure of β-CD, (c) Chemical structure of β-CD-Ferrocene, (d) SEM-EDX image of the PIfBCD cross section membrane

The thermal decomposition of the PI membrane in nitrogen and in air is shown in Figure5.2a. A decline in membrane weight in both nitrogen and air can be observed when the temperature reaches 350 °C. This is mainly due to the release of carbon dioxide from the decarboxylation of the DABA moiety of the polyimide [26]. At 400 °C, a distinctive difference is seen from the decomposition profile in air compared to that in nitrogen. There is an

accelerated weight loss, leaving almost no char at 800 °C. In nitrogen, the polyimide exhibits a substantial 40 wt% decrease from 500 to 800 °C, corresponding to the degradation of the polymer backbone. The final residual weight is 54 wt%. Oxygen in air may induce other reactions on the polymer backbone and cause it degrade at a faster rate.

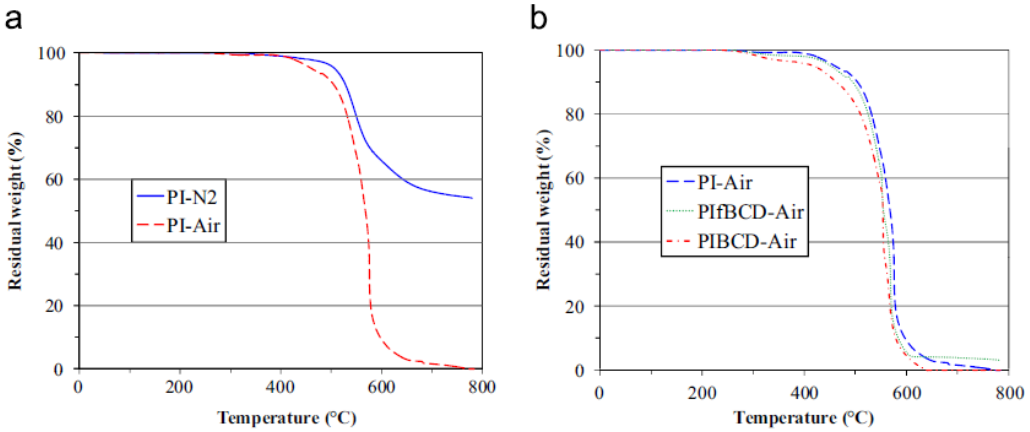

Figure 5.2 Comparison of thermal decomposition profiles of (a) the synthesized polyimide membrane in nitrogen and in air and (b) the modified membranes in air

InFigure 5.2b, the weight loss after 250 °C follows this order, PIBCD > PIfBCD > PI. The final residual weight of 4% in the PIfBCD membrane is attributed to the iron from ferrocene in the membrane. The excess weight loss in the PIBCD membrane compared to the PI membrane is owing to the decomposition of thermally labile β-CD. Figure 5.3adepicts the decomposition profile of β-CD, ferrocene and the β-CD-ferrocene complex. β-CD melts and decomposes at around 300 °C, while Ferrocene decomposes below 200 °C. The complex of β-CD and ferrocene is stable up to 200 °C. This indicates that the ferrocene present in β-CD-Ferrocene is tightly included in the β-CD cavity [35]. It does not independently decompose below 200 °C like the free ferrocene. In addition, the complex decomposes at a lower temperature compared to β-CD. This is in consistent with other literatures that the inclusion of a guest molecule into β-CD affects the thermal stability of β-CD [36-37]. Though ferrocene affects the stability of β-CD, interestingly asshown in Figure 5.2b, the resultant weight loss of the PIfBCD membrane is lesser than that of PIBCD. It is speculated that electrostatic interactions

between ferrocene and polyimide chains cause reduced chain mobility, hence less prone to degradation.

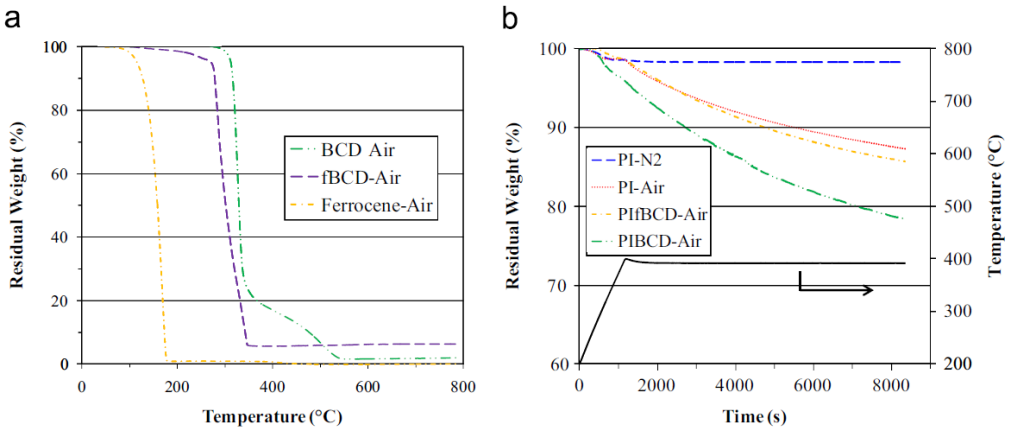

Figure 5.3 Thermal decomposition profiles of (a) β-CD, ferrocene and β-CD-ferrocene in air, (b) the modified membranes held at 400 ^{o}C in air

As the majority of the decomposition of β-CD and β-CD-Ferrocene are completed by 400 °C, an annealing temperature of 400 °C is chosen to study the effect of heat treatment environment and thermally labile groups on the membranes.Figure 5.3bis the thermal analysis performed to simulate the annealing process of the fabricated membranes.The PI membrane shows superior stability in nitrogen at 400 °C because its weight loss is only 1.7 %. On the contrary, the weights of PI, PIBCD and PIfBCD membranes continue to decline at prolonged heating at 400 °C in air due to oxidation of polymer chains when held for a long period of time at high temperatures. The higher decomposition of the PIBCD membrane is attributed to the decomposition of the β-CD structure as mentioned earlier. Further characterizations are performed to examine the change in polymer structure and the effect on gas separation performance.

Comparing the gel content of the membranes fabricated and annealed at 400 °C, the PI membrane dried at 200 °C is found to be completely soluble in NMP. All other heat treated membranes have a gel content of over 98% due to the thermal induced cross-linking reactions. This crosslinking effect may have an impact on the resistance against CO_2 induced plasticization, which will be discussed later. O1s spectra of the polyimide membrane annealed at 400 °C in vacuum, in air, and grafted with β-CD and then annealed at 400 °C in air are

shown inFigure 5.4a. The reduced intensity of the peak might be due to the oxidative cleavage of some imide bond linkages in the polyimide by oxygen in air, which agrees with the monotonic weight loss seen in the TGA analysis at prolonged heating. In addition, there seems to be an additional peak in PI-A400 and PIBCD-400 membranes. Upon deconvolution, a single peak at 532.6 eV in the O1s spectrum of the PI-400 membrane, pertaining to the oxygen in the carbonyl group (O=C) in the imide bond linkages, is observed inFigure 5.4b. The O1s spectrum of the PI-A400 membrane comprises of two component peaks (Figure 5.4c): (1) peak at 532.6 eV, pertaining to the oxygen in the carbonyl group (O=C) in the imide bond linkages of the polyimide, (2) peak at 534.5 eV, possibly pertaining to the single bond of oxygen-carbon atom (O-C). It is speculated that annealing with air introduces polar functional groups (O-C) to the polyimide chains. A slight shift in the O1s spectrum of PIBCD-A400 and similar two peaks with higher intensity as the spectrum of PI-A400 are observed inFigure 5.4d. The O1s spectrum of PIfBCD-400, not depicted in the figure, follows a similar trend as PIBCD-A400.

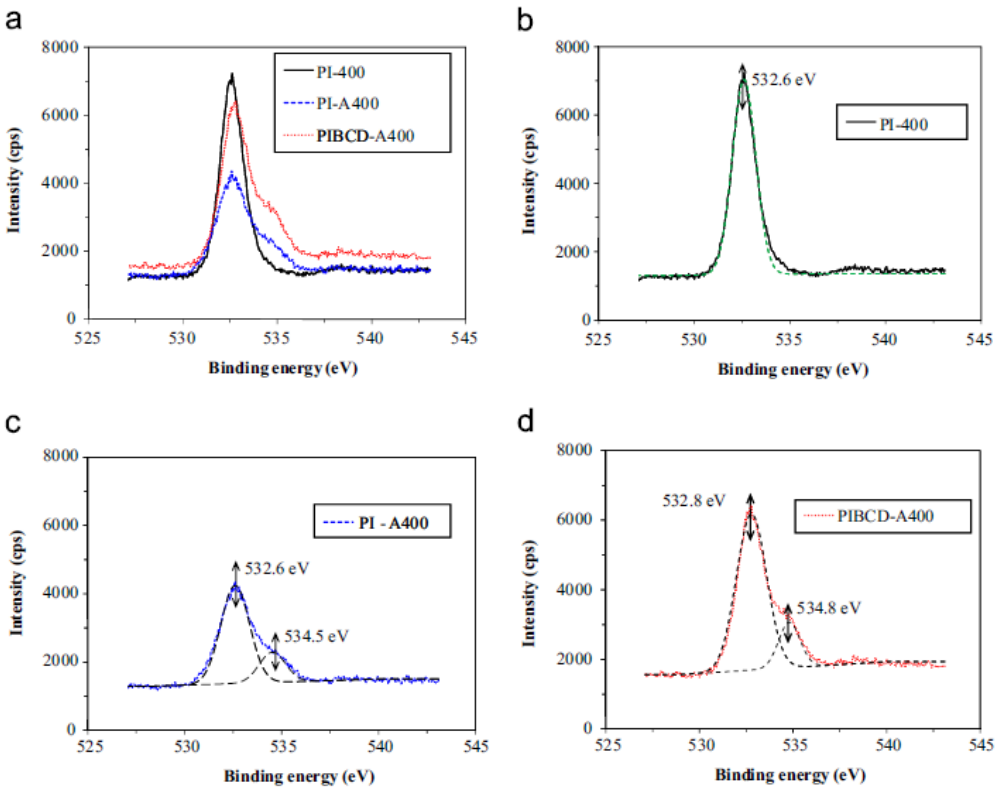

Figure 5.4 XPS O1s spectra of the PI membrane fabricated and annealed

5.2.2 Gas separation performance of the membranes and comparison with CO_2/CH_4 upper bound

Table 5.1 lists the pure gas permeability and selectivity of the membranes prepared in this study. For the PI membrane annealed at 400 °C in vacuum, the permeability and selectivity are much higher than the PI membrane dried at 200 °C. It is attributed to (1) the decarboxylation of the DABA moiety of the polyimide and the crosslinking effect, as mentioned previously and (2) the breaking of the strong hydrogen bonds between the DABA moiety[30]. For the PI membrane treated under air atmosphere, an increase in CO_2/CH_4 selectivity is attained at the expense of gas permeability.The increase in selectivity may be due to the introduction of polar functional groups, as seen by the second peak in XPS O1s spectra.

Table 5.1Pure gas permeability and selectivity of the membranes, tested at 2 atm and 35 °C

	P_{CO_2} (barrer)	P_{CH_4} (barrer)	α_{CO_2/CH_4}
PI-200	324	13.9	23.3
PI-400	640	26.1	24.5
PI-A400	202	5.6	36.0
PIBCD-A400	430	10.0	42.9
PIfBCD-A400	243	5.2	47.3

The permeability of the polyimide annealed under air atmosphere doubles when β-CD is incorporated.The decomposition of thermally labile units, as discussed in the previous section, creates microvoids in the polymer matrix. These microvoids increase the free volume of the membranes and therefore enhance permeability. The selectivity also increases by 20%. This possibly causes by the additional crosslinking reactions of the radicals left by the decomposition of β-CD. With the inclusion of ferrocene, a decline in gas permeability is observed but a further 10% increase in CO_2/CH_4 selectivity is attained for the PIfBCD-A400 membrane comparing to the PIBCD-A400 membrane.Iron in ferrocene may enhance the affinity of the membrane to CO_2 [38-39],while the electrostatic crosslinking between ferrocene and polymer

chains and the space occupation by ferrocene may be the causes for the permeability reduction.

In Figure 5.5, the gas separation performance is compared to the existing CO_2/CH_4 upper bound and to some of the studies on thermally annealed membranes at near 400 °C. Due to the considerable increment in CO_2/CH_4 selectivity, the gas separation performance of PIBCD-A400 and PIfBCD-A400 membranes lies above the CO_2/CH_4 upper bound curve compared to other studies.The annealed membranes at 400 °C lie closer to the upper bound compared to the pristine PI membrane and the annealed membranes in air have better gas separation performance compared to that in vacuum.

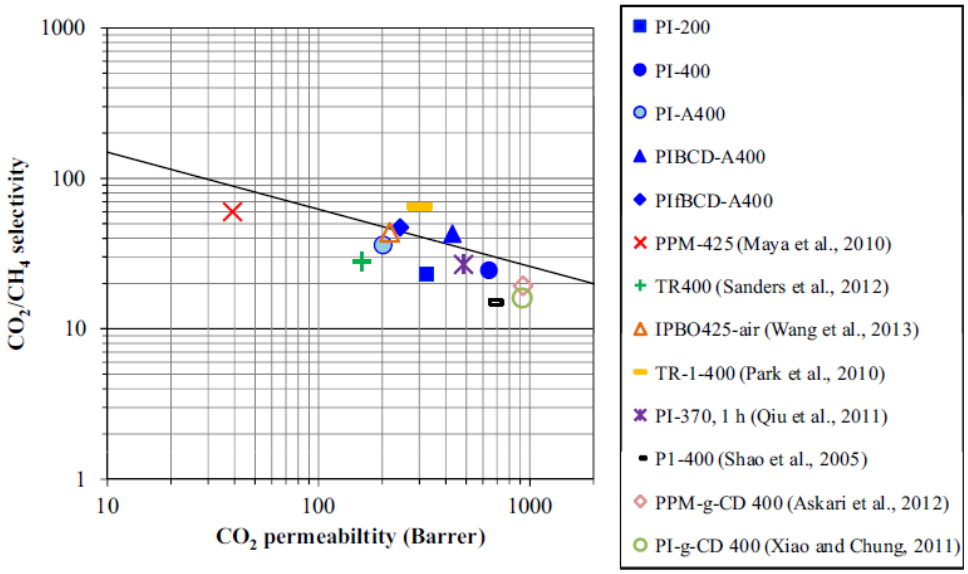

Figure 5.5 Comparison with the upper bound curve for CO_2/CH_4 gas-pair

5.2.3 Effects on plasticization resistance, mixed gas tests and mechanical strength

Figure5.6 shows the plasticization resistance against CO_2 of some of the membranes. The membranes exhibit decline in the CO_2 permeability when pressure increases, which is caused by the saturation of Langmuir sites. The PI-200 membrane exhibits an increment in CO_2 permeability at 10 atm. This is due to the swelling of polymer chains by CO_2. Plasticization phenomenon is also observed for the PI-400 membrane after 15 atm. Plasticization is not

observed for the membranes after heat treatment in air. They are able to resist plasticization up to 30 atm of CO_2. This is a result of the crosslinking reactions in air.

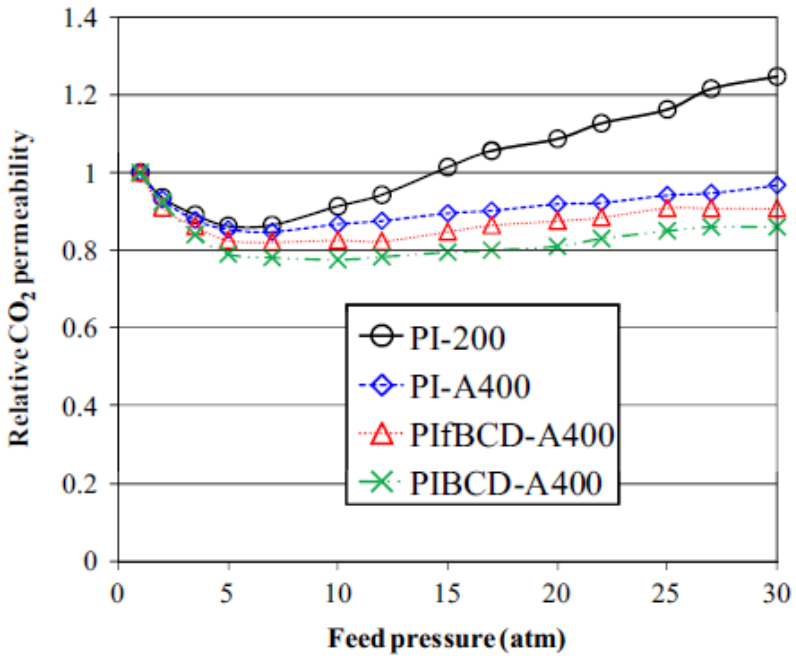

Figure 5.6 CO_2 plasticization resistance of the membranes

When the PIBCD-A400 and PIfBCD-400 membranes are subjected to a CO_2/CH_4 binary gas mixture, the permeability and selectivity in Table 5.2 remain almost the same for the binary gas tests. The membranes are able to maintain the structure integrity under mixed gas. The pictures in Figure5.7 demonstrate the toughness and flexibility of the membranes after heat treatment. They are unlike carbon molecular sieve membranes, which are brittle. Even the membranes treated under air atmosphere maintain its mechanical strength. Overall, the polymeric membranes that we have annealed in air and incorporated with β-CD and β-CD-Ferrocene exhibit enhanced CO_2 plasticization resistance, good stability under mixed gas and strong mechanical strength.

Table 5.2Binary gas permeability and selectivity of the membranes, tested with a CO_2/CH_4 50:50 molar gas mixture at CO_2 partial pressure of 2 atm and 35 ^oC

	P_{CO_2} (barrer)	P_{CH_4} (barrer)	α_{CO_2/CH_4}
PIBCD-A400	414 (430)	9.6 (10.0)	43.0 (42.9)
PIfBCD-A400	235 (243)	5.0 (5.2)	47.0 (47.3)

* Results in parentheses are obtained from the pure gas test

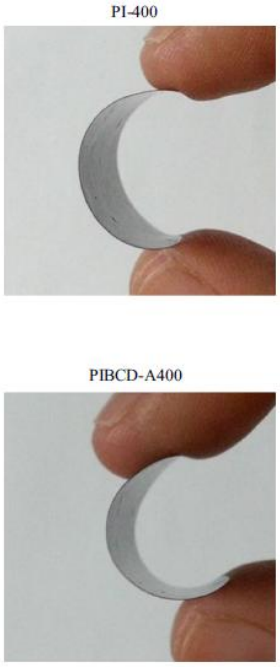

Figure 5.7 Mechanical strength of the membranes annealed

5.3 Conclusion

In this study, polyimides comprising carboxylic acid group and grafted with β-CD and β-CD-Ferrocene have been synthesized. The changes in molecular structure and gas separation performance of polyimide membranes by annealing in air and incorporating β-CD and β-CD-Ferrocene were investigated.

(1) TGA analyses show a difference in the decomposition profiles of the membranes fabricated. The weight loss at 400 °C follows this order, PIBCD-Air > PIfBCD-Air > PI-Air > PI-N_2. XPS analyses reveal additional functional groups on the polymer backbone when the membranes are annealed in air.

(2) When annealing at 400 °C in air, the competing effects between decarboxylation of the DABA moiety, the breaking of the strong hydrogen bonds between the DABA moiety, and the reactions of polymer chains with air, result in the improvement in CO_2/CH_4 (55 %) selectivity at the expense of permeability.

(3) The incorporation of β-CD into the polyimide results in decomposition of the thermally labile group, creating microvoids in the polymer matrix. A twofold improvement in the permeability of the PIBCD membrane annealed under air at 400 °C, compared to that of PI membrane. Due to electrostatic crosslinking and steric hindrance brought by ferrocene, the PIfBCD membrane annealed under at 400 °C exhibits a higher selectivity but a lower permeability.

(4) Significant increments in CO_2/CH_4 selectivity with performance lies above the CO_2/CH_4 upper bound have been observed for both PIBCD and PIfBCD membranes annealed under air atmosphere. Swelling of the polymer chains of the annealed membranes by CO_2 is suppressed. The membranes are able to resist CO_2 plasticization up to 30 atm and exhibit toughness and flexibility after heat treatment. The permeability and selectivity of PIBCD-A400 and PIfBCD-A400 membranes remain almost the same for the binary gas tests.

This approach of annealing in air, which is a simpler process, coupled with incorporating thermally labile groups, has shown feasibility to modify the polymer structure and tune the polymer matrix to achieve mechanically strong membranes with enhanced gas separation, good stability in carbon dioxide and binary gas.

References:

[1] R. W. Baker andK. Lokhandwala, Natural gas processing with membranes: an overview, Ind. Eng. Chem. Res. 47 (2008) 2109-2121.

[2] Y. Xiao, B. T. Low, S. S. Hosseini, T. S. Chung, D. R. Paul, The strategies of molecular architecture and modification of polyimide-based membranes for CO_2 removal from natural gas – A review, Prog. Polym. Sci. 34 (2009) 561-580.

[3] L. Shao. B. T. Low, T. S. Chung, A. Greenberg, Polymeric membranes for the hydrogen economy: Contemporary approaches and prospects for the future, J. Membr. Sci. 327 (2009) 18-31.

[4] X. He, M. B. Hägg, Membranes for environmentally friendly energy processes, Membranes 2 (2012) 706-726.

[5] N. Peng, N. Widjojo, P. Sukipaneenit, M. M. Teoh, G. G. Lipscomb, T. S. Chung, J. Y. Lai, Evolution of polymeric hollow fibers as sustainable technologies: Past, present, and future, Prog. Polym. Sci. 37 (2012) 1401-1424.

[6] H. Ohya, V. V. Kudryavtsev, S. I. Semenova, Polyimide membranes: applications, fabrications and properties, Kodansha Japan and Gordon and Breach Science Publishers, 1996.

[7] L. M. Robeson, W. F. Burgoyne, M. Langsam, A. C. Savoca, C. F. Tien, High performance polymers for membrane separation, Polymer 35 (1994) 4970-4978.

[8] B. D. Freeman, Basis of permeability/selectivity tradeoff relations in polymeric gas separation membranes, Macromolecules 32 (1999) 375-380.

[9] L. M. Robeson, The upper bound revisited, J. Membr. Sci. 320 (2008) 390-400.

[10] S. A. Stern, Y. Mi, H. Yamamoto, Structure/permeability relationships of polyimide membranes. Applications to the separation of gas mixtures, J. Polym. Sci. Part B: Polym. Phys 27, (1989) 1887–909.

[11] M. R. Coleman, W. J. Koros, Isomeric polyimides based on fluroinated dianhydrides and diamines for gas separation applications, J. Membr. Sci. 50 (1990) 285-297.

[12] S. X. Cheng, T. S. Chung, R. Wang, R. H. Vora,Gas-sorption properties of 6FDA-durene/1,4-phenylenediamine (pPDA) and 6FDA-durene/1,3-phenylenediamine (mPDA) copolyimdes, J. Appl. Polym. Sci. 90 (2003) 2187-2193.

[13] D. Ayala, A. E. Lozano, J. D. Abajo, C. G. Perez, J. G. de la Campa, K. V. Peinemann, B. D. Freeman, R. Prabhakar, Gas separation properties of aromatic polyimides, J. Membr. Sci. 215 (2003) 61–73.

[14] Y. Álvarez-Gallego, S. P. Nunes, A. E. Lozano, J. G. de la Campa, J. de Abajo, Synthesis and properties of novel polyimides bearing sulfonated benzimidazole pendant groups, Macromol. Rapid Comm. 28 (2007) 611-622.

[15] S. Xiao, X. Feng, R. Y. M. Huang, Synthesis and Properties of 6FDA-MDA copolyimide membranes: effects of diamine and dianhydrides on gas separation and pervaporation properties, Macromol. Chem. Phys. 208 (2007) 2665-2676.

[16] M. B. Hägg, J. A. Lie, A. Lindbrathen, Carbon molecular sieve membranes: a promising alternative for selected industrial applications, Ann. N. Y. Acad. Sci. 984 (2003) 329-345.

[17] S. M. Saufi andA. F. Ismail, Fabrication of carbon membranes for gas separation—a review, Carbon 42 (2004) 241-259.

[18] J. N. Bersema, S. D. Klijnstra, J. H. Balster, N.F.A. van der Vegt, G. H. Koops, M. Wessling, Intermediate polymer to carbon membranes based on Matrimid PI, J. Membr. Sci. 238 (2004) 93-102.

[19] L. Shao, T. S. Chung, K. P. Pramoda, The evolution of physicochemical and transport properties of 6FDA-durene toward carbon membranes; from polymer, intermediate to carbon, Micropor. Mesopor. Mater. 84 (2005) 59-68.

[20] P. S. Tin, Y. C. Xiao, T. S. Chung, Polyimide-carbonised membranes for gas separation: structural, composition and morphological control of precursors, Sep. Purif. Reviews 35 (2006) 285-318.

[21] H. B. Park, S. H. Han, C. H. Jung, Y. M. Lee, A. J. Hill, Thermally rearranged (TR) polymer membranes for CO_2 separation, J. Membr. Sci. 359 (2010) 11-24.

[22] D. F. Sanders, Z. P. Smith, C. P. Ribeiro Jr., R. Guo, J. E. McGrath, D. R. Paul, B. D. Freeman, Gas permeability, diffusivity, and free volume of thermally rearranged polymers based on 3,3’-dihydroxy-4,4’-diamino-

biphenyl (HAB) and 2,2'-bis-(3,4-dicarboxyphenyl) hexafluoropropane dianhydride (6FDA), J. Membr. Sci. 409-410 (2012) 232-241.

[23] Y. F. Yeong, H. Wang, K. P. Pramoda, T. S. Chung, Thermal induced structural rearrangement of cardo-copolybenzoxazole membranes for enhanced gas transport properties, J. of Membr. Sci. 397– 398 (2012) 51–65.

[24] H. Wang, D. R. Paul, T. S. Chung, The effect of purge environment on thermal rearrangement of ortho-functional polyamide and polyimide, Polymer 54 (2013) 2324-2334.

[25] M. N. Islam, W. Zhou, T. Honda, K. Tanaka, H. Kita, K. Okamoto, Preparation and gas separation performance of flexible pyrolytic membranes by low-temperature pyrolysis of sulfonated polyimides, J. Membr. Sci. 26 (2005) 17-26.

[26] A. M. Kratochvil, W. J. Koros, Decarboxylation-induced cross-linking of a polyimide for enhanced CO_2 plasticization resistance, Macromolecules 41 (2008) 7920-7927.

[27] W. Qiu, C.-C. Chen, L. Xu, L. Cui, D. R. Paul, W. J. Koros, Sub-T_g cross-linking of a polyimide membrane for enhanced CO_2 plasticization resistance for natural gas separation, Macromolecules 44 (2011) 6046-6056.

[28] E. M. Maya, A. Tena, J. de Abajo, J. G. de la Campa, A. E. Lozano, Partially pyrolyzed membranes (PPMs) derived from copolyimides having carboxylic acid groups. Preparation and gas transport properties, J. Membr, Sci. 349 (2010) 385-392.

[29] Y. C. Xiao, T. S. Chung, Grafting thermally labile molecules on cross-linkable polyimide to design membrane materials for natural gas purification and CO_2 capture, Energy & Environ. Sci. 4 (2011) 201-208.

[30] M. Askari, Y. Xiao, T. S. Chung, Natural gas purification and olefin/paraffin separation using cross-linkable 6FDA-Durene/DABA co-polyimides grafted with α, β and γ-cyclodextrin, J. Membr. Sci. 390-391 (2012) 141-151.

[31] M. L. Chua, Y. Xiao, T. S. Chung, Effects of thermally labile saccharide units on the gas separation performance of highly permeable polyimide membranes, J. Membr. Sci. 415-416 (2012) 375-382.

[32]R. Singh, N. Bharti, J. Madan, S. N. Hiremath, Characterization of cyclodextrin inclusion complexes – a review, J. Pharm. Sci. & Technol. 2 (2010) 171-183.

[33] J. Meier-Haack, W. Lenk, S. Berwald, T. Riesar, K. Lunkwitz, Influence of thermal treatment on the pervaporation separation properties of polyamide-6 membranes, Sep. Purif. Technol. 19 (2000) 199-207.

[34] C.-C. Chen, S. J. Miller, W. J. Koros, Characterization of thermally cross-linkable hollow fiber membranes for natural gas separation, Ind. Eng. Chem. Res. 52 (2013) 1015-1022.

[35] A. Harada andS. Takahashi, Preparation and properties of cyclodextrin inclusion compounds of organometallic complexes. Ferrocene inclusion compounds, J. Incl. Phenom. 2 (1984) 791-798.

[36] A. Harada, Cyclodextrin-based molecular machines, Acc. Chem. Res. 34 (2001) 456-464.

[37] L. X. Song, P. Xu, A comparative study on the thermal decomposition behaviors between β-cyclodextrin and its inclusion complexes of organic amines, J. Phys. Chem. A 112 (2008) 11341-11348.

[38] F. Li, T. S. Chung, S. Kawi, Facilitated transport by hybrid POSS®–Matrimid®–Zn^{2+} nanocomposite membranes for the separation of natural gas, J. Membr. Sci. 356 (2010) 14-21.

[39] Y. Li, T. S. Chung, Silver ionic modification in dual-layer hollow fiber membranes with significant enhancement in CO_2/CH_4 and O_2/N_2 separation, J. Membr. Sci. 350 (2010) 226-231.

Chapter 6: Using iron (III) acetylacetonate as both a cross-linker and micropore former to develop polyimide membranes with enhanced gas separation performance

6.1 Introduction

Over the past three decades, the industrial application of membrane technology in the separation of gas mixtures such as natural gas and olefin/paraffin has expanded significantly and further growth is likely to continue [1-3]. In comparison with conventional gas separation technologies such as amine absorption, membrane technology has a higher energy efficiency, possesses asmaller footprint and it is easy to scale up and is environmentally friendly [4]. Polymeric membranes are commonly used as polymers are of low costs and easy to process into different configurations. On the other hand, it has several drawbacks, which include the tradeoff existingbetween permeability and selectivity and losing its separation performance in the presence of plasticizing components such as carbon dioxide (CO_2) and hydrocarbons [5-7]. Therefore, in the selection of materials to fabricate an effective and efficient polymeric membrane for gas separation, factors to be taken into consideration consist of high separation properties such as high permeability and selectivity, strong chemical resistance, mechanical strength and good thermal stability.

Generally, glassy polymers with rigid structure and poor chain packing offer best combinations of permeability and selectivity. One glassy polymer of interest is polyimide containing 4,4′-(hexafluoroisopropylidene) diphthalic anhydride (6FDA)[8-16]. It consists of bulky CF_3 groups that reduce chain packing and increase chain stiffness due to steric hindrance. Thus, most 6FDA-based polyimide membranes display good gas permeability and selectivity. However, similar to other glassy polymers, they are also prone to be plasticized by high sorbing gases like carbon dioxide (CO_2). Occurrence of plasticization is often marked by the upward increase in CO_2 permeability at high upstream pressures [17]. CO_2 swells up the polymer chains, resulting an increase in inter-chain spacing and chain mobility. In mixed gas tests, there

will be an increase in permeability of all components, leading to a loss in membraneselectivity.

Some of the approaches to modify the properties of polyimide membrane are by blending it with other polymers, with inorganic particles and cross-linking [18-20].Cross-linking can be obtained by radiation (ultraviolet, ion beam etc), thermal treatment and chemical treatment [5]. It often results in chain mobility reduction, hence suppressing swelling induced by highly sorbing components. UV irradiation of the polyimide containing benzophenone moiety brought cross-linking between the polymer chains, resulting a significant enhancement in gas selectivity at the expense of permeability [21]. Through exposure to ion beam irradiation, there were simultaneous increments of permeability and selectivity in Matrimid membranes. However, the ion beam led to degradation of the polymer backbone [22-23].

Extensive research efforts have also been focused on modifying the polymer properties via thermal treatment. Thermal treatment of polyimides such as Matrimid and 6FDA-based polymers at elevated temperatures for short periods of time has shown increased resistance to plasticizationcompared to untreated membranes [24-30]. In a study by Barsema et al., they observed structure densification of Matrimid when annealing it below the glass transition temperature (T_g), forming a charge transfer complex at above T_g and transiting it to a carbon membrane at a higher annealing temperature [25]. Decarboxylation occurred at 15 °C above $T_g$for the 6FDA-based polymer containing cross-linkable carboxylic acid, generating phenyl radicals to form linkages and a more open matrix [26-27]. Thermal treatment of 6FDA-based polymers grafted with thermally labile units such as cyclodextrin and saccharrides not only induced thermal cross-linking, but also led to the decomposition of thermally labile units to form microvoids, resulting simultaneous enhancements in permeability, selectivity and the integrity of the polymer backbone [28-30]. There are varying results obtained for cross-linking polyimides via thermal treatment. However, thermal treatment at elevated temperatures incurs a higher cost for membrane fabrication. It may also compromise the mechanical strength of the resultant membranes.

Chemical cross-linking is another commonly employed method. Hayes found that diamino cross-linked polyimide membranes at ambient temperature with an increased O_2/N_2 selectivity [31-32]. Chung and his co-workers further explored the use of different diamines and multi-arm amines with various immersion times as cross-linkers to post-treat polyimide flat sheet and hollow fiber membranes [33-42]. The modified membranes showed an enhanced CO_2/CH_4 selectivity and plasticization resistance but the permeability decreased [33]. Drawbacks of this method include methanol swelling, reversibility of amidation reaction at high temperatures and considerable time to dry the membranes[43]. Vapor-phase cross-linking was devised as an alternative to solution-phase cross-linking of polyimides. Another chemical cross-linking method is to synthesize the polyimide containing carboxylic acid that can be cross-linked by diols [44-45]. Coupled with thermal treatment, the transesterification reaction occurred and brought forth cross-linking reaction with the removal of pendant diol groups. As a result, it improves plasticization resistance and increases permeability. Besides the organic cross-linkers, inorganic cross-linkers like metal and metal salts and metal complexes like metal acetylacetonates are also employed to modify polyimide and other polymers [46-51]. The affinity of the ions with the polymer hinders the mobility of the polymer chains.

From the above research findings, the preferred cross-linking method would be one that (1) causes a minimum loss in membrane permeability, (2) occurs at low temperatures, (3) integrity of polymer backbone is kept and (4) resistance to plasticization. Therefore, in this work we aimto cross-link a 6FDA-based polymer by means of an ionic thermally labile unit and examine if it can be developed into gas separation membranes with good permeability and selectivity as well as resistance to plasticization. Iron (III) acetylacetonate (FeAc), which has not been studied before, is selected from a few metal acetylacetonates as the thermally labile and potential cross-linking unit. Iron (III) acetylacetonate consists of iron (III) ion which has high charge density to possibly cross-link the polymer chains to hinder their mobility, and organic acetylacetonate which can improve the compatibility with the matrix polymer

and then be removed easily upon annealing. For performance comparison, iron (III) chloride ($FeCl_3$) and acetylacetonate (Ac) areused as reference additives. This study may provide a feasibleapproach to develop high performance membranes for gas separation.

6.2 Results and discussion

6.2.1 Polymer and membrane characterizations

The 6FDA-based polyimide was synthesized by a two-step polycondensation method via poly(amic acid) as the intermediate. The viscosity of the reaction mixture in NMP increased as the molecular weight of poly(amic acid) increased. Chemical imidization was performed and the resultant polyimde had an inherent viscosity of 0.76 g/dL. Preliminary trial tests in the selection of metal acetylacetonate for cross-linking polyimide were conducted using three metal acetylacetonates with ions of different charge density; namely, silver acetylacetonate (+1), zinc acetylacetonate (+2) and iron (III) acetylacetonate (+3). Clear solutions of polymer/additive blends and homogenous annealed membranes were observed by visual inspection. Gel content tests revealed that only iron (III) acetylacetonate effectively cross-linked polyimide. The membrane blended with iron (III) acetylacetonate remained insoluble in NMP before and after heat treatment. On the other hand, the other two polymer/metal acetylacetonate membranes dissolved in NMP completely.

In view of the cross-linking effect brought by iron (III) acetylacetonate, iron (III) chloride and acetylacetonate were then used as the blank additives to compare with the PI-2 wt% FeAc membrane to understand the cross-linking mechanism of iron (III) acetylacetonate. The PI-1.75 wt% Ac membrane dissolved in NMP. This shows that iron (III) ion is required for cross-linking. Interestingly, the PI-1 wt% $FeCl_3$ membrane, which has iron (III) ions, dissolved in NMP too, possibly due to the aggregation of inorganic iron (III) chloride in the polymer matrix. As a result, the function of iron (III) ions towards crosslinking cannot be effectively manifested. An organic ligand is essential for iron (III) ions to be homogenously distributed in the polymer matrix. Hence, iron (III) acetylacetonate, with its highly charge density to cross-link the polymer and organic acetylacetonate group that aids compatibility with the polymer matrix, is chosen for further studies.Figure 6.1 depicts the uniform distribution of iron (III) element across an annealed and cross-linked PI-6 wt% FeAc membrane as observed by SEM-EDX.

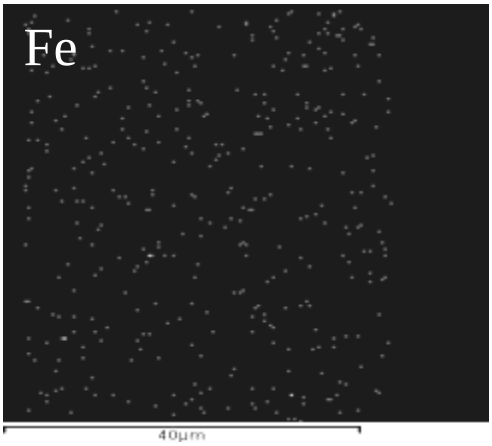

Figure 6.1 SEM-EDX scan of an annealed PI-6 wt% FeAc membrane

Figure 6.2 shows the thermal analyses of as-cast PI and PI-FeAc membranes and iron (III) acetylacetonate as a function of temperature. The iron (III) acetylacetonate powders show weight decline starting at about 180 ◦C. Three distinct regions of weight loss can be observed for the as-cast membranes. The first region takes place below 170 °C, it showed similar rates and weight declines of around 10 wt% for both PI and PI-FeAc membranes. This was mainly due to the removal of the residual NMP solvent from the membranes. When the temperature was increased to 200 °C and held for 15 minutes, different weight loss profiles were observed. PI-6 wt% FeAc and PI-2 wt% FeAc membranes have larger weight losses compared to the PI membrane owing to the evolution of the thermally labile acetylacetonate group. The PI-6 wt% FeAc membrane has a greater weight loss than the PI-2 wt% FeAc membrane because the former contains more iron (III) acetylacetonate than the latter. In the third region (i.e., 200 °C and held more than 15 minutes), the weight profiles gradually reach plateaus, indicating the complete thermal decomposition of acetylacetonate groups in the membranes. Since PI-FeAc membranes thermally treated at 200 °C for 30 minutes did not dissolve in NMP, they were chosen for further studies to examine (1) polymer structural changes due to the electrostatic cross-linking by iron (III) ions and the evolution of acetylacetonate and (2) their effects on gas separation performance.

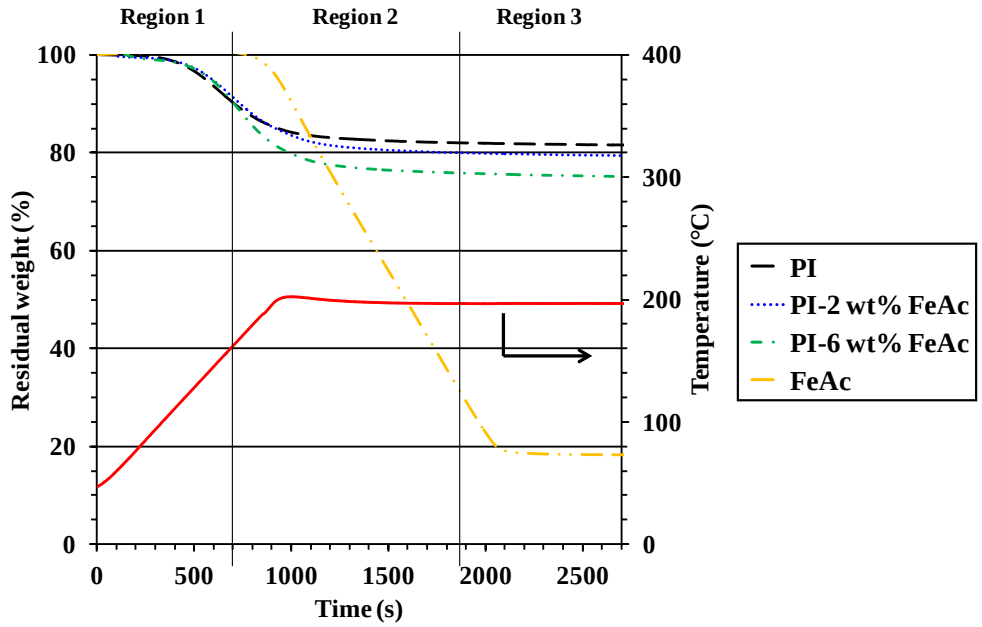

Figure6.2 Thermal analyses of the fabricated membranes and iron (III) acetylacetonate

The FTIR spectra, as shown in Figure6.3, confirm that the polymer backbone of the membranes is intact after the electrostatic cross-linking by iron (III) ions and thermal decomposition of acetylacetonate. The characteristic peaks of imide linkagessuch as (1) symmetric stretching of the C=O bond at approximately 1780 cm^{-1}, (2) asymmetric stretching of the C=O bond at 1716 cm^{-1}, (3) asymmetric stretching of the C-N bond at 1350 cm^{-1} and (4) asymmetric bending of the C=O bond at 717 cm^{-1}, are seen in the FTIR spectra of the pristine membrane. These peaks are also identified for the annealed PI-6 wt% Fe membrane. Clearly, the integrity of the polymer backbone remains intact. It could also be observed that the intensity of –OH peak at 3700 cm^{-1}, which is attributed to the carboxylic group of DABA, decreases upon the addition of iron (III) acetylacetonate. This agrees with the proposed schemethat there is interaction between the carboxylic acid group and iron (III) acetylacetonate.

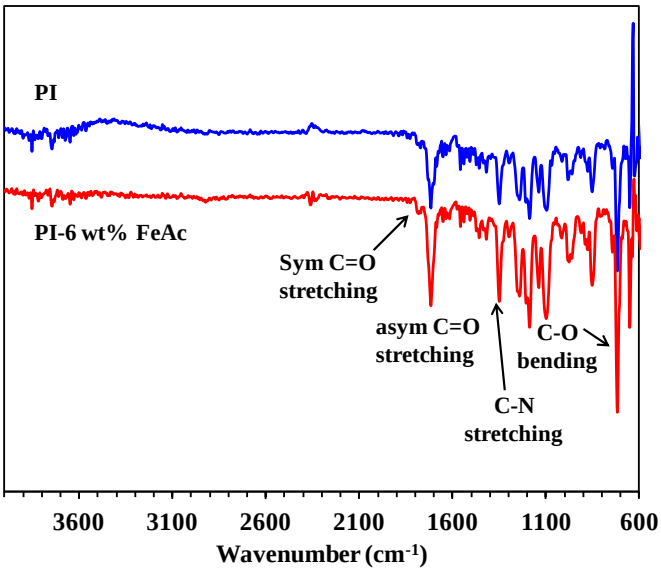

Figure6.3 FTIR spectra of annealed PI and PI-6 wt% FeAc membranes

Table 6.1 summarizes the gel content, glass transition (T_g) and density of annealed PI and PI-FeAc membranes. When the annealed membranes were immersed in NMP which was the original casting solvent, the PI membrane dissolved completely while PI-FeAc membranes stayed intact because they have high gel content of more than 89 wt%. Clearly, a cross-linked network was formed by adding a small amount of iron (III) acetylacetonate into the polyimide, followed by annealing at 200 °C. The formation of the cross-linked network was also evident from the T_g increment from 375 °C to 390 °C. A higher T_g is an indication of enhanced polymer chain rigidification resulting from the cross-linking reaction [52]. Though a cross-linked network was formed in the polymer matrix, a reduction in membrane density from 1.375 g/cm^3 to 1.296 g/cm^3 was noticed. It was speculated that the overriding factor to density reduction was the decomposition of the acetylacetonate group, which created micropores in the rigidified polymer matrix [28].

Table 6.1 Gel content, glass transition temperature and density of the membranes annealed at 200 °C for 30 min

	Gel content (wt%)	T_g (°C)	Density (g/cm^3)
PI	-	375	1.375
PI-2 wt% FeAc	89	377	1.350
PI-3 wt% FeAc	91	380	1.339
PI-6 wt% FeAc	95	390	1.296

6.2.2 Gas separation performance and transport properties

Table 6.2 shows the ideal gas permeability and selectivity of all the membranes measured at 35 °C and 2 atm. For comparison, PI-10 wt% FeAc, PI-1 wt% $FeCl_3$ and PI-1.75 wt% Ac membranes were also fabricated, annealed and tested. It can be observed that there is a significant increase in permeability for membranes consisting of iron (III) acetylacetonate from 2 to 6 wt%. A permeability increase of more than 88 % is achieved for the PI-6 wt% FeAc membrane as compared to that of the pristine PI membrane. This permeability enhancement is different from most conventional cases where cross-linking coupled with annealing tends to tighten polymer chains and reduce permeability. The iron (III) acetylacetonate not only performs as a cross-linker but also functions a micropore former during annealing, thus leads to an enhanced permeability.

Table 6.2 Pure gas permeability and selectivity of the annealed membranes tested at 2 atm

	Permeability (Barrer)						Selectivity		
	O_2	N_2	CH_4	CO_2	C_3H_6	C_3H_8	O_2/N_2	CO_2/CH_4	C_3H_6/C_3H_8
PI	95	25	20	465	17	1.5	3.8	23.4	12.0
PI-2 wt% FeAc	125	33	27	599	24	2.2	3.7	22.4	11.8
PI-3 wt% FeAc	143	39	31	700	28	2.4	3.7	22.3	11.7
PI-6 wt% FeAc	175	48	39	877	35	3.0	3.6	22.2	11.7
PI-10 wt% FeAc	166	46	40	821	32	2.8	3.6	20.5	11.4
PI-1 wt% $FeCl_3$	108	29	22	528	19	1.6	3.7	23.4	11.9
PI-1.75 wt% Ac	126	34	26	610	25	2.1	3.7	22.7	11.8

Since PI-Ac and PI-2 wt% FeAc membranes have similar relatively higher gas permeability and PI-1 wt% $FeCl_3$ and pristine PI membranes exhibit similar relatively lower gas permeability as shown in Table 6.2, these suggest that the evolution of acetylacetonate during annealing is the main cause of decreasing membrane density and increasing membrane permeability. However, permeability does not increase further if adding 10wt% iron (III) acetylacetonate into the polymer matrix. This could be due to aggregations of iron (III) acetylacetonate in the polymer matrix. As a result, the function of Fe^{3+} ions towards crosslinking is compromised. A very slight decrease in ideal selectivity is also observed with an increase in iron (III) acetylacetonate content. This may be attributed to the variations of physicochemical properties (i.e., sorption selectivity and diffusion selectivity) with different degrees of cross-linking reaction and the amounts of Fe^{3+} ions.

The CO_2 and CH_4 sorption behaviors of PI, PI-3 wt% FeAc and PI-6 wt% FeAc membranes were measured to further validate the variation in gas transport properties. As depicted in Figure6.4, the isotherms are concave to the pressure axis, which are typical for glassy polymers. Comparing CH_4 and CO_2 isotherms, the sorption concentration follows this order: PI < PI-3 wt% FeAc < PI-6 wt% FeAc membranes. Upon comparing the dual mode sorption parameters as tabulated inTable 6.3, the observed sorption increment is contributed by the increase in C'_H. C'_H is the Langmuir capacity constant, which is indicative of the microcavities and defects (excess free volume) in glassy polymers. The evolution of the acetylacetonate group at 200 °C from the blend membranes leaves extra micropores between polymer chains and results in free volume increase as observed in decreasing membrane density. As a result, the gas sorption increases with the concentration of iron (III) acetylacetonate.

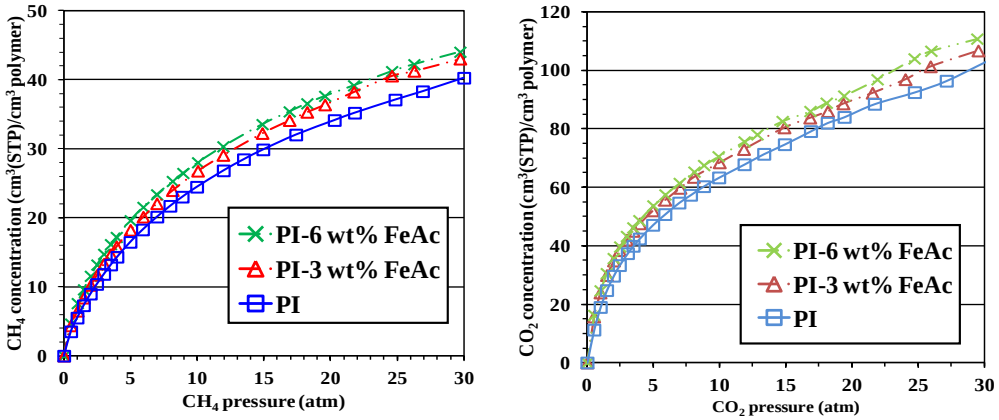

Figure6.4 Pure CH_4 and CO_2 sorption isotherms of the PI and PI-FeAc membranes

Table 6.3 Dual mode sorption parameters of the membranes

	Gas	k_D	C'_H	b
PI	CH_4	0.70	20.3	0.35
	CO_2	2.30	50.1	0.74
PI-3 wt% FeAc	CH_4	0.70	25.0	0.33
	CO_2	2.33	52.0	0.74
PI-6 wt% FeAc	CH_4	0.71	28.8	0.33
	CO_2	2.35	54.1	0.75

k_D: cm^3 (STP)/cm^3 (polymer) atm; C'_H: cm^3 (STP)/cm^3 (polymer); b: atm^{-1}

Table 6.4 shows and compares gas solubility and diffusivity between PI-6 wt% FeAc and pristine PI membranes. Both the solubility and diffusivity coefficients increase when the amount of iron (III) acetylacetonate added increases. However, the diffusivity coefficient has a higher percentage of increment than the solubility coefficient. Compared to the PI membrane, there is a 78% increase in D_{CO2}, 53 % in D_{CH4}, 28 % in S_{CH4} and 6 % S_{CO2} in the PI-6 wt% FeAc membrane. In addition, the solubility selectivity decreases while diffusivity selectivity increases. The excess free volume due to the formation of micropores by the decomposition of the acetylacetonate group allows more gas molecules to be soluble in the matrix, contributing to the decrease in solubility selectivity. The increase in diffusivity selectivity further proves the formation of a cross-linked structure.

Table 6.4 Solubility and diffusivity coefficients of the membranes at 2 atm

	S_{CH4}	D_{CH4}	S_{CO2}	D_{CO2}	S_{CO2}/S_{CH4}	D_{CO2}/D_{CH4}
PI	59.3	33.7	222	209	3.7	6.2
PI-3 wt% FeAc	67.3	46.8	228	307	3.4	6.6
PI-6 wt% FeAc	76.0	51.6	236	372	3.1	7.2

S: 10^{-3} cm^3 (STP)/cm^3 (polymer) cm Hg; D: 10^{-9} cm^2/s; Measurements were repeated within 1% error.

Figure6.5 plots the gas separation performance of the pristine and Fe^{3+} cross-linked membranes against the O_2/N_2, CO_2/CH_4 and C_3H_6/C_3H_8 upper bound curves. The annealed and cross-linked polyimides with the aid of iron (III) acetylacetonate shift gas transport properties towards the upper bound curves as the concentration of iron (III) acetylacetonate increases [6, 53]. For the C_3H_6/C_3H_8 gas pair, the gas separation performance of the PI-6 wt% FeAc membrane lies above the upper bound. Clearly, using iron (III) acetylacetonate as a cross-linking and micropore forming agent is a feasible strategy to surpass the trade-off line between permeability and selectivity.

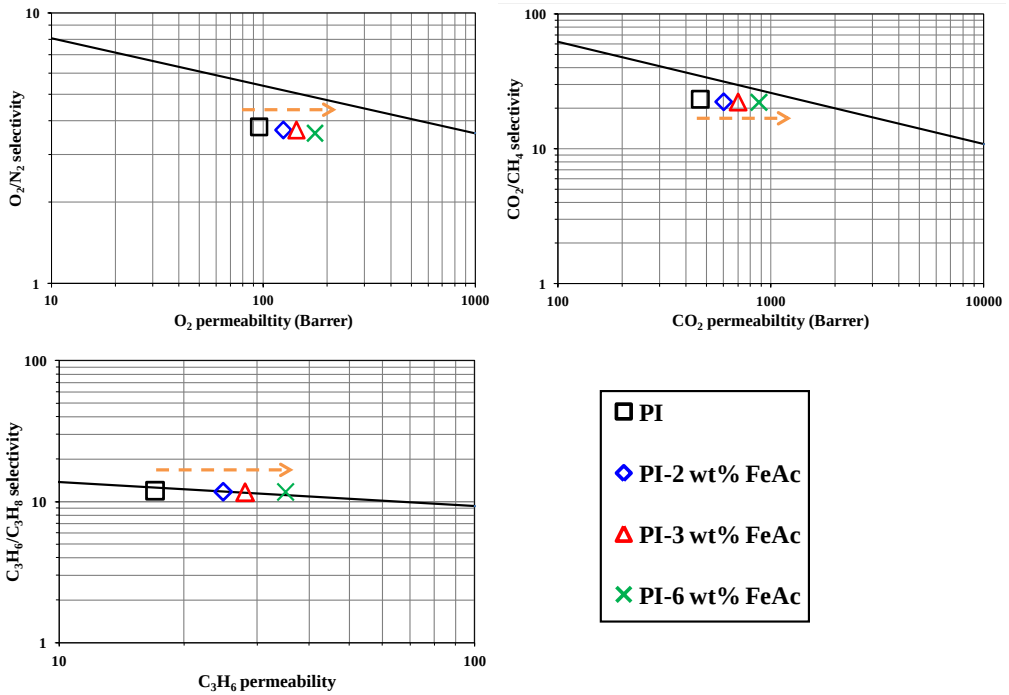

Figure6.5 Comparison with O_2/N_2, CO_2/CH_4 and C_3H_6/C_3H_8 upper bound

6.2.3 CO_2 plasticization and CO_2/CH_4 pure and binary gas tests

Figure 6.6 shows the plasticization behavior of PI, PI-Ac and PI-FeAc membranes as a function of CO_2 pressure from 0 to 30 atm in pure CO_2 tests. The initial decline in CO_2 permeability at low pressures is due to the saturation of Langmuir sites. As CO_2 pressure increases, these membranes behave differently. An upward increase in permeability for the pristine PI membrane occurs at 7 atm due to CO_2 swelling up polymer chains, increasing chain mobility and inter-chain spacing, thus allowing more CO_2 to permeate through. The PI-Ac membrane with no cross-linking is prone to plasticization like the pristine PI membrane. With the addition of a small amount of 2 wt% iron (III) acetylacetonate into the polyimide membrane, the plasticization pressure increases by two-fold. The PI-6 wt% FeAc membrane does not exhibit plasticization till 30 atm. The formation of a cross-linked network in the polyimide restricts chain mobility, hence suppresses plasticization by CO_2.

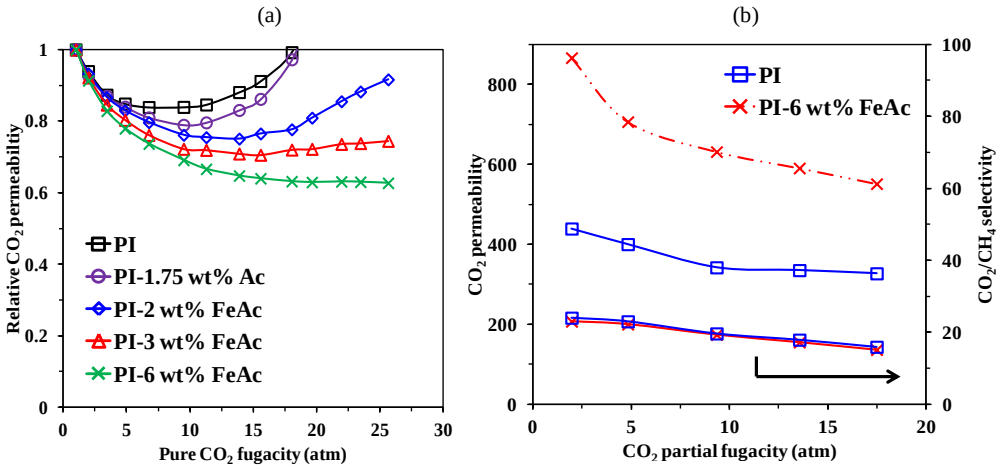

Figure 6.6 Resistance of the membranes against (a) increasing pure CO_2 feed pressure, (b) increasing CO_2/CH_4 binary gas feed pressure

The resilience of some aforementioned membranes towards a binary gas feed was also investigated. Table 6.5 compares the CO_2 and CH_4 permeability and CO_2/CH_4 selectivity of the PI and PI-6 wt% FeAc membranes when subjected to a 50:50 binary molar CO_2/CH_4 mixture at aCO_2 partial pressure of 2 atm. When the results are compared to the pure gas tests, there is only a small decline of less than 6% in gas permeability while the selectivity remains almost unchanged. The variations of CO_2 permeability and CO_2/CH_4

selectivity of these two membranes as a function of feed pressure in mixed gas tests were also studied. As shown in Figure 6b, both PI and PI-6 wt% FeAc membranes show declines in their CO_2 permeability and CO_2/CH_4 selectivity with an increase in feed pressure. Based on dual-mode sorption model for glass polymers, the reduction in CO_2 permeability is due to the saturation of Langmuir sites. Since CO_2 has a higher condensability than CH_4, the former has a greater drop in permeability than the latter. As a consequence, the CO_2/CH_4 selectivity of both membranes decreases with increasing feed pressure. However, the plasticization pressure of the pristine PI membrane occurs at CO_2 partial pressure of 12 atm while the cross-linked PI-6 wt% FeAc membrane exhibits no plasticization till CO_2 partial pressure of 20 atm. The improvement in plasticization resistance of the pristine PI membrane could be attributed to the presence of CH_4 which reduces the CO_2 plasticizing effect on the membrane [54]. Nevertheless, the high resistance of the PI-6 wt% FeAc membrane against CO_2 inducedplasticization suggests that the use of iron (III) acetylacetonate as both a cross-linker and micropore former may have potential to develop novel gas separation membranes.

Table 6.5 Binary gas permeability and selectivity of the membranes at CO_2 partial pressure of 2 atm and 35 ^oC

	P_{CH4} (Barrer)	P_{CO2} (Barrer)	$\alpha_{CO2/CH4}$
PI	19 (20)	439 (465)	23.0 (23.4)
PI-6 wt% FeAc	38 (39)	866 (877)	22.7 (22.2)

* Results in parentheses are obtained from pure gas tests

6.3 Conclusion

In this study, membranes of a 6FDA-polyimide blending with iron (III) acetylacetonate have been fabricated. The structural changes and gas transport properties of the membranes due to electrostatic cross-linking and thermal decomposition of iron (III) acetylacetonate have been investigated.

(1) The formation of cross-linked network is evident from the gel content measurements of the annealed PI-FeAc membranes and the increase in the glass transition temperature. Though cross-linking typically leads to tightening of polymer chains, a reduction in the density of the annealed PI-FeAc membranes is observed. TGA analyses of the fabricated PI-FeAc membranes reveal larger weight losses at 200 °C compared to the pristine PI membrane. Hence, the reduction in membrane density is attributed to the evolution of the thermally labile acetylacetonate group during annealing at 200 °C, which leaves micropores in the rigidifed polymer.

(2) In pure gas tests, a significant increase in membrane permeability with the concentration of iron (III) acetylacetonate is attained. Both solubility and diffusivity coefficients increase. However, the increase in diffusivity coefficient has a higher magnitude than that in solubility coefficient because of the formation of a cross-linking network and micropores.

(3) The newly developed cross-linked polyimide show enhanced resistance against CO_2 induced plasticization in both pure CO_2 and binary CO_2/CH_4 tests. In binary gas tests, only a small decline in membrane permeability is observed while the selectivity remains almost unchanged.

In summary, the approach of incorporating iron (III) acetylacetonate to cross-link a 6FDA-based polyimide containing carboxylic acid group not only improves the plasticization resistance of the membranes, but also enhances the gas transport properties.

References:

[1] R. W. Baker, K. Lokhandwala, Natural gas processing with membranes: an overview, Ind. Eng. Chem. Res. 47 (2008) 2109-2121.

[2] N. Peng, N. Widjojo, P. Sukipaneenit, M. M. Teoh, G. G. Lipscomb, T. S. Chung, J. Y. Lai, Evolution of polymeric hollow fibers as sustainable technologies: Past, present, and future, Prog. Polym. Sci. 37 (2012) 1401-1424.

[3] D. F. Sanders, Z. P. Smith, R. Guo, L. M. Robeson, J. E. McGrath, D. R. Paul, B. D. Freeman, Energy-efficient polymeric gas separation membranes for a sustainable future: a review, Polymer 54 (2013) 4729-4761.

[4] X. He, M. B. Hägg, Membranes for environmentally friendly energy processes, Membranes 2 (2012) 706-726.

[5] Y. Xiao, B. T. Low, S. S. Hosseini, T. S. Chung, D. R. Paul, The strategies of molecular architecture and modification of polyimide-based membranes for CO_2 removal from natural gas – A review, Prog. Polym. Sci. 34 (2009) 561-580.

[6] L. M. Robeson, The upper bound revisited, J. Membr. Sci. 320 (2008) 390-400.

[7] B. W. Rowe, L. M. Robeson, B. D. Freeman, D. R. Paul, Influence of temperature on upper bound: theoretical considerations and comparison with experimental results, J. Membr. Sci. 360 (2010) 58-69.

[8] D. J. Liaw, K. L. Wang, Y. C. Huang, K. R. Lee, J. Y. Lai, C. S. Ha, Advanced polyimide materials: syntheses, physical properties and applications, Prog. Polym. Sci. 37 (2012) 907-974.

[9] H. Ohya, V. V. Kudryavtsev, S. I. Semenova, Polyimide membranes: applications, fabrications and properties, Kodansha Japan and Gordon and Breach Science Publishers, 1996.

[10] C. E. Sroog, Polyimides, Prog. Polym. Sci. 16 (1991) 561-694.

[11] S. A. Stern, Y. Mi, H. Yamamoto, Structure/permeability relationships of polyimide membranes. Applications to the separation of gas mixtures, J. Polym. Sci. Part B: Polym. Phys 27 (1989) 1887–909.

[12] M. R. Coleman, W. J. Koros, Isomeric polyimides based on fluroinated dianhydrides and diamines for gas separation applications, J. Membr. Sci. 50 (1990) 285-297.

[13] S. X. Cheng, T. S. Chung, R. Wang, R. H. Vora, Gas-sorption properties of 6FDA-durene/1,4-phenylenediamine (pPDA) and 6FDA-durene/1,3-phenylenediamine (mPDA) copolyimdes, J. Appl. Polym. Sci. 90 (2003) 2187-2193.

[14] D. Ayala, A. E. Lozano, J. D. Abajo, C. G. Perez, J. G. Campa, K. V. Peinemann, B. D. Freeman, R. Prabhakar, Gas separation properties of aromatic polyimides, J. Membr. Sci. 215 (2003) 61–73.

[15] Y. A´lvarez-Gallego, S. P. Nunes, A. E. Lozano, J. G. de la Campa, J. de Abajo, Synthesis and properties of novel polyimides bearing sulfonated benzimidazole pendant groups, Macromol. Rapid Commun. 28 (2007) 616-622.

[16] S. Xiao, X. Feng, R. Y. M. Huang, Synthetic 6FDA-ODA copolyimide membranes for gas separation and pervaporation: correlation of separation properties with diamine monomers, Polym. Eng. Sci. 48 (2008) 795-805.

[17] E. S. Sanders, Penetrant-induced plasticization and gas permeation in glassy polymers, J. Membr. Sci. 37 (1998) 63-80.

[18] L. M. Robeson, Polymer blends in membrane transport processes, Ind. Eng. Chem. Res. 49 (2010) 11859-11865.

[19] T. S. Chung, L. Y. Jiang, Y. Li, S. Kulprathipanja, Mixed matrix membranes (MMMs) comprising organic polymers with dispersed inorganic filters for gas separation, Prog. Polym. Sci. 32 (2007) 483-507.

[20] M. A. Aroon, A. F. Ismail, T. Matsuura, M. M. Montazer-Rahmati, Performance studies of mixed matrix membranes for gas separation: A review, Sep. Sci. Technol. 75 (2010) 229-242.

[21] H. Kita, T. Inada, K. Tanaka, K. I. Okamoto, Effect of photocrosslinking on permeability and permselectivity of gases through benzophenone-containing polyimide, J. Membr. Sci. 87 (1994) 139-147.

[22] J. Won, M. H. Kim, Y. S. Kang, H. C. Park, U. Y. Kim, S. C. Choi, S. K. Koh, Surface modification of polyimide and polysulfone membranes by ion beam for gas separation, J. Appl. Polym. Sci. 75 (2000) 1554–60.

[23] L. Hu, X. Xu, M. R. Coleman, Effect of H^+ and N^+ irradiation on structure and permeability of the polyimide Matrimid, Sep. Sci. Tech. 43 (2008) 4030-4055.

[24] A. Bos, I. G. M. Pünt, M. Wessling, H. Strathmann, Plasticization-resistant glassy polyimide membranes for CO_2/CH_4 separations, Sep. Purif. Tech. 14 (1998) 27-39.

[25] J. N. Barsema, S. D. Klijnstra, J. H. Balster, N.F.A. van der Vegt, G. H. Koops, M. Wessling, Intermediate polymer to carbon membranes based on Matrimid PI, J. Membr. Sci. 238 (2004) 93-102.

[26] A. M. Kratochvil, W. J. Koros, Decarboxylation-induced cross-linking of a polyimide for enhanced CO_2 plasticization resistance, Macromolecules 41 (2008) 7920-7927.

[27] W. Qiu, C.-C. Chen, L. Xu, L. Cui, D. R. Paul, W. J. Koros, Sub-T_g cross-linking of a polyimide membrane for enhanced CO_2 plasticization resistance for natural gas separation, Macromolecules 44 (2011) 6046-6056.

[28] Y. C. Xiao, T. S. Chung, Grafting thermally labile molecules on cross-linkable polyimide to design membrane materials for natural gas purification and CO_2 capture, Energy & Environ. Sci. 4 (2011) 201-208.

[29] M. Askari, Y. C. Xiao, T. S. Chung, Natural gas purification and olefin/paraffin separation using cross-linkable 6FDA-Durene/DABA co-polyimides grafted with α, β and γ-cyclodextrin, J. Membr. Sci. 390-391 (2012) 141-151.

[30] M. L. Chua, Y. C. Xiao, T. S. Chung, Effects of thermally labile saccharide units on the gas separation performance of highly permeable polyimide membranes, J. Membr. Sci. 415-416 (2012) 375-382.

[31] R. A. Hayes, Polyimide gas separation membranes, E. I. Du Pont de Nemours and Company, US patent 4,717,393 (5 January 1988).

[32] R. A. Hayes, Amine-modified polyimide membranes, E. I. Du Pont de Nemours and Company, US patent 4,981,497 (1 January 1991).

[33] Y. Liu, R. Wang, T. S. Chung, Chemical cross-linking modification of polyimide membranes for gas separation, J. Membr. Sci. 189 (2001) 231–239.

[34] C. Cao, T. S. Chung, Y. Liu, R. Wang, K. P. Pramoda, Chemical cross-linking modification of 6FDA-2,6-DAT hollow fiber membranes for natural gas separation, J. Membr. Sci. 216 (2003) 257–68.

[35] P. S. Tin, T. S. Chung, R. Wang, Y. Liu, S. L. Liu, K. P. Pramoda, Effects of crosslinking modification on gas separation performance of Matrimid membranes, J. Membr. Sci. 225 (2003) 77–90.

[36] L. Shao, T. S. Chung, S. H. Goh, K. P. Pramoda, Polyimide modification by a linear aliphatic diamine to enhance transport performance and plasticization resistance, J. Membr. Sci. 256 (2005) 46–56.

[37] Y. C. Xiao, T. S. Chung, M. L. Chng, Surface characterization, modification chemistry and separation performance of polyimide and PAMAM dendrimer composites, Langmuir 20 (2004) 8230–8238.

[38] L. Shao, T. S. Chung, S. H. Goh, K. P. Pramoda, Transport properties of cross-linked polyimide membranes induced by different generations of diaminobutane (DAB) dendrimers, J. Membr. Sci. 238 (2004) 153-163.

[39] B. T. Low, Y. C. Xiao, T. S. Chung, Y. Liu, Simultaneous occurrence of chemical grafting, cross-linking, and their etching on the surface of polyimide membranes and their impact on H_2/CO_2 separation, Macromolecules 41 (2008) 1297-1309.

[40] L. Shao, C. H. Lau, T. S. Chung, A novel strategy for surface modification of polyimide membranes by vapor-phase ethylenediamine (EDA) for hydrogen purification, Int. J. Hydrogen Energy 34 (2009) 8716-8722.

[41] C. H. Lau, B. T. Low, L. Shao, T. S. Chung, A vapor-phase surface modification method to enhance different types of hollow fiber membranes for industrial scale hydrogen separation, Int. J. Hydrogen Energy 35 (2010) 8970-8982.

[42] H. Wang, D. R. Paul, T. S. Chung, Surface modification of polyimide membranes by diethylenetriamine (DETA) vapor for H_2 purification and moisture effect on gas permeation, J. Membr. Sci. 430 (2013) 223-233.

[43] C. E. Powell, X. J. Duthie, S. E. Kentish, G. G. Qiao, G. W. Stevens, Reversible diamine cross-linking of polyimide membranes, J. Membr. Sci. 291 (2007) 199-209.

[44] C. Staudt-Bickel, W. J. Koros, Improvement of CO_2/CH_4 separation characteristic of polyimides by chemical crosslinking, J. Membr. Sci. 155 (1999) 145–154.

[45] J. D. Wind, C. Staudt-Bickel, D. R. Paul, W. J. Koros, Solid-sate covalent cross-linking of polyimide membranes for carbon dioxide plasticization reduction, Macromolecules 36 (2003) 1882–1888.

[47] S. Yoda, A. Hasegawa, H. Suda, Preparation of a platinum and palladium/polyimide nanocomposite film as a precursor of metal-doped carbon molecular sieve membrane via supercritical impregnation, Chem Mater 16 (2004) 2363–2368.

[48] F. Li, Y. Li, T. S. Chung, S. Kawi, Facilitated transport by hybrid POSS®–Matrimid®–Zn^{2+} nanocomposite membranes for the separation of natural gas, J. Membr. Sci. 356 (2010) 14-21.

[49] M. B. Davydova, Y. P. Yampol'skii, N. K. Gladkova, S. G. Durgaryan, Permeability through membranes prepared from polyvinylmethylsilane with transition metal acetylacetonate additives, Polym. Sci. U. S. S. R. 30 (1988) 545-551.

[50] C. C. Chao, D. S. Tsai, Si-Al-C gas separation membranes derived from polydimethylsilane and aluminium acetylacetonate, J. Membr. Sci. 192 (2001) 209-216.

[51] J. D. Wind, C. Staudt-Bickel C, D. R. Paul, W. J. Koros, The effect of crosslinking chemistry on CO_2 plasticization of polyimide gas separation membranes, Ind. Eng. Chem. Res. 4 (2002) 6139–6148.

[52] M. L. Chua, L. Shao, B. T. Low, Y. C. Xiao, T. S. Chung, Polyetheramine-polyhedral oligomeric silsequioxane organic-inorganic hybrid membranes for CO_2/H_2 and CO_2/N_2 separation, J. Membr. Sci. 385-386 (2011) 40-48.

[53] R. L. Burns, W. J. Koros, Defining the challenges for C_3H_6/C_3H_8 separation using polymeric membranes, J. Membr. Sci. 211 (2003) 299-309.

[54] J. Z. Xia, T. S. Chung, D. R. Paul, Physical aging and carbon dioxide plasticization of thin polyimide films in mixed gas permeation, J. Membr. Sci. 450 (2014) 457-468.

Chapter 7: Polyetheramine–polyhedral oligomeric silsesquioxane organic–inorganic hybrid membranes

7.1 Introduction

The typical separation of carbon dioxide from gas mixtures using amine absorption is an energy-intensive process and it involves the need to regenerate the solvent. Membrane technology offers an attractive alternative to amine absorption due to its higher energy efficiency, small footprint and environmental friendliness feature [1]. A suitable candidate for fabricating gas separation membranes is polymeric materials as the cost is low and it can be easily processed into different configurations [2]. However, the relatively low performance of commercial polymers and the sensitivity towards harsh process conditions of gas streams (pressure, temperature, high flow rates) are some of the drawbacks of polymeric membranes [3-4]. This drives the researchers to develop membrane materials that exhibit better performance and that are robust enough for long-term operations.

Over the last few years, poly(ethylene oxide) (PEO), a semi-crystalline polymer, has gained interests as a feasible material to fabricate carbon dioxide-selective membranes for carbon dioxide/hydrogen (CO_2/H_2) and carbon dioxide/nitrogen (CO_2/N_2) separations [5-14]. Its strong affinity to carbon dioxide due to the polar ether groups present allows preferential removal of carbon dioxide. However, its shortcomings such as tendency to crystallize due to its semi-crystalline nature and weak mechanical strength have restricted its applications [5]. Incorporating PEO with other monomers as copolymers or as polymer blends or crosslinking it are some of the strategies done to overcome the drawbacks of PEO and improve the gas separation performance. Okamoto and co-workers fabricated PEO-segmented copolymers with various hard segments [6]. Peinemann's group blended different low molecular weights of poly(ethylene glycol) (PEG) with synthesized PEO-PBT (Poly(butylene terephthalate) and commercial Pebax® respectively [7-8]. Enhancement in the gas separation performance of the membranes was observed. CO_2 permeability increased by eight-fold to more than 850 Barrer for the Pebax membrane blended with 50 wt% of PEG-dimethyl ether. The CO_2/N_2 selectivity was 31. Reijerkerk et al. also attempted

to blend an additive, PDMS (poly(dimethyl siloxane))-PEG, into Pebax with the aim to enhance the membraneperformance with the aid of highly permeable and flexible PDMS and highly selective PEO [9]. CO_2 permeability was improved by five times to 530 Barrer at 50 wt% of PDMS-PEG. The increase in permeability was mainly ascribed to the increase in diffusivity due to the incorporation of PDMS. Freeman's group applied ultraviolet light to crosslink different ratios of PEG diacrylate (PEGDA) and PEG methyl ethyl acrylate (PEGMEA) [10]. The resultant structure had a hyperbranched network in which crystallisation of PEO was restricted. Siloxane-based monomers were incorporated with PEO acrylates with the intention to increase permeability [11-12]. The CO_2 permeability was enhanced while the selectivity decreased. Shao and Chung also explored the addition of silane as acrosslinking agent to form PEO-based membranes. This strategy hindered the formation of crystals which in turn increased the permeability of PEO [13]. Further studies by grafting PEG methacrylate (PEGMA) and blending PEG into the polymer matrix had improved the performance of the membranes significantly by 5 folds and 2.5 folds, respectively [14-15]. Thus, combining with highly permeable groups and fabricating it as an organic-inorganic hybrid network seems to be a promising strategy to enhance the inherent properties of CO_2-selective PEO.

Polyhedral oligomeric silsesquioxane (POSS), a molecule with cage-like rigid structure of particle size ranging from 1 to 3 nm, may be another suitable candidate to crosslink PEO to attain high performance gas separation membranes. The functional side groups available on the POSS cage structure allow POSS molecules to possess good chemical reactivity and compatibility with many polymer systems [16]. Furthermore, the small particle size of POSS enables it to have better dispersion at molecular level in the membranes [17-18]. The formation of a crosslinked network may disrupt the PEO crystals arrangement and potentially reduce the crystallinity. In addition, the bulky POSS molecules may aid to increase free volume and the cage may provide a possible pathway for gas transport. Simulation results showed that the distance between two diametrical opposite silicon atoms in each face was approximately 4.442 Å, which is larger than the kinetic diameter of carbon

dioxide and nitrogen [19]. An attempt by Dominguez et al. to exploit the above-mentioned advantages of POSS molecules has demonstrated that the permeability of oxygen and nitrogen increased with the inclusion of POSS with polystyrene as copolymers [20]. This rise in permeability could be attributed to the increase in free volume contributed by the bulky POSS molecules.

In this study, we aim to explore the feasibility of fabricating an organic-inorganic hybrid membrane combining the various advantages of a polyetheramine (PEA), which contains predominately PEO backbone, and POSS for CO_2/H_2 and CO_2/N_2 separation, which are the major components in the pre-combustion and post-combustion capture of carbon dioxide respectively. Different compositions of PEAand POSS are fabricated. The physiochemical and mechanical properties of the membranes are characterized and the effects of varying POSS composition, testing pressure and temperature on gas performance of the membranes are evaluated.

7.2 Results & Discussion

7.2.1 Membrane fabrication and structure verification

One of the challenges encountered in the fabrication of membranes consisting PEO and silica-containing monomers is the compatibility between the organic and inorganic segments [11, 21]. As mentioned earlier, POSS have functional side groups which provide chemical reactivity. With eight epoxy functional groups, it could potentially make POSS molecules more compatible with PEA and crosslink it to fabricate organic-inorganic hybrid membranes. The POSS cage with another side group, epoxycyclohexyl, is the first monomer to be tried before glycidyl POSS. The bulky epoxycyclohexyl group is chosen with the aim to increase the free volume of the membrane. Following the fabrication procedure, the solution ofPEA and POSS cages with epoxycyclohexyl side groups is casted in the oven. However, only a viscous liquid is obtained upon the evaporation of solvent in the oven. The membrane is formed after annealing at 120°C, suggesting that the epoxy-amine reaction may occur slowly and high extent of crosslinking is achieved only at higher temperatures. Thereafter, POSS cages with glycidyl groups are used to cross-link PEA. A dried film is obtained. The aliphatic group next to the epoxy functional group makes the ring-opening reaction between epoxy and amino groups occur at a lower temperature. The membrane is annealed for complete reaction and removal of residual solvent. The glycidyl POSS cage mixture is selected for further study. The composition of PEA and POSS with glycidyl side groups is varied according to weight percentage (90:10, 80:20, 70:30, 50:50 and 30:70) and the membranes are used for characterizations and gas permeation.

As illustrated in Figure7.1, FTIR-ATR results confirm the structure of the resultant membranes and verify that the crosslinking reaction has occurred. Pure PEA has characteristic peaks at approximately 2862 cm^{-1}, 1454 cm^{-1} and 1083 cm^{-1} which corresponds to the stretching of the C-H bond, the scissoring of the H-C-H bondand the stretching of the C-O-C bond, respectively [22]. When the composition of POSS increases, it can be observed that similar peaks corresponding to the PEO structure exist and new peaks appear at approximately 3300-3600 cm^{-1} (stretching of O-H or N-H bond), 1630 cm^{-1}

(scissoring of N-H bond) and 1015 cm^{-1} (stretching of Si-O-Si bond). The peak at 1015 cm^{-1} corresponds to the POSS cage while the two other peaks prove the occurrence of the epoxy-amine reaction between PEA and POSS and the intensity increases when the POSS content increases. For the peak that appears at approximately 1730 cm^{-1}, it corresponds to the stretching of carbonyl group which is unexpected. It should not be a product of the crosslinking reaction. In addition, it could be observed that the intensity of the peak increases with the increase in POSS content. Therefore, it could be due to the impurity in POSS.

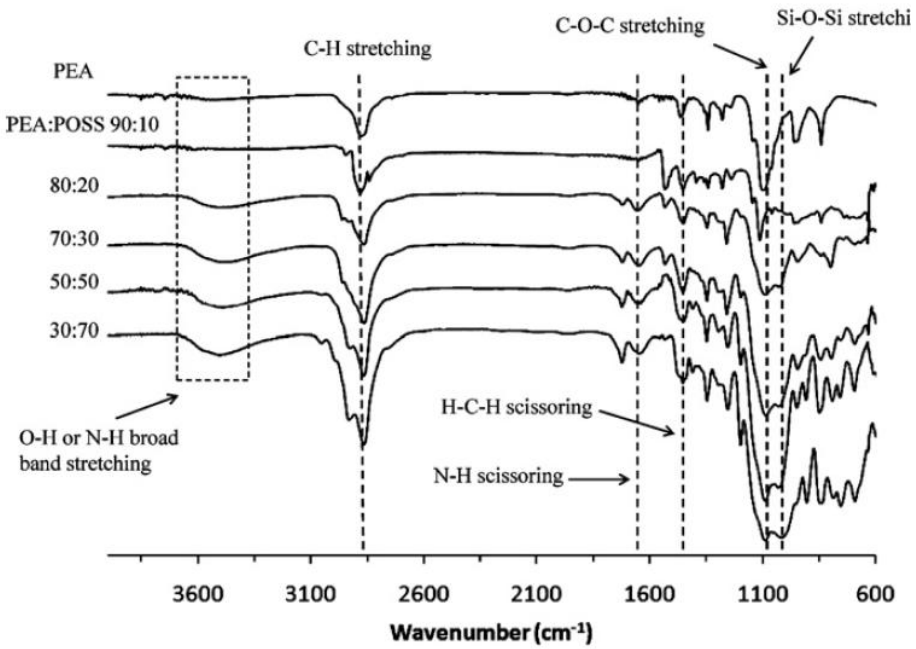

Figure 7.1 FTIR spectra of the hybrid membranes

A uniform distribution of silicon element across the membranes as seen from an example of the SEM-EDX analysis of the cross-section of the PEA:POSS 50:50 membrane in Figure7.2 is attributed to two factors: (1) a good compatibility between organic PEA and inorganic POSS due to the functional organic groups on the POSS cage and (2) the nano particle size of POSS allowing it to be able to disperse and react with PEA.

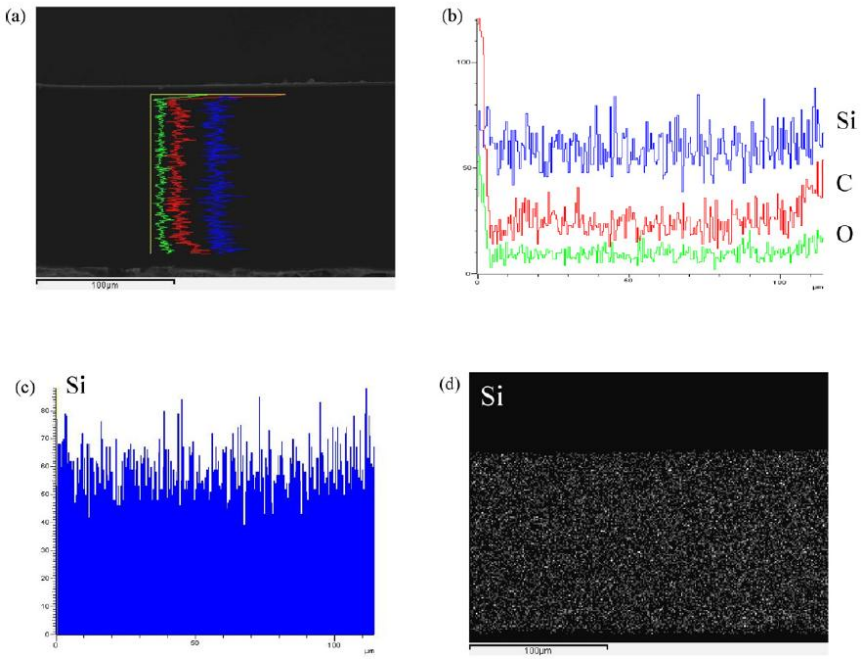

Figure 7.2 SEM-EDX results of the cross-section of the PEA:POSS 50:50 membrane
(a)–(c) Line-scan of the cross-section
(d) Distribution of silicon element through elemental mapping of the cross-sectional area

Figure7.3 shows the variation of density with the amount of POSS in the hybrid membranes measured using the gas pycnometer. The increase in membrane density with the addition of POSS could be attributed to the higher crosslinking extent between PEA and POSS and the higher density of POSS starting materials. In addition, it is observed that the density for the PEA:POSS 30:70 membrane seems to deviate further from the others. It is speculated that the affinity between the PEA chains becomes weaker at low PEA content and they interpenetrate with POSS molecules. As a result, the fractional free volume decreases and the density increases. The higher crosslinking extent and interpenetration of PEA in POSS may cause rigidification of PEA chains and partial pore blockage, which would in turn affect the chain mobility and the gas permeability (will be discussed later)[23-24].

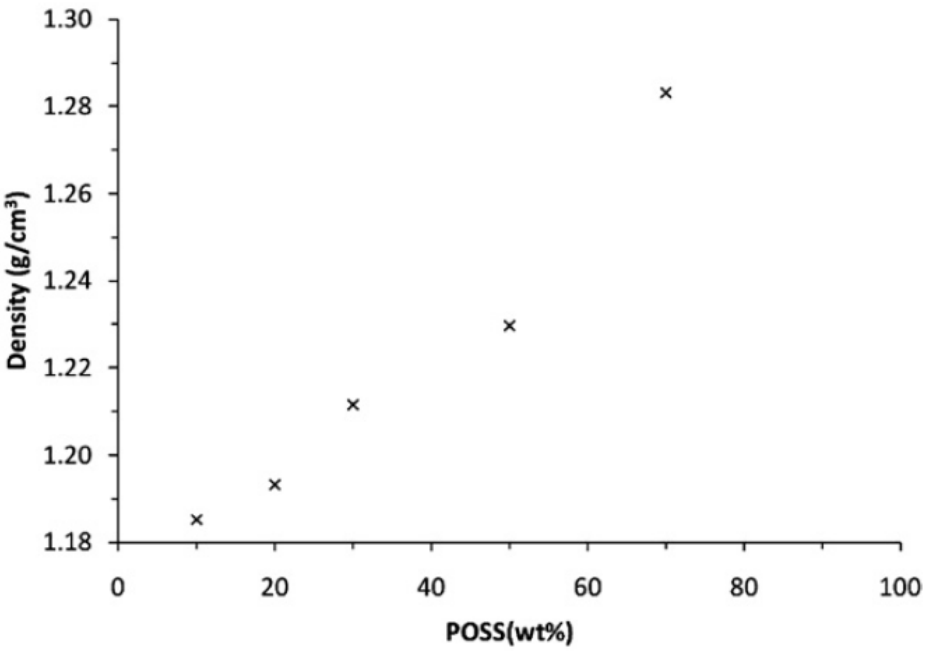

Figure 7.3 Density of the hybrid membranes measured using the gas pycnometer

Figure7.4 shows the XRD spectra of the membranes. Sharp crystal peaks at 2θ = 19.1° and 23.1° can be vividly seen for the membrane with 90 wt% of PEA and 10% of POSS. These two peaks are characteristic peaks of crystalline PEO, which are in consistent with other literature [25-26]. Hence, for the membrane with 10 wt% of POSS, the degree of crystallinity in the network is still very high. As mentioned previously, PEO have strong solubility selectivity to CO_2 but one of its drawbacks is the tendency for linear PEO chains to crystallize. The crystals are impermeable for gas transport. Crosslinking is a strategy to disrupt the orderly packing of PEO segments. A broad amorphous peak is detected and absence of PEO crystal peak is observed for the membranes with higher POSS content. This indicates that the PEO crystallization is successfully restricted by POSS.

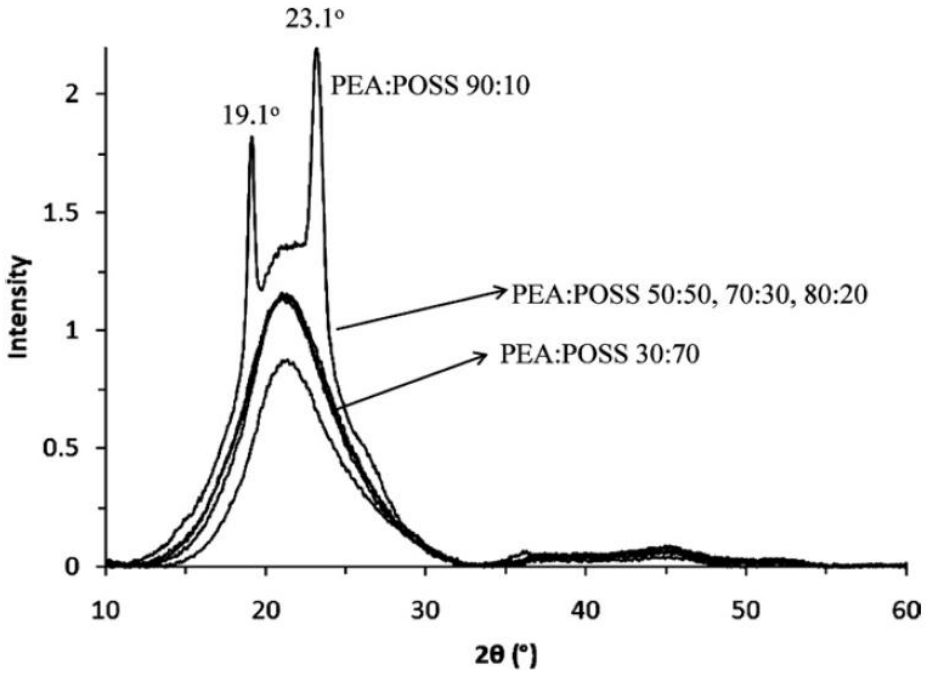

Figure 7.4 XRD spectra of the hybrid membranes

7.2.2 Thermal and mechanical properties of the membranes

The degree of crystallinity in the membranes could also be examined using DSC. Figure 7.5 shows the second heating curve of the membranes. The temperature equivalent to the midpoint of the gradual heat change at approximately - 50 to - 60 °C is the glass transition temperature (T_g) of the membranes. The low T_g is a feature of rubbery materials. T_g of the membranes becomes more obvious for higher POSS content. The magnitude of T_g shifts to the higher temperature range when the weight percentage of POSS increases from 30 (-57.0 °C) to 50 (-56.7 °C) to 70 (-55.0 °C). This is due to the rigidifying of the PEA chains by POSS. This observation is seen in other literature. It agrees with the results from the density measurement in Figure 7.3. The higher crosslinking extent of PEA with POSS results in a higher density and T_g, which may produce a smaller fractional free volume (FFV) in the membranes.

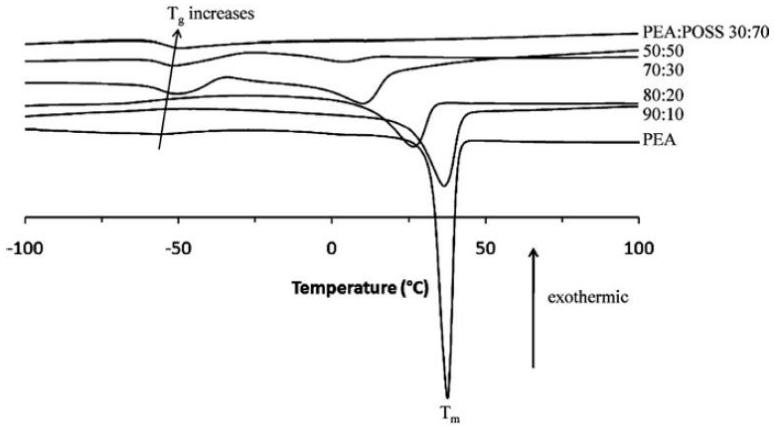

Figure 7.5 Second heating DSC curves for the hybrid membranes

An endothermic peak which corresponds to the melting point (T_m) of the crystalline PEA segments can be observed for some of the compositions. The PEA used in this study has a melting point of 37.4 °C. The melting point shifts to the lower temperature range for a higher composition of POSS. It decreases from 37.4 °C (PEA) to 36.2 °C (PEA:POSS 90:10) to 25.5 °C (PEA:POSS 80:20) to 8.6 °C (PEA:POSS 70:30) to 2.6 °C (PEA:POSS 50:50). For the membrane with 70 wt% of POSS, no obvious endothermic peak can be observed. The crosslinking of POSS with PEA completely disrupts the chain arrangement of PEA to form crystals. The results from DSC coincide with that from XRD as discussed in the previous section. The XRD experiment is carried out at room temperature. PEA:POSS 90:10, which has crystal peaks in the XRD results, has shown a melting point of 36.2 °C. The membrane still contains a significant amount of crystallinity at room temperature. These two results show good agreement. The other compositions, which have lower melting points, exhibit amorphous peak.

TGA was performed to analyze the thermal stability of the membranes. The residual weight of the membranes was plotted against the increase in the heating temperature in Figure7.6. The degradation temperature (T_d) is defined as the temperature at which the weight of the sample is decreased by 5% [27]. PEA has the lowest T_d of 337 °C. The increment of POSS content shifts the degradation temperature to the right and increases the residual weight at the end of the experiment. The thermal stability of PEA is improved in the range of 20 °C to 30 °C.

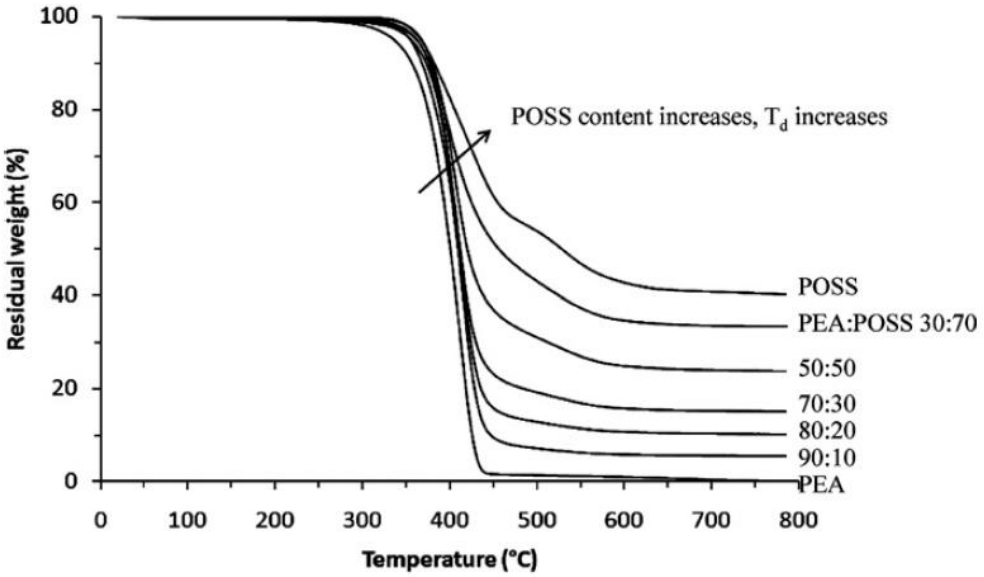

Figure 7.6 TGA curves of the hybrid membranes

A robust membrane with strong mechanical strength is crucial for usage in real industrial applications. Hence, data regarding the Young's modulus and hardness of the membranes are critical. It is observed that limited information about the mechanical strength of other crosslinked PEO networks in the literature was provided. In this study, the mechanical strength of the membranes was tested using a nano-indentor. The results are listed in Table 7.1. The Young's modulus and hardness of the PEA:POSS hybrid membranes doubles when the weight percentage of POSS increases from 20 to 30 and remain fairly constant for higher compositions of POSS. The mechanical strength of the membranes is enhanced from the formation of crosslinked network and the presence of the inorganic POSS.

Table 7.1 Young's modulus and hardness of the hybrid membranes

Ratio of PEA POSS	Young's modulus (MPa)	Hardness (MPa)
30:70	18.4 ± 0.8	4.44 ± 0.21
50:50	18.0 ± 0.4	4.54 ± 0.29
70:30	19.5 ± 1.3	4.33 ± 0.50
80:20	10.1 ± 1.1	1.65 ± 0.33

7.2.3 Gas permeation performance

As concluded from the previous results, the crosslinking of PEA and POSS has resulted in inorganic-organic hybrid membranes with reduced crystallinity and enhanced mechanical strength. Next, the gas permeation performance was measured. The pure gas was fed at 1 bar and the operating temperature was varied from 30 °C to 50 °C. The PEA:POSS 90:10 hybrid membrane has a low CO_2 permeability of 194 at 30 °C as there is a significant amount of crystals in the membrane which inhibits the gas transport and the CO_2 permeability increases tremendously to 821 at 50 °C due to the melting of the crystals. The H_2, N_2 and CO_2 permeability and the CO_2/H_2 and CO_2/N_2 selectivity of the membranes with other compositions at 30 °C to 50 °C are listed in Table 7.2. The fabricated hybrid membranes in this study possess higher permeability than semi-crystalline PEO, which exhibited a CO_2 permeability of 13 Barrers at 35 °C and 4.5 bar [28]. One point to be noted is that the melting of PEO may lead to the destruction of the membrane structure due to the lack of a force to support the structure. However, in this study, the reaction of PEA and POSS strengthens the membrane structure as seen from the nano-indention results. Hence, the structural integrity is maintained.

The activation energy for permeation in Table 7.3 is computed based on the Arrhenius equation [29].

$$P = P_o \exp\left(\frac{-E_p}{RT}\right) \tag{7.1}$$

It is noted that the activation energy for CO_2 permeation through the membranes range between 18.7 to 23.0 kJ/mol, which is similar to other crosslinked PEO-based membranes and is lower than the pure semi-crystalline PEO [13, 27, 30]. This affirms the formation of crosslinked network in the hybrid membranes and explains the high gas permeability results obtained. The activation energy for H_2 and N_2, which falls in the range of 30.8 to 41.3 kJ/mol and 37.7 to 42.0 kJ/mol, is much higher than that for CO_2 due to its

lower diffusivity and solubility in the network. N_2 has a larger kinetic diameter and lower condensability than CO_2.

Table 7.2 Pure H_2, N_2 and CO_2 permeation results for PEA:POSS 30:70 and 50:50, tested at 1 bar

Ratio of PEA POSS	T_m (°C)	T_{cell} (°C)	Permeability (Barrer)			Selectivity	
			H_2	N_2	CO_2	CO_2/H_2	CO_2/N_2
(a)							
30:70	–	30	45.0 ± 0.4	7.3 ± 0.1	321 ± 2	7.1 ± 0.2	44.1 ± 0.7
		35	57.5 ± 0.5	9.6 ± 0.1	372 ± 3	6.5 ± 0.1	38.8 ± 0.6
		40	70.5 ± 0.5	12.9 ± 0.1	416 ± 3	5.9 ± 0.1	32.2 ± 0.4
		45	87.5 ± 0.6	16.1 ± 0.2	464 ± 4	5.3 ± 0.1	28.9 ± 0.4
		50	109 ± 1	20.1 ± 0.2	510 ± 4	4.7 ± 0.1	25.4 ± 0.4
50:50	2.6	30	44.1 ± 0.4	8.2 ± 0.1	335 ± 3	7.6 ± 0.1	40.7 ± 0.8
		35	54.2 ± 0.2	9.7 ± 0.1	380 ± 2	7.0 ± 0.1	39.1 ± 0.6
		40	76.2 ± 0.6	15.0 ± 0.1	453 ± 4	5.9 ± 0.1	30.2 ± 0.4
		45	92.3 ± 1.0	18.5 ± 0.1	520 ± 3	5.6 ± 0.2	28.0 ± 0.4
		50	120 ± 1	21.5 ± 0.2	579 ± 4	4.8 ± 0.1	26.9 ± 0.5
(b)							
70:30	8.6	30	42.7 ± 0.4	7.3 ± 0.1	335 ± 3	7.8 ± 0.1	46.2 ± 0.6
		35	51.6 ± 0.4	9.4 ± 0.1	401 ± 2	7.7 ± 0.2	42.4 ± 0.5
		40	63.3 ± 0.5	12.5 ± 0.1	457 ± 4	7.2 ± 0.1	36.5 ± 0.5
		45	76.3 ± 0.3	15.4 ± 0.2	499 ± 5	6.5 ± 0.1	32.3 ± 0.8
		50	90.3 ± 0.8	18.5 ± 0.2	560 ± 4	6.2 ± 0.1	30.3 ± 0.4
80:20	25.5	30	30.5 ± 0.2	5.9 ± 0.1	275 ± 2	9.0 ± 0.1	46.7 ± 0.7
		35	40.7 ± 0.4	8.1 ± 0.1	329 ± 2	8.1 ± 0.1	40.7 ± 0.5
		40	49.7 ± 0.4	10.5 ± 0.1	369 ± 3	7.4 ± 0.1	35.2 ± 0.4
		45	60.3 ± 0.4	13.4 ± 0.1	415 ± 3	6.9 ± 0.1	30.9 ± 0.5
		50	75.7 ± 0.5	16.5 ± 0.2	462 ± 2	6.1 ± 0.1	28.0 ± 0.4

Table 7.3 Activation energy for pure gas permeation for the hybrid membranes

Ratio of PEA:POSS	Activation energy for permeation (kJ/mol)		
	H_2	N_2	CO_2
30:70	35.7 ± 1.1	41.5 ± 0.3	18.7 ± 0.5
50:50	41.3 ± 0.5	42.0 ± 0.4	23.0 ± 0.3
70:30	30.8 ± 0.4	38.5 ± 0.5	20.3 ± 0.7
80:20	36.0 ± 0.8	41.9 ± 0.4	20.8 ± 0.4
PEO [35]	76 ± 5	95 ± 5	70 ± 7

The CO_2 permeability is higher for membranes with 30 wt% and 50 wt% of POSS compared to PEA:POSS 80:20 membrane. But the permeability decreases slightly when the POSS content increases to 70 wt%. This can be attributed to multiple factors. Sorption measurements were carried out to fully understand the individual contribution of solubility and diffusivity of the gases in the membranes. The CO_2 solubility and the calculated diffusivity are reported in Table 7.4. The sorption of H_2 and N_2 was not included in this study due to the low solubility in the membranes. It is noted that the solubility of CO_2 remained fairly constant for the various compositions of the membranes. CO_2 affinity in the membranes should decrease when the PEA content decreases as the presence of polar ether groups in PEA increase the

compatibility of the membrane with CO_2 due to their relatively similar solubility parameter [5]. However, the incorporation of non-polar POSS aids to decrease the cohesive energy density of the polymer, which would result in the increase in gas solubility. Hence, the decrease in the solubility of CO_2 in PEAis compensated by the decrease in cohesive energy density. The membranes have strong sorption of CO_2, hence leading to high CO_2 permeability.

Table 7.4 CO_2 solubility and diffusivity coefficients at 35 °C and 1 bar

Ratio of PEA:POSS	P_{CO2} (Barrer)	S_{CO_2} ($\times 10^{-3}$ cm^3 (STP)/cm^3 (polymer) cm Hg)	S_{CO_2} ($\times 10^{-7}$ cm^2/s)
30:70	372	18.1	20.6
50:50	380	18.2	20.8
70:30	401	18.4	21.8
80:20	329	18.2	18.1

The CO_2 diffusivity increases when the weight percentage of POSS increases from 20 to 30 and decreases again at higher POSS content. This can be ascribed to a series of competing factors. The decrease in the chain mobility and FFV as seen from the increase in T_g and density as discussed earlier would tend to decrease the diffusivity of the gases through the membranes with higher POSS content. On the other hand, the effect of crystallinity and the strong holding force of CO_2 due to the affinity between PEO and CO_2 may affect the diffusivity of gases through the membranes with lower POSS content. Hence, the diffusivity of CO_2 for PEA:POSS 30:70 and 80:20 is lower compared to PEA:POSS 50:50 and 70:30.

A gradual increase in the permeability of the permeants at the expense of selectivity can be seen with the increase in operating temperature. This is a result of faster gas diffusion due to chain mobility and lower solubility at higher temperatures, which is consistent with observations from other literatures [10, 13]. The effect of pressure on separationperformance of the PEA:POSS 50:50 membrane is plotted inFigure7.7. The CO_2 permeability can be observed to be increasing from 380 Barrer to 412 Barrer with the increase in the upstream pressure from 1 bar to 10 bar while the H_2 and N_2 permeability decreases. The ideal CO_2/N_2 selectivity increases by 33% and the ideal CO_2/H_2 selectivity increases by 24%. This could be ascribed to the CO_2 plasticization phenomenon in the membranes and the increase in solubility of

CO_2 in the membranes. With the increase in CO_2 concentration, the sorbed CO_2 plasticizes the flexible PEA polymer chains and increases FFV of the membranes, which in turn enhance the CO_2 diffusivity. Interestingly, an approximately stable CO_2 permeability is observed when the PEA:POSS 50:50 membrane is subjected under a constant CO_2 pressure of 1 bar over a period of 4 days. CO_2 plasticization is not time-dependent. It could be probably due to the cross-linked network. It stabilizes the membrane structure after CO_2 gas plasticizes the polymer chains.

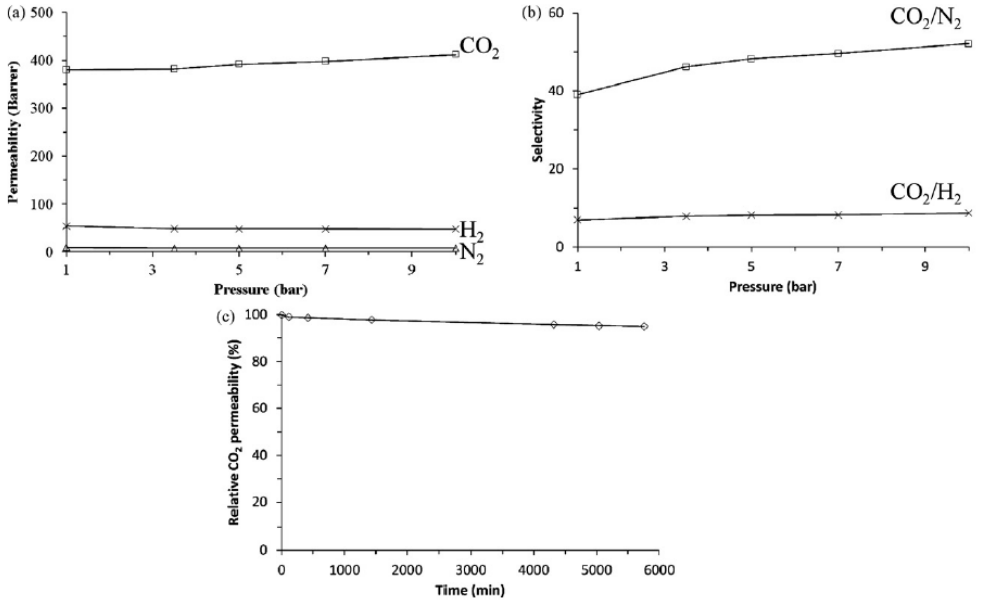

Figure 7.7 Pressure effect on (a) H_2, N_2 and CO_2 permeability and (b) ideal CO_2/H_2 and CO_2/N_2 selectivity (c) relative CO_2 permeability with conditioning at 1 bar for PEA:POSS 50:50 membrane

As seen fromFigure7.8,the pure gas separation performance of the membranes falls slightly below the upper bound for CO_2/H_2 and CO_2/N_2 gas pair[31-32]. With the increase in the upstream pressure, the pure gas performance for CO_2/N_2 separation surpasses the upper bound. Under a binary CO_2/H_2 50:50 mixture, the CO_2/H_2 selectivity of PEA:POSS 50:50 membrane remains approximately the same while the CO_2 permeability decreases slightly. A larger decline in the CO_2 permeability and CO_2/N_2 selectivity is seen under a binary CO_2/N_2 50:50 mixture. This could be ascribed to the stronger competitive sorption between CO_2 and N_2 in the membranes. N_2 is more condensable in the membranes compared to H_2.

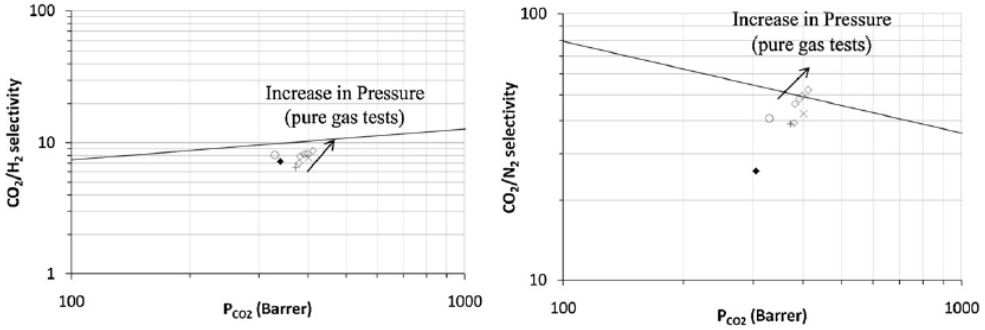

Figure 7.8 Comparison with the upper bound for CO_2/H_2 and CO_2/N_2 gas pair at 35 ^oC + represents the pure gas permeability and selectivity for PEA:POSS 30:70, - 50:50, x – 70:30, o – 80:20 represents the binary gas permeability and selectivity for the PEA:POSS 50:50 membrane at CO_2 partialpressure of 1 bar

7.3 Conclusion

In this study, organic-inorganic hybrid membranes consisting of CO_2-selective PEA and rigid POSS have been successfully fabricated for separation of CO_2 from H_2 and N_2. Two types of epoxy-POSS molecules were chosen to react with a diamine functional PEA. Only the POSS cage with glycidyl side groups reacted readily with PEA to form a hybrid membrane. The effect of the composition of this POSS structure with PEA was investigated further. The formation of the crosslinked network enhanced the compatibility between the polar ether groups of PEA and nonpolar POSS. In addition, the crystallinity of PEA is suppressed and the thermal stability improves with increase in POSS content. The permeation performance of the hybrid membranes is affected by competing factors such as decrease in solubility of PEA and cohesive energy density, chain rigidifying and crystallinity of the membranes. The strong sorption and affinity to CO_2 result in a high CO_2 permeability with a moderate selectivity. Competitive sorption between CO_2 and N_2 results in the decrease of the selectivity of the membrane under a binary CO_2/N_2 gas mixture.

References:

[1] D. R. Paul, Y. P. Yampol'skii, Polymeric gas separation membranes, CRC Press, Boca Raton, FL, 1994.

[2] L. Shao, B. T. Low, T. S. Chung, A. Greenberg, Polymeric membranes for the hydrogen economy: Contemporary approaches and prospects for the future, J. Membr. Sci. 327 (2009) 18-31.

[3] R. W. Baker, Future directions of membrane gas separation technology, Ind. Eng. Chem. Res. 41 (2002) 1393-1411.

[4] A. Hussain, M. B. Hagg, A feasibility study of CO_2 capture from flue gas by a facilitated transport membrane, J. Membr. Sci. 359 (2010) 140-148.

[5] H. Lin, B. D. Freeman, Materials selection guidelines for membranes that remove CO_2 from gas mixtures, J. Mol. Struct. 739 (2005) 57-74.

[6] M. Yoshino, K. Ito, H. Kita, K. I. Okamoto, Effects of hard segment polymers on CO_2/N_2 gas-separation properties of poly(ethylene oxide)-segmented copolymers, J. Polym. Sci. B: Polym. Phys. 38 (2000) 1707-1715.

[7] W. Yave, A. Car, S. S. Funari, S. P. Nunes, K. V. Peinemann, CO_2-Philic polymer membrane with extremely high separation performance, Macromolecules 43 (2010) 326-333.

[8] W. Yave, A. Car, K. V. Peinemann, Nanostructured membrane material designed for carbon dioxide separation, J. Membr. Sci. 350 (2010) 124-129.

[9] S. R. Reijerkerk, M. H. Knoef, K. Nijimeijer, M. Wessling, Poly(ethylene glycol) and poly(dimethyl siloxane): Combining their advantages into efficient CO_2 gas separation membranes, J. Membr. Sci. 352 (2010) 126-135.

[10] H. Lin, B. D. Freeman, Plasticization-enhanced hydrogen purification using polymeric membranes, Science 311 (2006) 639-642.

[11] V. A. Kusuma, G. Gunawan, Z. P. Smith, B. D. Freeman, Gas permeability of cross-linked poly(ethylene-oxide) based on poly(ethylene glycol) dimethacrylate and a miscible siloxane co-monomer, Polymer 51 (2010) 5734-5743.

[12] V. A. Kusuma, B. D. Freeman, S. L. Smith, A. L. Heilman, D. S. Kalika, Influence of TRIS- based co-monomer on structure and gas transport properties of cross-linked poly(ethylene oxide), J. Membr. Sci. 359 (2010) 25-36.

[13] L. Shao, T. S. Chung, In situ fabrication of cross-linked PEO/silica reverse-selective membranes for hydrogen purification, Int. J. Hydrogen Energy 34 (2009) 6492-6504.

[14] C. H. Lau, S. L. Liu, D. R. Paul, J. Z. Xia, Y. C. Jean, H. Chen, L. Shao, T. S. Chung, Silica nanohybrid membranes with high CO_2 affinity for green hydrogen purification, Adv. Energy Mat. 1 (2011) 634-642.

[15] J. Z. Xia, S. L. Liu, C. H. Lau, T. S. Chung, Liquid-like poly(ethylene glycol) supported in the organic-inorganic matrix for CO_2 removal, Macromolecules 44 (2011) 5268-5280.

[16] D. R. Paul, L. M. Robeson, Polymer nanotechnology: nanocomposites, Polymer 49 (2008) 3187-3204.

[17] Y. Li, T. S. Chung, Molecular-level mixed matrix membranes comprising Pebax® and POSS for hydrogen purification via preferential CO_2 removal, Int. J. Hydrogen Energy 35 (2010) 10560-10568.

[18] T. S. Chung, L. Y. Jiang, Y. Li, S. Kulprathipanja, Mixed matrix membranes (MMMs) comprising organic polymers with dispersed inorganic fillers for gas separation, Prog. Polym. Sci.32 (2007) 483–507.

[19] B. Tejerina, M. S. Gordon, Insertion mechanism of N_2 and O_2 into T_n (n = 8, 10, 12)-silsesquioxane framework, J. Phys. Chem. B 106 (2002) 11764-11770.

[20] H. R. Dominguez, F. A. Trevino, R. C. Reyes, A. G. Montiel, Syntheses and evaluation of gas transport properties in polystyrene-POSS membranes, J. Membr. Sci. 271 (2006) 94-100.

[21] L. Matejka, A. Strachota, J. Plestil, P. Whelan, M. Steinhart, M. Slouf, Epoxy networks reinforced with polyhedral oligomeric silsesquioxanes (POSS). Structure and morphology, Macromolecules 37 (2004) 9449-9456.

[22] S. Ramesh, T. F. Yuen, C. J. Shen, Conductivity and FTIR studies on PEO-LiX [X: CF3SO3-, SO42-] polymer electrolytes, Spectrochimica Acta A Mol. Biomol. Spectr. 69 (2008) 670-675.

[23] F. Li, Y. Li, T. S. Chung, S. Kawi, Facilitated transport by hybrid POSS-Matrimid-Zn^{2+} nanocomposite membranes for the separation of natural gas, J. Membr. Sci. 356 (2010) 14-21.

[24] P. Iyer, G. Iyer, M. Coleman, Gas transport properties of polyimide-POSS nanocomposites, J. Membr. Sci. 358 (2010) 26-32.

[25] K. Y. Mya, K. P. Pramoda, C. B. He, Crystallization behavior of star-shaped poly(ethylene oxide) with cubic silsesquioxane (CSSQ) core, Polymer 47 (2006) 5035-5043.

[26] Y. W. Chen-Yang, Y. L. Wang, Y. T. Chen, Y. K. Li, H. C. Chen, H. Y. Chiu, Influence of silica aerogel on the properties of polyethylene oxide-based nanocomposite polymer electrolytes for lithium battery, J. Power Sources 182 (2008) 340-348.

[27] L. Shao, T. S. Chung, K. P. Pramoda, The evolution of physiochemical and transport properties of 6FDA-durene toward carbon membranes; from polymer, intermediate to carbon, Microporous Mesoporous Mater. 84 (2005) 59-68.

[28] H. Lin, B. D. Freeman, Gas solubility, diffusivity and permeability in poly(ethylene oxide), J. Membr. Sci. 239 (2004) 105-117.

[29] K. Ghosal, B. D. Freeman, Gas separation using polymer membranes: an overview, Polym. Adv. Tech. 5 (1994) 673–697.

[30] H. Lin, E. V. Wagner, J. S. Swinnea, B. D. Freeman, S. J. Pas, A. J. Hill, S. Kalakkunnath, D. S. Kalika, Transport and structural characteristics of crosslinked poly(ethylene oxide) rubbers, J. Membr. Sci. 276 (2006) 145-161.

[31] B. D. Freeman, Basis of permeability/selectivity tradeoff relations in polymeric gas separation membranes, Macromolecules 32 (1999) 375-380.

[32] L. M. Robeson, The upper bound revisited, J. Membr. Sci. 320 (2008) 390-400.

Chapter 8: Conclusions and recommendations

8.1 Conclusions

Development of polymeric membranes for gas separation applications faces tradeoff between permeability and selectivity for polymers, CO_2-induced plasticization and low mechanical strength. New membrane materials or modifications of existing membrane materials to improve its physiochemical properties and its gas separation performance are studied extensively in research. The purpose of this study is to improve the properties of polyimide and poly(ethylene oxide) membranes through chemical modifications.

8.1.1 Modification of polyimide with thermally labile saccharide units

Thermalannealingpolymericmembranesconsistingofthermallysaccharidelabileunitshave been proventobeafeasibleapproachtoproducehighlypermeablegasseparationmembranes.Inthiswork, thermallabileunitswithdifferentmolecularweightsandstructures,glucose(180g/mol),sucrose (342 g/mol)andraffinose(504g/mol),arechosentobegraftedontothesidechainsofapolyimideand the membranesareannealedtoinvestigatetheeffectsofthermallylabileunitsonitsproperties.The gas separationperformanceofthemembranesforvariousgasessuchasO_2, N_2, CO_2, CH_4, C_2H_6, C_3H_6 and C_3H_8 areexamined.Itisobservedthatwhenthegraftedandannealedmembranesareannealed from 200to 400 °C, asubstantialincreaseingaspermeabilityisachievedwithmoderategas-pair selectivity.Itcouldbeattributedtotheformationofmicrovoidsuponthedegradation ofthethermally labile unit.Dependingonthethermallylabileunitgrafted,afourtoeight-foldincreaseingaspermeabilitywasseen.Thevariationofthegasseparationperformancewiththethermallylabileunit is elucidatedbythethermaldecompositionbehaviorofthethermallylabileunitsandthe interaction with thepolymermatrix.ThemembraneresistancetoCO_2 plasticizationisalsoinvestigated.The

annealedmembranesshowgoodflexibilitywithenhancedgaspermeabilityandCO_2 plasticization resistance.ThemembranesexhibitexcellentCO_2/C_2H_6 and C_3H_6/C_3H_8 separationperformance.The selectivityforCO_2/C_2H_6 is over34.The separation performanceforO_2/N_2, CO_2/N_2 and CO_2/CH_4 gas pairs fall slightlybelowtheupperbound.TheCO_2 permeabilityofthemembranegraftedwithglucose declinesslightlyfrom1389Barrersto1339BarrerswhilemaintainingthesameCO_2/CH_4 selectivityof about26.6whensubjectedtoabinarygasmixture.

8.1.2 Modification of polyimide via annealing in air and incorporation of β-CD and β-CD–ferrocene

Thermal annealingis further explored in this study. Annealingin air andincorporating β-CD and β-CD–ferrocene areemployedtochangethemolecularstructureand improvetheCO_2/CH_4 gas-pair separationandstabilityofpolyimidemembranes.A55%incrementinCO_2/CH_4 selectivity attheexpenseofpermeabilityareobservedforthePImembraneannealedunderair at 400 °C comparedtotheas-castmembrane.Afurthertwofoldimprovementinthepermeabilityofthe β-CD containingmembraneannealedunderairat400 °C isachieved.TheCO_2/CH_4 selectivityalso increases by20%.Withtheinclusionofferrocene,themembraneexhibitsadeclineinpermeability with an improvementofCO_2/CH_4 selectivity to47.3whenannealedinairat 400 °C. Thestructuralchangesare elucidated bycharacterizationtechniques(TGA,XPSandgelcontent).Theannealedmembranesinair haveshownimprovedresistancetoCO_2 plasticization andexhibitgoodmechanicalstrength.When subjected toabinaryCO_2/CH_4 gas mixture,thegasseparationperformanceremainsalmostunchanged compared tothepuregastests.Membraneswithhighstabilityunderbinarygastests,resistanceto CO_2 plasticization andstrongmechanicalstrengtharedeveloped.

8.1.3 Using iron (III) acetylacetonate as both a cross-linker and micropore former to develop polyimide membranes with enhanced gas separation performance

An ionic thermally labile unit, iron (III) acetylacetonate (FeAc), coupled with low temperature annealing, is employed in this study to improve the gas separation performance and plasticization resistance of polyimide membranes. Cross-linking polymer chains has proved to be one of the feasible ways to improve its gas separation performance and plasticization resistance, but often at the expense of permeability. However, not only a cross-linked network is established in this study, an increment of more than 88 % in permeability is attained for the PI-6 wt% FeAc membrane as compared to pristine PI membrane. The permeability enhancement is resulted from increments in both solubility and diffusivity coefficients. The modified membranes also show improved resistance to CO_2 plasticization in both pure CO_2 and binary CO_2/CH_4 gas tests. Various characterization techniques such as TGA, DSC, FTIR, gel content and density measurement were employed to elucidate the structural changes of the PI-FeAc membranes during the cross-linking and annealing processes. A moderate post thermally treated polyimide membranes blended with iron (III) acetylacetonate with enhanced gas separation performance, improved CO_2 plasticization resistance and good stability under mixed gas has been developed.

8.1.4 Polyetheramine–polyhedral oligomeric silsesquioxane organic–inorganic hybrid membranes

In this study, composite polyetheramine (PEA)–polyhedral oligomeric silsesquioxane (POSS) membranes were successfully fabricated for carbon dioxide/hydrogen (CO_2/H_2) and carbon/nitrogen (CO_2/N_2) separation.The organic functional groups on the POSS cage and its small particle size enhanced its compatibility with PEA. With the optimized conditions for membrane fabrication, a uniform distribution of POSS particles across the membranes could be observed from the SEM–EDX analysis. With the weight ratio of PEA:POSS 50:50, the crystallinity of the membranes is significantly suppressed as observed in the reduction of the melting point to 2.6 ◦C,

compared with the original PEA melting point of 37.4 ◦C. In addition, the mechanical strength of the soft PEA is enhanced. A high CO_2 permeability of 380 Barrer with a moderate CO_2/N_2 selectivity of 39.1 and a CO_2/H_2 selectivity of 7.0 are achieved at 35 ◦C and 1 bar for PEA:POSS50:50 membrane. The relationship between gas transport properties and membrane composition is elucidated in terms of PEA/gas interaction and nanohybrid structure. Fundamental study on the effect of temperature and pressure on the performance of the membranes were also carried out. The gas permeability through the membrane is found to increase at the expense of selectivity with the increase in temperature. At higher upstream gas pressure during permeation tests, improvements are observed in both CO_2 permeability and ideal CO_2/H_2 and CO_2/N_2 selectivity due to the plasticization effect of CO_2. The CO_2/N_2 selectivity of the membrane is found to decrease considerably under the binary mixture because of competitive sorption between CO_2 and N_2 in the membranes.

8.2 Recommendations

8.2.1 Preparation of polyimide hollow fiber membranes modified with iron (III) acetylacetonate

In this study, dense films were fabricated in laboratory scale for fundamental study of intrinsic membrane properties. The next step would be to scale them up to hollow fiber form, which is more useful for industrial applications. Hollow fiber membranes have higher surface area per volume compared to other configurations. Single layer asymmetric hollow fibers, dual layer asymmetric hollow fibers and composite hollow fibers are common types of hollow fiber structures. To obtain high performance hollow fiber membranes, high permeance (ultra-thin dense selective layer) and high selectivity (defect-free) are desirable.

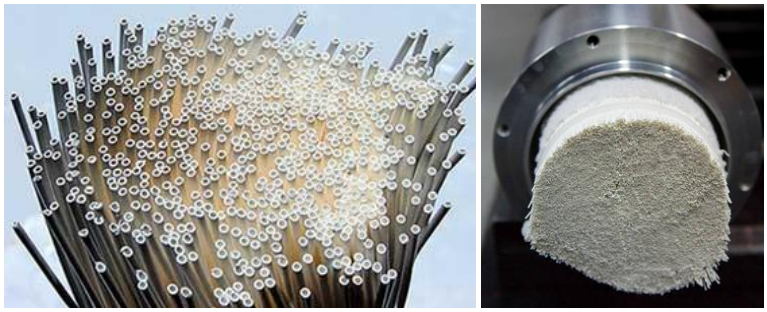

Figure 8.1 Hollow fiber membranes and module

For high performance and expensive material like polyimide modified with iron (III) acetylacetonate, it would save cost if it is scale up as dual layer hollow fibers. The outer layer is the high performance material and the inner layer is a low cost material with good mechanical properties to provide support. Preliminary studies were carried out with the spinning parameters in

Table 8.1. Matrimid was chosen as the inner layer as the hollow fibers had to be thermal annealed at 200 °C to evolve the acetylacetonate group in iron (III) acetylacetonate. Hence, a polymer with higher T_g than 200 °C was required. The concentration of polyimide blended with iron (III) acetylacetonate was prepared as 24 wt% initially. Due to its high viscosity, the concentration was lower prior to spinning. The gas tests revealed that the membranes were defective. The spinning parameters have to be examined further for the future works.

Table 8.1 Spinning conditions for polyimide hollow fiber membranes

Parameter	
Inner layer dope extrusion rate (ml/min)	1.5
Inner layer dope composition	Matrimid (22.8 wt%)/NMP/Ethanol (4/1)
Outer layer dope composition	Polyimide (24 wt%)-FeAc/NMP/Ethanol
Bore fluid	NMP/DI water (95/5 wt%)
External coagulant	Tap water
External coagulant temperature (°C)	25
Air Gap (cm)	2.5
Bore fluid flow rate (ml/min)	0.8

8.2.2 Preparation of poly(ethylene oxide) compositehollow fiber membranes

The work on polyetheramine–polyhedral oligomeric silsesquioxane organic–inorganic hybrid membranes can be scale up to composite hollow fiber form. The proposed composite hollow fiber structure consists of the outer ultra-thin selective layer, the gutter layer and the porous hollow fiber substrate. The selective layer is the PEA-POSS blend. The gutter layer provides a bridge between the selective layer and the substrate. The substrate provides the support for the entire composite membrane. The proposed gutter layer is silicon rubber and the proposed support is polyacrylonitrile. For the future work, the substrate will be fabricated, the gutter layer will be coated onto the substrate followed by the selective layer. The morphology and the gas separation performance of the membranes will be examined.

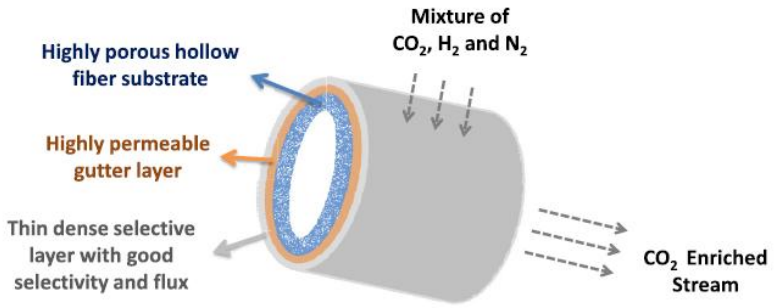

Figure 8.2 Composite hollow fiber structure

8.2.3 Fabrication of poly(ethylene oxide) membranes with enhanced gas separation performance

Blending poly(ethylene oxide) with poly(ethylene glycol) units have proven to be a feasible method to improve the gas separation performance of poly(ethylene oxide) membranes. A future work could be to enhance the gas separation performance is to blend them with poly(ethylene glycol) units and to examine possible cross-linking method like ozonolysis and ultraviolet light.

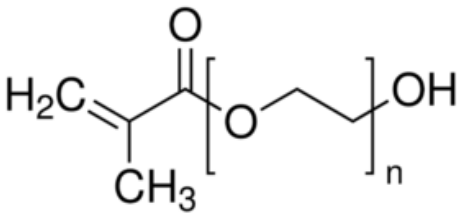

Figure 8.3 Poly(ethylene glycol) methacrylate